

DISS. ETH Nr. 26434

# Development of a long-term *ex vivo* liver perfusion system

A dissertation submitted to attain the degree of  
DOCTOR OF SCIENCES of ETH ZURICH  
(Dr. sc. ETH Zurich)

presented by  
Dustin Alexander Becker  
MSc ETH  
born on May 25<sup>th</sup>, 1991  
from Germany

accepted on the recommendation of  
Prof. Dr. Dr. h.c. Philipp Rudolf von Rohr, examiner  
Prof. Dr. med. Pierre-Alain Clavien, co-examiner  
Prof. Dr. Christopher Onder, co-examiner  
Prof. Dr. Mark Tibbitt, co-examiner

2020



*Wege entstehen dadurch, dass man sie geht.*

Franz Kafka



# Preface

The presented doctoral thesis was written at the Institute for Process Engineering at ETH Zürich as part of the Liver4Life project, a collaboration between ETH Zürich and the University Hospital Zurich, bringing together surgeons, biologists and engineers. The success of this ambitious project can undoubtedly mainly be attributed to its interdisciplinary nature. I would like to use this opportunity to appreciate that I was given the chance and trust to write my doctoral thesis within the framework of this project.

First of all, I would like to thank my supervisor Prof. Rudolf von Rohr for granting me the opportunity and honor to be his last doctoral student before retirement and putting trust in me with this exciting project. The journey was pretty unclear upon commencing and we had no idea of the road that was laying ahead. The project is mainly funded by the Wyss Zurich who envision to bring projects from the research phase to the clinical application. With us starting basically from scratch, it was clear from the beginning that the journey was going to be a long one. I would gratefully like to thank the Wyss Zurich for providing us with the funding to approach this challenging task. I would also like to thank my coexaminers Prof. Pierre Alain Clavien, Prof. Christopher Onder and Prof. Mark Tibbitt for agreeing to coexamine this exciting thesis.

I would like to thank the entire Liver4Life project team. We had a great team spirit which surely contributed to the success of the project and enjoyed each other occasionally also outside of the lab, be it at e.g. fishing adventures or at the Oktoberfest. Starting with Dima, who made sure that it would never get boring and delivered us of ETH with sufficient work. Be it cleaning up after he quickly did the experimental analysis or providing him with some tools to present the data where he never ran out of ideas or new features he wanted. Without him, the project wouldn't have been the success it was and he was always ready to "patiently" explain the medical background to us illiterates. Martin,

usually seen with gloves and a mop in his hands, was sure to always have a smart adage fitting the current situation. My repertoire of randomness surely profited from his presence. Jokes aside he was also helpful when problems arose and one could approach him with any concerns, be it thesis related or of other matter. Max joined the project after my first year because he was not yet ready to leave the ML building of ETH. So instead of continuing as a postdoc in the G floor he rose to the H floor to experience a better view from above. Many times he was able to add valuable input to my current issues and surely gave me a different perspective to my problems when I was once again stuck. Lucia provided valuable biological input and Cathy made sure we always had enough data to analyse. Matteo ensured we often had a good laugh with stories about the USZ - never have I met someone with his impersonation skills. Brian, who left the project after my first year, made sure I had a good start.

With me being the last PhD student starting with Philipp, it was inevitable that at some point the group would shrink and leave us of the liver project to ourselves. Nonetheless, I would like to thank the former members of the LTR group who accompanied me in my PhD journey at some point in time. We had a great time during our lunch and coffee breaks and I greatly enjoyed the occasional activity outside of the lab such as Skiweekends or an evening beer at bQm. The successor to the LTR was Prof. Mark Tibbitt who introduced new faces into the corridor. With him and his group, who grew quickly over the last years of my thesis, I had a great time. Thanks to all of them for also making the time here on the floor cheerful.

Last but not least I would like to thank my family for supporting me in this entire journey. My parents paved the way for me by providing me with the means to pursue my entire pre-doctoral studies and enabled for me to approach this exciting voyage of a doctoral thesis. They supported me morally, made sure I had advice when needed and were an inspiration to me in many ways. A special thanks also goes to my sister, Bianca, who was always there for me in difficult times. Surely, all my friends, who accompanied me during my entire studies in different ways, made the whole journey worthwhile.

Thank you.

# Abstract

Life outside the body, or *ex vivo* organ perfusion, has interested the scientific community for almost a century. With the first successful liver transplantation in the 1960s by Thomas Starzl, excitement around *ex vivo* liver perfusion intensified. However, the main competitor of *ex vivo* perfusion – placing the organ on ice – remained the most commonly applied method for storing an organ prior to transplantation. In recent years, with more and more people requiring an organ and consequently two to three times more patients awaiting one as compared to transplantations taking place, interest in *ex vivo* organ perfusion has revived. Currently, organ perfusion for up to a day allows to prolong storage time and assess graft quality prior to transplantation, thereby enhancing organ reach and outcome certainty. Extending this duration lays the foundation to enable further treatment such as organ recovery and repair. Taking it one step further, one would provide a sufficient time window to enable *ex vivo* liver regeneration, which is possible within one week *in vivo*. In this thesis, an *ex vivo* perfusion technology has been developed which is capable of perfusing pig and human livers for one week.

The perfusion system was developed based on pig liver experiments. Initial experiments were conducted with a commercially available machine. Based on this experience, a first prototype was constructed. From this point on, incremental changes were conducted, evaluating their effect on the perfusion quality of the liver. First, glucose supplementation and metabolism was improved by controlling the glucose infusion rate, hence ensuring physiological blood glucose levels and avoiding hyperglycemia. Secondly, pulsatile operation of the pump and, thereby, hepatic artery (HA) pressure lead to reduced hemolysis rates in the perfusion system. Thirdly, an integrated dialysis unit provided a mean to ensure physiological electrolyte levels in the perfusate and enabled the removal of metabolic waste products such as urea from the system. Further, hematocrit could be controlled with the dialysis by defining the amount of fluid

within the blood. Lastly, a physiological oxygen concentration in the portal vein (PV) reduced the vascular resistance in the HA, leading to a lower demand for vasodilator infusion. With the final machine prototype, livers could be perfused viably for seven days, which was evaluated based on various parameters such as metabolic function, damage markers and tissue integrity.

The liver plays a central role in maintaining the body's glucose homeostasis. With the motivation of ensuring physiological perfusate conditions in the perfusion system, the liver's functionality was utilized to control the glucose level in the perfusate. Thereby, insulin and glucagon are infused in a closed-loop manner based on a continuous glucose sensor. The insulin controller was elaborated in detail and two controllers were compared, namely a P-controller and a model based controller. There was no significant difference in the performance of the two controllers with respect to their ability to maintain glucose in the physiological range. Further, blood glucose could be kept within the physiological range for most of the perfusion time for both, human and pig livers. The main reason for occasions of blood glucose lying outside of the physiological range was the initial ischemia reperfusion injury, when the liver releases glucose in an uncontrollable manner. Concluding, blood glucose can be maintained in the physiological range and a P-controller is able to ensure such in the presented *ex vivo* liver perfusion system.

With the presented system, hemodynamic studies were conducted with pig livers. More specifically, the hepatic arterial buffer response (HABR) was studied in the *ex vivo* system. The HABR describes the relation of PV flow to HA flow resistance, where an increase in PV flow leads to an increase in HA flow resistance and vice versa. In order to study the HABR on the perfusion systems, the in- and outputs of the liver, namely HA, PV and vena cava (VC), were controlled and varied individually. First, the HABR showed to be unimpaired in the *ex vivo* perfusion system with a similar behaviour as previously reported *in vivo*. Secondly, in addition to the already known effect of PV flow variations on the HA resistance, an influence of VC pressure on the HA resistance was identified. By applying a hemodynamic model, the interpretation of the HABR and VC pressure variation experiments was supported and a sole washout theory - which is commonly applied for HABR nowadays - seems unlikely. A myogenic response must also play a role during HABR.



Concluding, washout and myogenic effects both influence the HABR, and hepatic sinusoidal pressure levels strongly influence the HA resistance.

The developed system was further evaluated with declined human livers, which were rejected for transplantation in entire Switzerland due to poor quality. These livers were declined for various reasons and, hence, very heterogeneous in their quality. Of ten livers, six livers were able to recover on the perfusion system and could be perfused for seven days. In the case of the other four livers, the livers could not show viability on the system and failed after four days latest. With the ability to evaluate borderline organs prior to transplantation, such organs could already be transplanted back into a patient if the perfusion on the machine renders those as transplantable. In the end, this would at this stage allow more organs to be brought to patients, ultimately showing the potential of the developed system.



# Zusammenfassung

Das Wunder des Lebens ausserhalb des Körpers interessiert die wissenschaftliche Gemeinschaft seit fast einem Jahrhundert. Mit der ersten erfolgreichen Lebertransplantation in den 1960er Jahren durch Thomas Starzl wuchs das Interesse an der *ex vivo* Leberperfusion. Der Hauptkonkurrent der *ex vivo* Perfusion - die Lagerung des Organs auf Eis - blieb jedoch für lange Zeit die Standardmethode zur Aufbewahrung eines Organs vor der Transplantation. In den letzten Jahren, in denen immer mehr Menschen ein Organ benötigen und damit zwei- bis dreimal mehr Patienten auf ein Organ warten als zur Transplantation verfügbar sind, hat sich das Interesse an der *ex vivo* Organperfusion wieder verstärkt. Die derzeitigen Systeme ermöglichen es, Lebern bis zu einem Tag aufzubewahren und erlauben es dadurch einerseits, die Reichweite für den Organtransport zu vergrössern und andererseits, die Organe vor der Transplantation zu beurteilen - wodurch die Sicherheit einer Transplantation erhöht werden kann. Diese Aufbewahrungsdauer zu verlängern bildet die Grundlage für weitere Behandlungsmöglichkeiten - wie zum Beispiel Organerholung oder -reparatur vor einer Transplantation. Zieht man dies einen Schritt weiter, bietet dies ein ausreichendes Zeitfenster, um *ex vivo* Leberregeneration zu ermöglichen, was *in vivo* innerhalb einer Woche gelingt. In dieser Arbeit wurde eine *ex vivo* Perfusionstechnologie entwickelt, die in der Lage ist, Schweine- und Menschenleber eine Woche lang am Leben zu erhalten.

Das Perfusionssystem wurde anhand von Schweinelebern entwickelt. Erste Versuche wurden mit einer kommerziellen Maschine durchgeführt. Basierend auf diesen Erfahrungen wurde ein erster Prototyp gebaut. Darauffolgend wurden inkrementelle Veränderungen durchgeführt und deren Einfluss auf die Perfusionsqualität der Leber evaluiert. In einem ersten Schritt wurde der Glukosestoffwechsel durch die Kontrolle der Glukoseinfusionsrate verbessert, wodurch physiologische Blutzuckerwerte gewährleistet und eine Hyperglykämie vermieden wurde. Als zweiter

Schritt führte die pulsierende Betriebsweise der Pumpe, respektive Druck in der Leberarterie (HA), zu einer reduzierten Hämolyserate im Perfusionssystem. Drittens konnten anhand einer integrierten Dialyseeinheit physiologische Elektrolytwerte im Perfusat gewährleistet werden und Stoffwechselendprodukte, wie zum Beispiel Harnstoff, aus dem System entfernt werden. Darüber hinaus erlaubte die Dialyse die Kontrolle des Hématokrits, indem die Menge der Flüssigkeit im Blut definiert wurde. Schlussendlich reduziert eine physiologische Sauerstoffkonzentration in der Portalvene (PV) den Gefäßwiderstand in der HA, was zu einem geringeren Bedarf an gefässerweiternden Medikamenten führte. Mit dem finalen Maschinenprototypen konnten die Leber sieben Tage lang lebensfähig perfundiert werden, was anhand verschiedener Parameter wie Stoffwechselfunktion, Schadensmarker und Gewebeatrität bewertet wurde.

Die Leber spielt eine zentrale Rolle bei der Aufrechterhaltung der Glukosehomöostase des Körpers. Mit der Motivation, physiologische Perfusatbedingungen im Perfusionssystem zu gewährleisten, wurde diese Funktionalität der Leber genutzt, um den Blutzuckerspiegel im Perfusat zu kontrollieren. Dabei werden Insulin und Glukagon mithilfe eines Reglers basierend auf einem kontinuierlichen Glukosesensor infundiert. Der Insulinregler wurde detailliert ausgearbeitet und zwei Regler verglichen, nämlich ein P-Regler und ein modellbasierter Regler. Es gab keinen signifikanten Unterschied in den Resultaten der beiden Regler im Bezug auf deren Fähigkeit den Blutzucker im physiologischen Bereich zu halten. Der Blutzuckerspiegel konnte für einen Grossteil der Perfusionszeit im physiologischen Bereich gehalten werden. Der Hauptgrund, dass der Blutzucker teilweise ausserhalb des physiologischen Bereichs war, war der anfängliche Ischämie-Reperfusionsschaden, wodurch die Leber Glukose auf unkontrollierbare Weise freisetzt. Zusammenfassend lässt sich sagen, dass der Blutzuckerspiegel im physiologischen Bereich gehalten werden kann und ein P-Regler in der Lage ist, dies im vorgestellten *ex vivo* Leberperfusionssystem zu gewährleisten.

Mit dem entwickelten System wurden hämodynamische Studien mit Schweinelebern durchgeführt. Genauer gesagt wurde die sogenannte hepatisch-arterielle Pufferreaktion (HABR) im *ex vivo* System untersucht. Die HABR beschreibt das Verhältnis von PV Strömung zu HA Strömungswiderstand, wobei eine Erhöhung der PV Strömung zu einer

Erhöhung des HA Strömungswiderstandes führt und umgekehrt. Um die HABR mittels des Perfusionssystems zu untersuchen, wurden die Ein- und Ausgänge der Leber, nämlich HA, PV und Vena Cava (VC), einzeln kontrolliert und variiert. Einerseits wurde gezeigt, dass die HABR im *ex vivo* Perfusionssystem ähnlich ausgeprägt ist wie in zuvor berichteten *in vivo* Untersuchungen. Andererseits wurde neben der bereits bekannten Wirkung der HABR auch ein Einfluss des VC-Drucks auf den HA Strömungswiderstandes identifiziert. Anhand eines hämodynamischen Modells wurde die Interpretation der HABR- und VC Druckvariationsexperimenten unterstützt. Eine reine Auswaschtheorie, anhand deren aktuell HABR beschrieben wird, erscheint unwahrscheinlich. Eine myogene Reaktion muss auch bei HABR eine Rolle spielen. Schlussendlich kann geschlossen werden, dass beides, auswaschende und myogene Effekte, die HABR beeinflussen und die intrahepatischen Druckniveaus einen starken Einfluss auf den HA Strömungswiderstand haben.

Das entwickelte System wurde mit menschlichen Lebern evaluiert, die aufgrund schlechter Qualität zur Transplantation in der ganzen Schweiz abgelehnt wurden. Diese Lebern wurden aus verschiedenen Gründen abgelehnt und waren daher in ihrer Qualität sehr heterogen. Von zehn Lebern konnten sich sechs Leber am Perfusionssystem erholen und sieben Tage lang lebensfähig perfundiert werden. Im Falle der anderen vier Lebern konnten die Lebern keine Lebensfähigkeit auf dem System zeigen und fielen spätestens nach vier Tagen aus. In Anbetracht der Tatsache, dass alle Leber für die Transplantation abgelehnt wurden, zeigt diese Studie das Potenzial des entwickelten *ex vivo* Leberperfusionssystems. Dadurch, dass grenzwertige Organe auf dem System evaluiert werden können, könnten solche Organe nach einer positiven Beurteilung auf der Maschine wieder einem Patienten transplantiert werden. Schlussendlich könnten dadurch bereits jetzt mehr Organe an Patienten gebracht werden und zeigt damit den Mehrwert des entwickelten Systems.



# Contents

<b>Nomenclature</b>	<b>XV</b>
<b>1 Introduction</b>	<b>1</b>
1.1 Motivation . . . . .	1
1.2 Objectives . . . . .	4
1.3 Overview . . . . .	5
<b>2 Background about liver and perfusion technologies</b>	<b>7</b>
2.1 The liver . . . . .	7
2.1.1 Blood supply . . . . .	7
2.1.2 Liver structure . . . . .	8
2.1.3 Liver functions . . . . .	10
2.1.4 Liver viability assessment . . . . .	13
2.2 State of the art of normothermic <i>ex vivo</i> liver perfusion	15
2.2.1 Machine configurations and functionalities . . . . .	16
2.2.2 Perfusion additives . . . . .	24
2.2.3 Results for long-term perfusion . . . . .	25
2.3 Physical relations . . . . .	26
2.3.1 Blood oxygenation . . . . .	26
2.3.2 Liver oxygen uptake rate . . . . .	27
2.3.3 Vascular resistance . . . . .	28
<b>3 Description of the perfusion system</b>	<b>29</b>
3.1 Overview . . . . .	29
3.2 Technical details . . . . .	34
3.3 Fluiddynamic setup & control . . . . .	34
3.3.1 Basic perfusion . . . . .	36
3.3.2 Pulsation . . . . .	37
3.3.3 VC pressure . . . . .	39
3.3.4 Medicamentous flow control . . . . .	41

---

3.4	Blood physiology . . . . .	43
3.4.1	Temperature . . . . .	43
3.4.2	Blood gases . . . . .	43
3.4.3	Dialysis . . . . .	48
3.4.4	Glucose . . . . .	49
3.4.5	Infusions . . . . .	50
3.5	Liver storage . . . . .	52
3.5.1	Container . . . . .	52
3.5.2	Movement . . . . .	54
3.6	Further . . . . .	56
3.6.1	Liver cannulation . . . . .	56
3.6.2	Bile mass measurement . . . . .	57
3.6.3	Blood and box weight measurement . . . . .	57
<b>4</b>	<b>Development of the perfusion system</b>	<b>59</b>
4.1	Experimental Procedure . . . . .	59
4.1.1	Liver procurement . . . . .	59
4.1.2	Blood collection . . . . .	60
4.1.3	Preparation of the perfusion machine . . . . .	60
4.1.4	Connection and initial phase . . . . .	60
4.1.5	General perfusion . . . . .	61
4.2	Incremental steps . . . . .	61
4.2.1	Hyperglycemic group . . . . .	62
4.2.2	Normoglycemic group . . . . .	63
4.2.3	Pulsatile group . . . . .	65
4.2.4	Dialysis group . . . . .	68
4.2.5	Physiological PV saturation group . . . . .	71
4.3	Further features . . . . .	74
4.4	Seven day pig liver perfusion . . . . .	75
4.5	Conclusion . . . . .	81
<b>5</b>	<b>Glucose control</b>	<b>83</b>
5.1	Introduction . . . . .	83
5.2	Materials & Methods . . . . .	84
5.2.1	Perfused livers . . . . .	84
5.2.2	Perfusion machine . . . . .	84
5.2.3	Continuous glucose measurement . . . . .	85



---

5.2.4	System modelling . . . . .	89
5.2.5	Controller . . . . .	97
5.3	Results . . . . .	97
5.3.1	Sensor calibration . . . . .	97
5.3.2	Model validation . . . . .	98
5.3.3	Continuous glucose control . . . . .	99
5.3.4	Effect of AP on perfusion quality . . . . .	103
5.3.5	Course of glucose during perfusion . . . . .	105
5.4	Discussion . . . . .	106
5.5	Conclusion . . . . .	109
<b>6</b>	<b>Hepatic arterial buffer response</b>	<b>111</b>
6.1	Introduction . . . . .	111
6.2	Materials & Methods . . . . .	113
6.2.1	Experiments . . . . .	113
6.2.2	Data post-processing . . . . .	114
6.2.3	Hepatic hemodynamic model . . . . .	116
6.3	Results . . . . .	122
6.3.1	Observations . . . . .	122
6.3.2	Buffer capacity and time constants . . . . .	124
6.3.3	Model identification . . . . .	126
6.3.4	Model assisted data analysis . . . . .	129
6.4	Discussion . . . . .	133
6.5	Conclusion . . . . .	136
<b>7</b>	<b>Human liver perfusion</b>	<b>139</b>
7.1	Experimental procedure . . . . .	139
7.1.1	Source of organs . . . . .	139
7.1.2	Perfusion system . . . . .	140
7.1.3	Perfusion procedure . . . . .	140
7.2	Results . . . . .	140
7.3	Discussion . . . . .	146
<b>8</b>	<b>Conclusions &amp; Outlook</b>	<b>149</b>
8.1	Conclusions . . . . .	149
8.2	Outlook . . . . .	152

<b>A Appendix</b>	<b>155</b>
A.1 Machine components . . . . .	156
A.2 Overview human livers . . . . .	158
<b>Bibliography</b>	<b>161</b>

# Nomenclature

## Roman letters

$a$	mmol/L/nA	Glucose sensor calibration slope
$C$	L/mmHg	Compliance
$c_{O_2}$	mLO <sub>2</sub> /dL	Oxygen concentration in blood
$F$	L/min	Volume flow
$G$	mmol/L	Glucose concentration
$I$	U/L	Insulin concentration
$n$	rpm	Rotational speed pump
$p$	mmHg	Pressure (relative)
$p_{CO_2}$	kPa	Partial carbon dioxide pressure
$p_{O_2}$	kPa	Partial oxygen pressure
$R$	kPa/(L/min)	Flow resistance
$T$	°C	Temperature
$\dot{v}$	mLO <sub>2</sub> /min	Volume flux
$\dot{V}$	mL/h	Volume flow rate
$V$	L	Volume

## Abbreviations

ALT	Alanine aminotransferase
AP	Artificial pancreas
AST	Aspartate aminotransferase
BC	Buffer capacity
BG	Blood glucose
BP	Bypass
BUN	Blood urea nitrogen
CVP	Central venous pressure

---

ECD	Extended criteria donor
ET-1	Endothelin-1
fHb	Free hemoglobin
fV	Factor V
Glu	Glucose
H&E	Haemotoxylin and Eosin
HA	Hepatic artery
HABR	Hepatic arterial buffer response
Hb	Hemoglobin
Hct	Hematocrit
HMP	Hypothermic machine perfusion
HS	Hepatic sinusoid
HV	Hepatic vein
ID	Inner diameter
IRI	Ischemia reperfusion injury
Lac	Lactate
MAP	Mean arterial pressure
MB	Model based
NMP	Normothermic machine perfusion
NO	Nitric oxide
OUR	Oxygen uptake rate
PC	P controller
PEEP	Positive end-expiratory pressure
PiV	Pinch valve
PV	Portal vein
RBC	Red blood cells
SCS	Static cold storage
SISO	Single Input, Single Output
SNMP	Subnormothermic machine perfusion
sO <sub>2</sub>	Oxygen saturation
tBil	total Bilirubin
TMF	Transmembrane flow
VC	Vena cava

## Sub- and superscripts

<i>blo</i>	Blood
<i>dia</i>	Dialysis
<i>G</i>	Glucose
<i>hep</i>	Hepatic / Liver
<i>hic</i>	Hepatic insulin clearance
<i>I</i>	Insulin
<i>inf</i>	Infusion
<i>L</i>	Liver
<i>myo</i>	myogenic
<i>rbc</i>	Red blood cells
<i>wo</i>	wash out



# Chapter 1

## Introduction

### 1.1 Motivation

With the first successful liver transplantation in the 1960s<sup>1</sup>, the diagnosis of end stage liver diseases such as primary hepatic carcinoma or terminal cirrhosis were no longer an immediate death sentence. Nowadays, transplantation still remains the best alternative for many patients with end stage liver diseases. Despite significant achievements in the field of liver transplantation, the gap between the available organs for transplantation and patients on waiting list is increasing<sup>2</sup>. It is estimated that only 10% of the worldwide need for organs is currently met<sup>3</sup>. In 2016, of 13'600 people on the waiting list in Europe, only about one third received an organ (see Figure 1.1). Means to reduce this gap between patients on waiting lists and available organs are urgently required. A possible strategy to increase the available donor pool is to allocate extended criteria donor (ECD) grafts<sup>4</sup>. ECD grafts are organs of suboptimal quality, determined by various criteria such as extended cold and warm ischemia times, steatosis, elevated donor age, or prolonged donor hospital stay and can pose a higher risk for primary non function or further complications after transplantation<sup>5,6</sup>. These organs are especially vulnerable to the cold ischemic injury, an inevitable consequence due to the current standard method of organ transport; static cold storage<sup>7,8</sup>. Consequently, ECD organs have a high discard rate with about 10% being discarded in the USA<sup>9</sup>. Novel strategies are urgently sought to enhance the donor pool, making the utilization of ECD organs an eligible target<sup>7</sup>. As an alternative to the current standard preservation technique, static cold storage (SCS), machine perfusion has gained a lot of interest in the recent

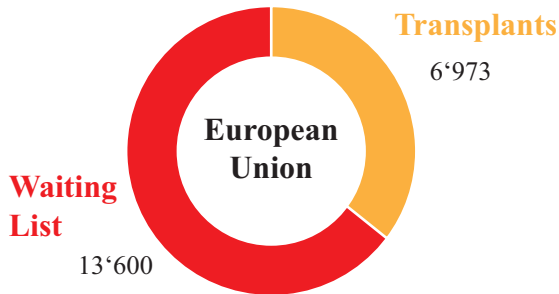


**Figure 1.1:** Number of patients on waiting list as compared to number of transplants in the European Union in 2016<sup>11</sup>.

years, potentially allowing to test the organ before transplantation or even manipulating its functions<sup>10</sup>.

With SCS, the organs are cooled and kept on ice, thereby reducing metabolism and allowing for livers to be stored for transplantation for a few hours. However, this is limited to eight to twelve hours of cold storage depending on the donor condition and graft quality and only provides a limited assessment of the organ<sup>12</sup>. With emerging technologies such as hypothermic (HMP), subnormothermic (SNMP) and normothermic machine perfusion (NMP), the assessment can be enhanced<sup>4</sup> and may even allow the recovery from ischemic injury<sup>13</sup>. In these perfusion systems, the livers are connected to a perfusion circuit and, depending on the type of system, perfused with whole blood or saline solution at different temperatures. These lie in the range from 4-8°C for HMP, 20-33°C for SNMP and at normal body temperature for NMP<sup>14</sup>. Figure 1.2 compares the different preservation methods with their respective preservation duration and possible applications. In the case of HMP, the liver is perfused with a saline solution at < 12°C, usually performed after the cold storage period, prior to implantation into a recipient<sup>10</sup>. This allows a certain evaluation of the liver while keeping metabolism low<sup>15,16</sup>. However, a full assessment and platform for therapeutic interventions is only given with normothermic machine perfusion, i.e. perfusion at normal body temperature. Although, along with the benefit of enhanced assessment of the liver's function and metabolism, comes the danger of human error



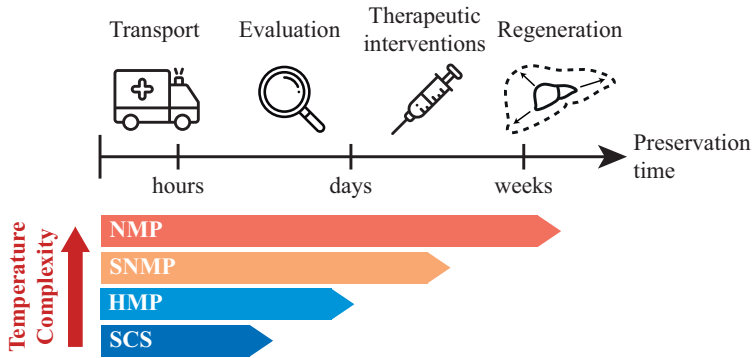


**Figure 1.2:** Comparison of preservation modes with their respective preservation times and possible applications.

and system failure at elevated temperatures. Nevertheless, normothermic machine perfusion<sup>4,17</sup> has gained a lot of interest in recent years<sup>4,17</sup>. There is currently an ongoing debate over the preferred perfusion technology and temperature, with, however, normothermic perfusion gaining increased interest as compared to the others<sup>9</sup>.

NMP enables to keep livers alive *ex vivo* with full metabolic function. This allows, on the one hand, to evaluate the performance of ECD livers and, on the other, to apply therapeutic measures<sup>18,5</sup>. One study has reported on the reduction of steatosis upon treatment of livers on the NMP circuit<sup>19</sup>. Other studies have shown a benefit of preserving organs with extended warm ischemia time by means of NMP as compared to SCS<sup>20,21</sup>. Further, the required lifelong administration of immunosuppressive medication to the patient, which are associated with long-term morbidity and mortality, may even be treated with the help of machine perfusion<sup>22,23,24</sup>. Treatment of patient with T-cell therapy to avoid need for immunosuppression after transplantation was shown effective in first studies in living donor liver transplantation<sup>25,26</sup> and in kidney<sup>27</sup>. A more moderate argument favouring NMP is the ability to schedule transplantations to staff-friendly hours<sup>9</sup>. As the goal is to keep ischemic times as short as possible, organ transplantation normally occur at odd hours. NMP would allow to keep organs viable for extended duration to schedule

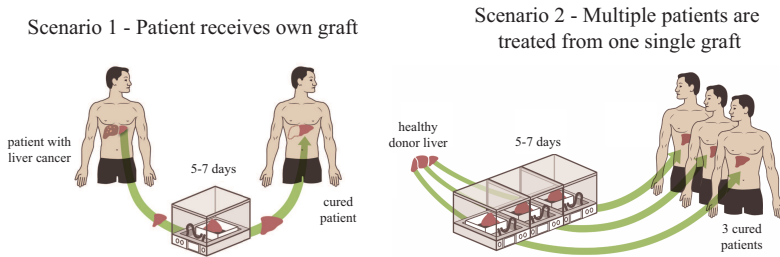


**Figure 1.3:** Illustration of two possible treatment scenarios by means of *ex vivo* liver regeneration in a perfusion machine.

transplants to working hours. Ultimately, normothermic *ex vivo* liver perfusion may even offer the mean to regenerate livers outside of the body<sup>28</sup>. This would enable novel therapeutic possibilities, with two depicted in Figure 1.3. In the first case, a patient diagnosed with liver cancer could have a healthy piece removed, regenerate it *ex vivo* in the perfusion machine and have it subsequently transplanted again. With the organ returning to its donor, there would be no need for immunosuppressive medication. In the second case, a healthy donor graft could be split into multiple pieces, with each regenerating inside the machine and ultimately curing multiple patients. Clinical experience *in vivo* has shown that livers are capable of doubling its size within 7 days post operation<sup>29,30,28</sup>. This duration sets the prerequisite for the perfusion machine, developed in the scope of this thesis. Overall, successful long-term normothermic perfusion of livers is urgently needed and may open the doors for novel therapeutic measures, whose scope may be revealed in the future<sup>8</sup>.

## 1.2 Objectives

This thesis is part of a project which is mainly funded by the Wyss Zurich. The Wyss Zurich was established by the generous donation of Hansjörg Wyss to ETH Zurich and the University of Zurich and is now funding projects in the various fields, including medicine and robotics.

In the scope of the project, a perfusion machine capable of regenerating

human livers in an *ex vivo* environment is sought to be developed. A multidisciplinary team consisting of surgeons, biologists and engineers was put together, each profiting from the expertise and knowledge of each other.

With the start of the project, the longest reported perfusion of human livers was 24 hours<sup>31</sup> and 72 hours in the case of pig livers<sup>32</sup>. It is known that human livers possess the ability to regenerate *in vivo* within seven days<sup>28</sup>. Therefore, a perfusion system had to be developed, being able to maintain livers alive for this duration in an *ex vivo* environment. For this purpose, experiments with porcine livers were conducted. Porcine livers are anatomically and physiologically similar to human livers, allowing to translate those findings to human livers<sup>33,34</sup>. With a systematic approach, a custom perfusion machine was developed, integrating various functionalities and thereby allowing to extend the duration of viable *ex vivo* liver perfusion to seven days.

## 1.3 Overview

The structure of the thesis is as follows. Following this introductory chapter, Chapter 2 provides relevant background information about liver physiology relevant for the understanding of the content of this thesis. Further, a summary about the state of the art of machine perfusion is provided, focusing on the functionalities of the various system available commercially or reported in scientific journals. The following Chapter 3 describes the developed perfusion machine in detail. All the functionalities of the system are elaborated, where the goal of the machine was to mimic the core body functions in the *ex vivo* setting. In Chapter 4, the step by step development of the machine is described. This provides the information and know-how obtained during the development, illustrating the purpose of the various components and functionalities which were integrated. At the end of the chapter, seven day pig liver perfusion is presented and discussed. In Chapter 5, a close look at the blood glucose control was taken. This is a core functionality of the machine and was elaborated in detail. A controller was implemented and tested, mimicking the *in vivo* pancreatic function of infusing insulin and glucagon based on real-time blood glucose level, i.e. an artificial pancreas. In the

subsequent Chapter 6, the hemodynamic interplay between the hepatic artery, portal vein and vena cava was studied. This was conducted by means of experiments and a mathematical model, supporting the interpretation of the data. Finally, Chapter 7 shows the significance of the developed perfusion machine by perfusing declined human livers for up to seven days.

# Chapter 2

## Background about liver and perfusion technologies

This chapter gives an introduction to the liver anatomy and physiology, as well as the state of the art of normothermic *ex vivo* liver perfusion.

### 2.1 The liver

The liver is the largest gland in the body and play many roles in the metabolism and digestion. *In vivo*, the liver is located in the upper right-hand abdominal cavity and extends to the left upper abdomen and is positioned beneath the diaphragm and on top of the right kidney, intestine and stomach. It is divided into two lobes, the left and right lobe.

#### 2.1.1 Blood supply

The liver is one of the largest organs inside the body, constituting about 2.5% of the body weight of an adult<sup>39</sup>. About 30% of hepatic volume is blood, constituting about 12% of the total body blood volume<sup>40</sup>. Further, the liver is the most well perfused organ of the body, obtaining approximately 100 mL/min/100 g liver if blood supply, approximately 25% of the cardiac output<sup>41</sup>.

Figure 2.1 illustrates the vessels entering and leaving the liver. The liver is particular with its two different blood supplies, namely hepatic artery (HA) and portal vein (PV). The blood leaves the liver via the central and hepatic veins (HV), before collectively draining into the

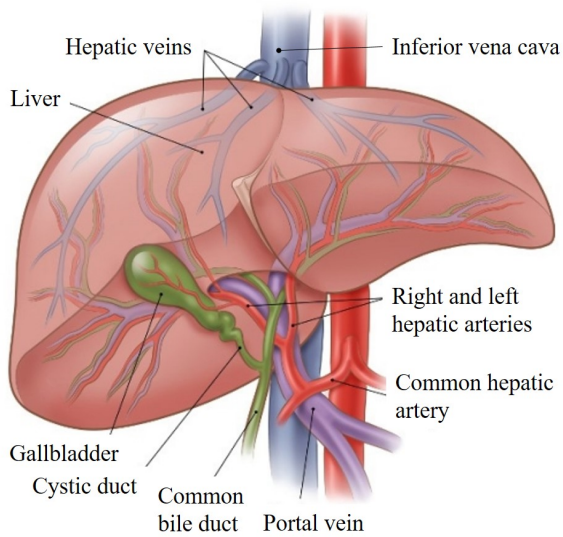


**Figure 2.1:** Liver illustration, indicating the vessels entering and leaving the liver. Adapted from [35]

inferior vena cava (VC). Oxygen rich blood enters the liver via the HA in a pulsatile manner, with typical flow levels of 0.3-0.6 L/min with pressure levels similar to the abdominal aorta. The PV on the other hand, originating from the intestinal tract and supplying the nutrients to the liver, provides about 1 L/min of flow at pressure levels between 6-10 mmHg<sup>42</sup>. The entire blood drains into the VC where pressure levels below 5 mmHg are present<sup>39</sup>, eventually leading to the heart.

### 2.1.2 Liver structure

In figure 2.2, the structure of the liver, from macro to micro scale is illustrated. The main cell of the liver are the hepatocytes, which make up about 80% of the liver volume<sup>36</sup>. The liver is divided into different segments (top left in figure 2.2), where each segment has a branch of HA and PV entering, and bile and HV leaving. This makes each segment

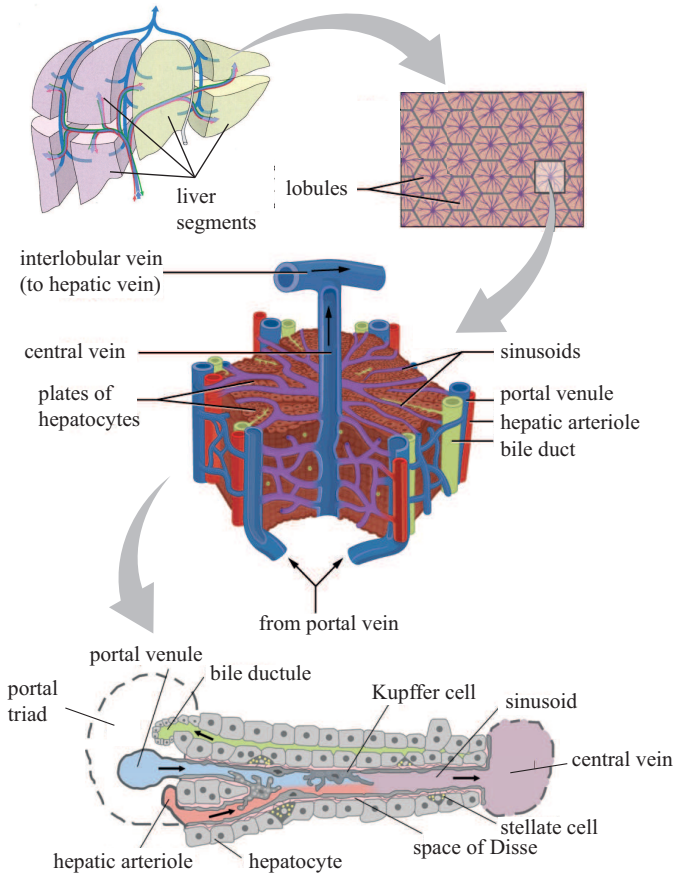


**Figure 2.2:** Illustration of hepatic structure from macro to micro scale. Top left: image of entire liver with separate segments isolated. Top right: repeating structure of hepatic lobules. Center: isolated lobule with respective vessels and elements indicated. Bottom: illustration of hepatic sinusoid. Concept and adapted from [36], extended with images from [37] and [38].

independent from each other, which allows to surgically remove entire segments and for the other segments to regenerate and compensate the missing liver piece. The segments are made up of repeating elements of lobules (top right and center of figure 2.2). These consist of the portal triad, where hepatic arteriole and portal venule enter and the bile ductule leave the liver, at each corner and the central vein in the center of the lobule. Hence, blood flows from the outside to the inside of the lobule, entering in the portal triads, flowing through the sinusoids and leaving in the central vein. This configuration leads to a concentration gradient from the portal triad to the central vein and different zones and functionalities of the hepatocytes, depending no their location. The liver further contains its own immune system consisting of Kupffer cells, phagocytes that remove dead cells or other foreign materials which enter the system.

### 2.1.3 Liver functions

The liver possesses numerous functions and responsibilities inside the body and is a central organ in the overall maintenance of physiological blood conditions. In the following paragraphs, central functions of the liver, relevant for the understanding of the underlying thesis, are briefly explained.

#### **Bile production**

Bile removes components from the blood which cannot, or only in limited amount, be removed by the kidney, such as bilirubin and excess of cholesterol. It also helps in the digestion of fats by means of bile salts and acids which, on the one hand, emulsify large fat droplets and, on the other hand, help in their subsequent adsorption. Bile is mainly made up of water, electrolytes, bilirubin, bile salts and fats. Its production is defined by two processes, with about one third defined by bile-salt dependent and the rest by bile-salt independent secretion<sup>43,44</sup>. Bile-salt independent production is further defined by two processes; the ductular secretion of bile by the bile ducts and canalicular secretion of bile by the hepatocytes<sup>45</sup>. Bile then enters the gallbladder from where it is released via the common bile duct into the duodenum on demand. On average,



the production of bile is between 20-30 mL/h<sup>44</sup>. Bile production is an important function of the liver, with its production immediately ending when the perfusion of the liver is stopped.<sup>46,47,45</sup>

### **Bilirubin metabolism**

The liver plays a central role in bilirubin metabolism. Bilirubin accrues due to the destruction of red blood cells (RBC) and the subsequent metabolism of its contents. RBCs have a typical lifespan of about six to twelve weeks *in vivo* and are rich in hemoglobin, an iron containing molecule capable of binding oxygen in the blood. With the destruction of RBCs, so called hemolysis, its contents are released into the blood plasma leading to an accumulation of free hemoglobin. Free hemoglobin is scavenged into its components heme and globin by the liver macrophages (Kupffer cells) and the heme is subsequently metabolised to bilirubin. In the plasma, bilirubin is bound to albumin, the transport protein produced by the liver, and eventually taken up by the hepatocytes and released into the biliary system. Elevated plasma bilirubin levels can have three causes. First, enhanced hemolysis could lead to more bilirubin being produced than the liver's capacity to remove. Second, due to failing liver function or insufficiency of hepatocytes, bilirubin may not be transported to the bile and lead to an accumulation of bilirubin in the plasma. Last, physical obstruction of the bile ducts could lead the cholestasis.<sup>48,49</sup>

### **Protein and coagulation factor synthesis**

The liver is responsible for the synthesis of numerous proteins and coagulation factors. Albumin, a protein only produced by the liver, binds various molecules, such as bilirubin or free fatty acids, to transport those in the blood. Also, a major role of albumin is to provide colloid osmotic pressure to prevent plasma loss from the capillaries<sup>46</sup>. With a half-life time of about three weeks, albumin is not useful as an indicator for acute liver failure<sup>50</sup>. Further, the liver exclusively synthesizes numerous proteins involved in secondary hemostasis and fibrinolysis, such as factor V, fibrinogen, antithrombin and many more<sup>47</sup>. Lack of these coagulation factors is a reliable indicator of acute liver failure, as those possess a half-life time in the range of hours to a few days<sup>51</sup>. Factor V for example,

has a half-life time of 20 h<sup>52</sup> and is primarily synthesized by the liver and clinically to assess liver failure<sup>51</sup>.

### **Glucose metabolism**

Glucose is the main energy supplier inside the body. It is tightly controlled by several hormones mainly excreted by the pancreas, with euglycemic levels of blood glucose (BG) lying in the range of 4-10 mmol/L<sup>53</sup>. While hypoglycemia can lead to brain disfunction and coma, prolonged hyperglycemia can have long-term effects in the form of diabetic retinopathy, neuropathy and nephropathy. The liver plays a vital role in BG homeostasis, as it is, next to the muscles, a major buffer site of glucose. It can take up an amount of glycogen, the storage form of glucose, equal to 10% of its own mass<sup>54</sup>. To avoid hyperglycemia, the pancreas releases insulin during elevated BG phases (e.g. fed state) to trigger glucose conversion to glycogen in the liver with the help of glucokinase, leading to a decrease in BG concentration. On the other hand, to avoid hypoglycemia, glucagon is released by the pancreas during glucose depleted times (e.g. fasting) to trigger glycogenolysis, the breakdown of glycogen to glucose, and gluconeogenesis, the synthesis of glucose from amino acids and lactate, yielding an increase in BG levels<sup>54</sup>. As the liver uses little of its stored glucose for its own energy supply but rather uses amino acids, its function related to glucose is mainly as a storage buffer and maintainer of constant blood glucose levels<sup>55</sup>.

### **Breakdown**

The liver is a central organ in drug metabolism and blood detoxification. All drugs which are absorbed by the gastrointestinal tract are transported via the portal vein into the liver. There, they first have to pass through the liver, which acts as a first filter for these before entering the system circulation by metabolizing part of those, the so called first pass effect. Further, the liver plays a major role in the removal of toxic products from the blood by usually metabolizing and subsequently removing those in the bile or by the kidneys.

### 2.1.4 Liver viability assessment

As described above, the liver performs numerous functions and carries many responsibilities to maintain blood components in the physiological range. In the clinical setting, these are monitored and evaluated to obtain feedback about the viability of the liver. In the *ex vivo* scenario, there is an ongoing debate about the applicability of *in vivo* parameters and which pose the most reliable measure to assess the liver<sup>43,56</sup>. In the following paragraphs, various viability tests from *in vivo* and *ex vivo* experience are explained. On the one hand, the liver's metabolic output is monitored, meaning the synthesis of various proteins and removal of toxic waste products. On the other hand, damages associated markers, which imply injury occurring in the liver, are measured. Overall, one cannot simply evaluate the liver based on a single criteria but needs to consider a picture of various liver functions<sup>57</sup>.

#### Damage associated markers

Many enzymes are active in the hepatocytes which are normally not, or only to a minor extend, present in the blood. Upon cellular damage or death, these are released into the blood stream, making the damage quantifiable. These comprise aspartate aminotransferase (AST), alanine transaminase (ALT), lactate dehydrogenase (LDH), alkaline phosphatase (ALP) and gamma-glutamyltranspeptidase (GGT). AST, ALT and LDH are most frequently reported with ALT being the more specific indicator for hepatocyte damage *in vivo* as AST and LDH are present in many other tissues as well<sup>58,59</sup>. An increase of these upon reperfusion after ischemic periods is usually observed during NMP<sup>60</sup>.

#### Hepatocellular function

Elevated **lactate** level in the perfusate is an indicator of poor perfusion with it being produced upon anaerobic metabolism due to lack of oxygen. However, its applicability as an indicator for healthy liver function, especially during NMP, is controversially discussed<sup>43</sup>. Elevated lactate levels are associated with liver dysfunction<sup>61</sup> and lactate clearance may be used as a sign of viability<sup>62</sup>. On the other hand, livers have failed after transplantation despite lactate clearance during NMP<sup>63</sup>.

The liver plays a central role in the **glucose** metabolism. *In vivo*, there are many sources and sinks of glucose, however, in the *ex vivo* system, glucose is only consumed by the red blood cells (RBC) or stored by the liver, which doesn't rely on glucose as an energy source. During NMP, an initial rise of glucose is inevitable due to ischemia reperfusion injury and a subsequent decline of glucose to physiological levels is generally seen as a sign of liver function<sup>43</sup>. This normally occurs within the first six to twelve hours of perfusion.

**Oxygen consumption** is generally seen as a sign of liver function with oxygen playing a central role in the metabolism. Oxygen depletion results in anaerobic metabolism, leading to lactate accumulation in the perfusate, which could ultimately cause perfusate acidosis. Oxygen consumption of the liver is also reported during *ex vivo* liver perfusion in some cases<sup>64,19</sup>

The liver is usually able to regulate *pH* in a close range. Therefore, these are used as an indirect marker of hepatic metabolism function<sup>65</sup>.

**Factor V**, being one of the coagulation factors synthesized by the liver, is clinically seen as a good indicator of liver function<sup>60</sup>. The half-life time of factor V is around 20 h, making it a reliable parameter to assess short-term viability<sup>52</sup>. However, one needs to keep in mind that factor V synthesis in the pig is about five-fold that of human livers<sup>66</sup>. Further, the perfusate during *ex vivo* perfusion is heparinized in order to prevent coagulation, making an assessment of factor V or other coagulation markers during *ex vivo* perfusion questionable.

**Ammonia** is a by-product of amino acid metabolism and is an important factor in the liver's ability to maintain acid-base homeostasis. Any disruption of the ammonia metabolism can lead to acidosis which could be indicative for metabolic disruption. In a healthy state, the liver metabolises ammonia to urea, which is then excreted by the kidneys to be removed from the system.<sup>43</sup>

**Urea** has recently also been identified as a reliable biomarker for post-transplantation outcome in a pig model<sup>67</sup>.

## Bile production & composition

Bile production during *ex vivo* perfusion is discussed controversially. On the one hand, bile production has been reported as a good sign of liver function and transplant predictor during *ex vivo* perfusion<sup>56,68</sup>, on the

other hand, reports have stated it not to correlate with post-transplant graft function<sup>69,57</sup> or even had livers fail which produced bile during *ex vivo* perfusion<sup>63</sup>. Nonetheless, bile production is commonly reported as a result during NMP<sup>70,71</sup>. As bile production consists bile-salt dependent and bile-salt independent secretion, bile-salts need to be replenished during *ex vivo* perfusion due to lack of recirculation as occurs *in vivo*<sup>72</sup>. Reason being that lack of bile production may lead to damage of the biliary canaliculi, possibly leading to the organs being non-transplantable<sup>72</sup>. The commonly infused bile-salt is sodium taurocholate<sup>72</sup>.

Next to bile production, bile components are also commonly analyzed, especially bicarbonates and glucose. Bicarbonates are believed to be required to maintain alkali *pH* and prevent damage of the cholangiocytes due to the bile acids<sup>73</sup>. Glucose is normally absorbed the cholangiocytes, leading to bile glucose levels of < 1 mmol/L in healthy state<sup>74</sup>. Therefore, presence of glucose in bile above this threshold may be an indicator of damage to cholangiocytes and could lead to post-transplant cholangiopathy. Some groups also report the ratio of bile/perfusate glucose level to evaluate cholangiocyte health<sup>67</sup>.

## Histology

Biopsy probes are normally taken to have a measure of tissue integrity. However, one needs to consider that these inherently induce damage to the liver tissue and the samples are local representations of the entire liver. Therefore, biopsy probes should be interpreted as part of the entire picture. The most commonly applied staining are Haemotoxylin and Eosin (H&E) staining to visualize tissue integrity<sup>60</sup> and periodic acid Schiff (PAS) to qualitatively examine glycogen content<sup>75</sup>. In the end, a pathologist is usually required to examine and interpret histology samples.

## 2.2 State of the art of normothermic *ex vivo* liver perfusion

There are a few normothermic *ex vivo* liver perfusion systems commercially available and many systems which have been developed by various

research groups in the world. These systems range from rat liver perfusion to pig and human. With the focus of this thesis lying on the perfusion of pig and the aim of perfusing human livers, this chapter only includes the ones from these two groups. Here, different machine configurations and functionalities, perfusion protocols, and results for long-term machine perfusion are summarized.

### 2.2.1 Machine configurations and functionalities

Considering the commercially available machines, three are currently available for normothermic *ex vivo* liver perfusion – the Organ Assist’s Liver Assist, the OrganOx metra and the Transmedics OCS<sup>9</sup>. These systems primarily focus on the evaluation of organs prior to transplantation, therefore, their incentive is to perfuse the organ in the range of a few hours to a day<sup>8</sup>. Next to these commercial machines, there are many more perfusion systems available which were developed by various research groups and differ greatly in terms of components and integrated functionalities. Table 2.1 gives an overview over these machines and their integrated components. In principle, all perfusion machines are based on an extracorporeal heart lung machine, consisting of a hemodynamic control aspect, such as pumps in combination with clamps, and an oxygen control given by an oxygenator, replacing the lung’s functions. Further, the system may either be open or closed, referring to the cannulation of the vena cava. In an open system, the venous blood flows into the surrounding environment of the liver, either air or some fluid, whereas in a closed system, the vena cava is cannulated and connected to a tube, leading the blood away from the liver. Last, a few systems also have a dialysis system integrated or added additional functionalities such as diaphragm movement.

#### General functionality

Table 2.1 gives an overview of the main functions of the three commercial systems and various reported systems in literature. It becomes apparent that all the commercially available and most of the research systems only include the basic perfusion functionality given by one or more pumps and an oxygenator. With the commercially available devices needing to

**Table 2.1:** Selection of reported machine configurations.

Group	Machine	CD	P	Oxy	Dia	cPHI	sDM	oBGA
<i>Commercial products</i>								
LiverAssist <sup>76,56</sup>		open	2CP	2	-	-	-	-
OrganOx metra <sup>77,20,32,78,68,31</sup>		closed	1CP	1	-	✓†	-	✓
Transmedics OCS <sup>§</sup>		open	1CP	1	-	-	-	-
<i>Research devices</i>								
Berlin 1 <sup>79,80</sup>	custom	closed	2PP+1RP	1	✓	-	-	-
Guangzhou <sup>81</sup>	custom	n.r.	3RP	2	-	-	-	-
St. Louis <sup>82</sup>	custom	open	2CP	1	✓	-	-	-
Cleveland <sup>83,84</sup>	custom	open	1CP+1RP	1	-	-	-	-
Leicester <sup>85</sup>	custom	open	1CP	1	-	-	-	-
Toronto <sup>86,87,88</sup>	OrganOx*	closed	1CP	1	✓	-	-	-
Barcelona <sup>89</sup>	LiverAssist*	open	2CP	2	-	-	-	-
Berlin 2 <sup>90</sup>	custom	closed	4RP	1	✓	-	✓	-
Brisbane <sup>91</sup>	custom	closed	1CP	1	-	-	-	-
Baltimore <sup>92</sup>	custom	open	3RP	1	-	✓†	-	-
Tianjin <sup>93</sup>	custom	open	1RP	1	-	✓†	-	-

*Notes:* Label descriptions: CD – circuit design (open/closed), P – pumps, Oxy – oxygenator, Dia – dialysis, cPHI – controlled pancreatic hormone infusion, sDM – simulated diaphragm movement, oBGA – online blood gas analysis. Abbreviations: CP – centrifugal pump, PP – pneumatic pump, RP – roller pump, n.r. – not reported, § – no publications available, \* – adapted machine, † – manual insulin adjustment

simplify the system to enhance the usability and reducing the number of roots of failure, minimizing the number of functionalities to a minimum is a comprehensible approach. On the other hand, reported research devices have more complexity with the main difference lying in the number of pumps integrated to control each liver input and perfusion circuit individually. Most of these systems are custom built whereas only a few use the commercially available ones in a modified version. Some of these systems apply centrifugal pumps (CP), some pneumatic pumps (PP), others roller pumps (RP) or a combination of those. A dialysis system is not integrated in any of the commercial systems whereas it is applied to some of the research devices for metabolic waste product removal. The only identified system with a closed loop oxygen control, requiring an online blood gas analysis (oBGA), is the commercial device OrganOx metra. Further, infusions are normally given in a continuous fashion, which also includes the supplement of the pancreatic hormone insulin. Only three systems, of which one is the commercial OrganOx metra<sup>31</sup>, were identified where insulin and/or glucose was adjusted based on current glucose readings, however, this was realized in a manual manner as opposed to a closed loop control. This requires the presence of trained staff to specify the respective infusion rate based on the manual glucose measurement.

## Hemodynamic

As described in 2.1.1, the HA receives blood in a pulsatile manner with pressure levels similar to the abdominal aorta and a flow in the range of 0.3-0.6 L/min. In contrast, the PV is supplied at a flow rate of approximately 1 L/min resulting in a PV pressure level of < 10 mmHg in healthy liver parenchyma. The HA and PV mix inside the liver's sinusoids, leaving the liver together and entering the VC. The pressure in the VC lies below 5 mmHg.

Table 2.2 lists the hemodynamic settings of the various available machines in literature. Generally, both the HA and the PV are cannulated and supplied with blood during NMP. The main difference in perfusion of these two inlets lies in the desired pressure level and resulting flow. In reported perfusion systems, the HA is either perfused pulsatile or continuous, with no clear consensus on the benefit or drawback of either.



**Table 2.2:** Overview of reported hemodynamic perfusion protocols.

Group	HA			PV		VC
	C/P*	P/F <sup>†</sup>	Target	P/F <sup>†</sup>	Target	
<i>Commercial products</i>						
Liver Assist <sup>76,56</sup>	P	P	50 mmHg	P	11 mmHg	open
OrganOx metra <sup>77,20,32,78,68,31</sup>	C	P	65-95 mmHg	P		0-2 mmHg
Transmedics OCS			no data reported			
<i>Research devices</i>						
Berlin 1 <sup>79,80</sup>	P	P	80 mmHg	P	7-13 mmHg	closed, not monitored
Guangzhou <sup>81</sup>	n.r.	P	90-100 mmHg	P	6-9 mmHg	n.r.
St. Louis <sup>82</sup>	C	F	0.5±0.1 L/min	F	1.2±0.2 L/min	open
Cleveland <sup>83,84</sup>	n.r.	P	90-95 mmHg	P	5-10 mmHg	open
Leicester <sup>85</sup>	n.r.	P	80-100 mmHg	P*	20-30 mmHg	n.r.
Toronto <sup>86,87,88</sup>	C	P	60 mmHg	P*	2-4 mmHg	closed, not monitored
Barcelona <sup>89</sup>	P	P	50 mmHg	P	8 mmHg	open
Berlin 2 <sup>90</sup>	P	P	100 mmHg	P	11 mmHg	closed, not described
Brisbane <sup>91</sup>	n.r.	P	70 mmHg	P*	n.r.	closed, not described
Baltimore <sup>92</sup>	P	P	60-80 mmHg	P	5-10 mmHg	open
Tianjin <sup>93</sup>	n.r.	F	0.13-0.24 L/min	F	0.32-0.58 L/min	open

Notes: n.r. - not reported, \* - continuous (C) or pulsatile (P), † - pressure (P) or flow (F) control, \* - gravity controlled

Further, the two inputs can either be pressure or flow controlled. Obviously, it is not possible to control pressure and flow in one input at the same time, as the combination of both results from the resistance in the liver. In general, the preferred perfusion mode is pressure control in both HA and PV. While the pressure in the HA is driven directly by the pump, the PV is in some cases perfused from a reservoir which is drained by gravity, fixing the reservoir height and yielding a constant pressure level in the PV. Target pressure levels in the HA vary strongly in the range from 50 to 100 mmHg, the same applies for the PV with some targeting 2-4 mmHg and others 20-30 mmHg drastically exceeding the bounds of the *in vivo* levels. In the case of an open system, the blood from the VC drains into the surrounding environment which is of atmospheric pressure level (0 mmHg). If the system is closed, the pressure in the VC can be controlled. However, in most of the systems, the target pressure levels are not reported, with the exception of the OrganOx metra system, where pressure levels between 0-2 mmHg are targeted<sup>94</sup>. The control mechanism, if present, is not reported.

## Oxygenation

*In vivo*, blood gases are closely regulated by the lungs. In particular, oxygen and carbon dioxide concentrations are controlled by respiration. Both gases are dissolved in the blood and measured in terms of partial pressures  $pO_2$  and  $pCO_2$ . Oxygen binds to hemoglobin, which increases the amount of oxygen that can be transported in the blood. Carbon dioxide is in equilibrium with carbonic acid, leading to an inverse relationship between carbon dioxide concentration in the blood and  $pH$ . An increase of  $pCO_2$  results in a reduction of  $pH$  and vice versa. Therefore, chemosensors in the body react to  $pO_2$ ,  $pCO_2$  and  $pH$ , whereby the response to changes in  $pCO_2$  and  $pH$  is more pronounced as compared to  $pO_2$ . Upon a reduction of  $pO_2$ , the body reacts by increasing respiration to supply more oxygen. Similarly, elevated  $pCO_2$  or reduced  $pH$  levels leads to an enhanced respiration, washing out more  $CO_2$  from the blood.<sup>52</sup>

Table 2.3 summarizes the oxygen and carbon dioxide control inside the perfusate of the various systems. These are controlled via the oxygenator which supplies a mixture of oxygen, nitrogen and carbon dioxide. Thereby,

**Table 2.3:** Overview of reported oxygenation modes and target levels.

Group	Oxygenator gas mixture	HA		PV $pO_2$
		$pO_2$	$pCO_2$	
<i>Commercial products</i>				
LiverAssist <sup>76,56</sup>	n.r.	hyper	n.c.	n.c.
OrganOx metra <sup>77,20,32,78,68,31</sup>	varied	controlled	controlled	n.c.
Transmedics OCS		no data reported		
<i>Research devices</i>				
Berlin 1 <sup>79,80</sup>	97.5% O <sub>2</sub> , 2.5% CO <sub>2</sub>	hyper	n.c.	hyper
Guangzhou <sup>81</sup>	varied	manual ctrl.	n.c.	n.r.
St. Louis <sup>82</sup>	95% O <sub>2</sub> , 5% CO <sub>2</sub>	hyper	n.c.	n.c.
Cleveland <sup>83,84</sup>	100% O <sub>2</sub>	hyper	n.c.	hyper
Leicester <sup>85</sup>	100% O <sub>2</sub>	hyper	n.c.	hyper
Toronto <sup>86,87,88</sup>	95% O <sub>2</sub> , 5% CO <sub>2</sub>	hyper	n.c.	hyper
Barcelona <sup>89</sup>	n.r.	hyper	n.c.	hyper
Berlin 2 <sup>90</sup>	95% O <sub>2</sub> , 5% CO <sub>2</sub>	hyper	n.c.	phys., no details
Brisbane <sup>91</sup>	n.r.	n.r.	n.r.	n.r.
Baltimore <sup>92</sup>	varied	controlled	n.r.	phys., no details
Tianjin <sup>93</sup>	varied	manual ctrl.	manual ctrl.	n.r.

*Notes:* n.r. - not reported, n.c. - not controlled, phys. - physiological level

either one oxygenator is used for both HA and PV or the two are equipped with an oxygenator individually.

Many systems provide a constant mixture of e.g. 95% O<sub>2</sub> and 5% CO<sub>2</sub> or 100% O<sub>2</sub>, not controlling the partial oxygen tension ( $pO_2$ ) of the blood, respectively oversupplying oxygen to ensure sufficient oxygen delivery to the liver. A few systems control the oxygen tension to physiological levels, although only the OrganOx metra reported an integrated sensor for online blood gas analysis allowing a closed loop oxygen control. In the other cases, details about the control are not reported or the control is realized manually with periodic manual measurements.

In contrast to oxygen, carbon dioxide is rarely controlled during NMP. Only two of the identified systems report a controlled  $pCO_2$ . One group manually controls  $pCO_2$  based on periodic blood gas measurements, whereas the OrganOx metra system has a closed loop control integrated to ensure physiological levels.

In most systems, the PV oxygen level is not controlled to defined to the same level as the HA. Two identified systems control PV oxygen content to physiological ranges, however, no details about the target level and control are reported. Control of carbon dioxide content in the PV is not explicitly mentioned in any of the reported systems.

## Dialysis

*In vivo*, the kidneys possess many important functions such as elimination of metabolic end products (e.g. urea) and toxic products, and regulation of osmotic blood pressure by controlling electrolyte balance and acid-base homeostasis. In case of a failure of the kidneys, their function can be replaced to a certain extend by a dialysis unit. This procedure is commonly applied in the clinic and has helped to save millions of patients. Applying this technology inside a perfusion system gives a mean to controllably remove components from the system. Depending on the type of dialysis, an equilibrium with certain blood components can be established.

Generally, dialysis is distinguished in two ways, hemodialysis and hemofiltration. In both cases, blood is cleaned by means of a filter. In the case of hemodialysis, a dialysate solution flows through the filter in a counter current manner to the blood. Thereby, two physical

processes are present; diffusion and convection. By means of diffusion, blood and dialysate equilibrate with each other due to a concentration gradient across the membrane. Different dialysate solutions are available, usually containing electrolytes, bicarbonates and glucose in physiologic concentrations, where the exact concentrations depend on the intended use. This allows the dialysate and blood to equilibrate with each other and gives a mean to indirectly control these parameters in the blood. By means of convection, fluid is pressed through the filter and thereby allows for a direct fluid exchange between the two sides. In the case of hemofiltration, only the blood flows through the filter, without a dialysate solution flowing on the other side of the filter. Thereby, only convection is taking place, filtering those components from the blood which can pass the membrane of the filter.

As listed in table 2.1, none of the commercially available systems have a dialysis unit integrated, whereas some of the reported research devices have one. These usually apply the hemodialysis as compared to hemofiltration to keep electrolytes and *pH* in physiological range<sup>80,82,90</sup> or control hemoglobin content of the perfusate by defining the filtration rate across the filter<sup>82</sup>.

## Further

**Vasoactive infusions** Studies have shown it to be beneficiary to infuse vasodilators during *ex vivo* liver perfusion<sup>86,95</sup> which has lead to most groups infusing vasoactive substances during perfusion. Most prominently, vasodilator prostacyclin is applied to ensure sufficient vasodilation during perfusion<sup>18,60</sup>. Next to their vasoactive property, the epoprostenol is applied due to their anti-inflammatory effect<sup>96</sup>. Many more factors influence the tension of the smooth muscle cells, with nitric oxide (NO) and endothelin-1 (ET-1) being the major antagonists derived in the endothelium<sup>97</sup>. NO has been shown to have a potent effect on arterial vasodilation<sup>98,99</sup>, whereas ET-1 acts as a potent vasoconstrictor<sup>100</sup>. However, reports about feedback controlled infusion of vasoactive substances could not be identified but those are rather infused in a constant manner or manually adjusted<sup>18,60</sup>.

**Pancreatic hormone infusion** As described in section 2.1.3, the liver plays an important role in the glucose metabolism inside the body. The release and uptake of glucose by the liver is mainly controlled by the pancreatic hormones insulin and glucagon. In reported *ex vivo* liver perfusion studies, insulin is in some cases supplied to the liver, but never glucagon. Either insulin is infused at a constant rate<sup>19,101,91</sup> or adjusted to meet desired BG levels based on periodic, manual glucose measurements<sup>31,93</sup>. The supplied insulin infusion rates vary greatly across protocols<sup>18</sup>. Further, some groups infuse additional glucose to keep a desired BG level, whose infusion rate is based on manual BG measurements<sup>31,93</sup>. However, no studies could be identified in which insulin and/or glucose were supplied in a closed-loop fashion with an integrated continuous glucose measurement and automated insulin infusion, i.e. an "artificial pancreas"<sup>18</sup>.

**Diaphragm movement** *In vivo*, the liver is position inferior to the diaphragm. During breathing the lung exerts pressure upon the liver leading to a periodic movement of the latter.

As listed in table 2.1, the diaphragm movement is not integrated or mimicked in most perfusion systems. Although, one group integrated an oscillating pressure in the organ chamber, thereby leading to variations in the venous pressure levels<sup>90</sup>. They observed a significant perfusion improvement of the peripheral lobules.

## 2.2.2 Perfusion additives

In order to ensure physiological blood conditions, various supplements need to be added to the perfusate. There is a large variation of which supplements are supplied and in what dosage<sup>18,60</sup>. In general, one needs to distinguish between two types of supplements; the ones added at the beginning of perfusion and the ones continuously supplied during the course of perfusion.

**Initial additives** The initial additives are added to the perfusion system once prior to beginning the perfusion. To prevent clotting, all systems add anticoagulant, mostly heparin. Commonly, antibiotics are added to reduce the risk on bacterial contamination in the *ex vivo* settings.

However, no clear consensus on the type of antibiotic is present and a wide variety of antibiotics are chosen. Next, most studies add bicarbonates to correct  $pH$  and other electrolytes such as calcium to ensure physiological ion balance. In some cases, steroids and albumin are added, the latter to ensure physiological oncotic pressure in the perfusate.<sup>18,60</sup>

**Continuous additives** During the perfusion, various additives are supplied in a continuous manner. Most study groups add parental nutrition, which includes amino acids and in some cases also glucose to maintain metabolism. Heparin is infused by some groups also continuously to prevent coagulation. Insulin is supplied in a continuous, not feedback controller manner by some groups. More details about this is given in chapter 5. *In vivo*, bile salts, which are excreted with the bile, are recycled by the intestinal tract, in a process called enterohepatic circulation. As the bile in the *ex vivo* perfusion system is not recycled, the lost bile salts need to be replenished. Especially for long-term perfusion ( $\geq 6$  h), bile salt replenishing seems to be mandatory<sup>60</sup>. Commonly, taurocholic acid is supplied as bile salt. Some groups also infused vasodilators such as prostacyclin or epoprostenol.<sup>18,60</sup>

### 2.2.3 Results for long-term perfusion

Long-term perfusion of livers has gained more interest in recent years. Up to now, short-term preservation had most clinical relevance leading to most studies focusing on only a few hours of perfusion. Nonetheless, long-term perfusion of livers may open doors for novel therapeutic interventions resulting in some studies also focusing on strategies to enable such. Up to writing of this thesis, longest reports of perfused human livers were 86 hours<sup>102</sup> and 72 hours<sup>32</sup> in the case of pig livers. Table 2.4 gives an overview of different studies in recent years, the respective perfusion durations and device used where focus was put on reports lasting longer than 10 h. Only very few studies perfused for a day or longer. During the 72 h pig liver perfusion, bile production ceased after 12 to 24 h<sup>32</sup>, which is generally accepted as a marker for liver function. A main limitation for long-term perfusion of livers is the hemolysis leading to some investigators suggesting the use of artificial oxygen carriers<sup>19</sup>. Overall, this overview

**Table 2.4:** Normothermic perfusion results reported in literature, lasting longer than 10 h.

Source	Year	Duration	Device	Goal
<i>Pig</i>				
Butler et al. [32]	2002	72 h	Custom	Eval.
St Peter et al. [20]	2002	24 h	Custom	TPS
Nassar et al. [83]	2015	10 h	Custom	Eval.
<i>Human</i>				
Liu et al. [102]	2018	86 h	Custom	Eval.
Vogel et al. [31]	2017	24 h	OM	Eval.
Nasralla et al. [94]	2018	1.4 – 23.1 h	OM	TP
Bral et al. [103]	2017	3.3 – 22.5 h	OM	TP
Ravikumar et al. [104]	2016	3.5 – 18.5 h	OM	TP
Pavel et al. [70]	2019	12 h	OM	Eval.

Notes: OM – OrganOx metra, LA – Liver Assist, Eval - evaluation, TPS - transplant simulation, TP - transplant

shows the need for a system which is capable of a long-term *ex vivo* liver perfusion to enable treatment of grafts prior to transplantation.

## 2.3 Physical relations

### 2.3.1 Blood oxygenation

Oxygen is present in blood in two ways. On the one hand, it's dissolved in blood plasma which is measured in terms of partial pressure  $pO_2$ . On the other hand, it's bound to hemoglobin which increases the capacity of blood to transport oxygen. This is described by means of the oxygen dissociation curve (see figure 2.3). The oxygen bound to hemoglobin depends on  $pO_2$  and ranges from 0 to 100%, which describes the percentage of binding sites for oxygen that are taken. The affinity of oxygen to hemoglobin also depends on other parameters such as  $pH$ ,  $pCO_2$  and  $T$ . Mathematical approximations are available to calculate the relation between  $pO_2$  and  $sO_2$ , considering the influence of  $pH$ ,  $pCO_2$  and temperature<sup>105</sup>.



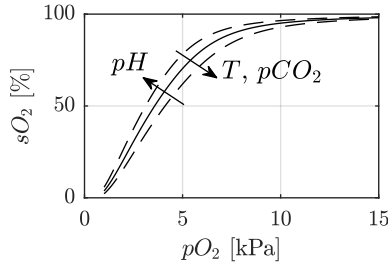


**Figure 2.3:** Oxygen dissociation curve

In order to obtain the oxygen concentration of blood, one needs to consider both the contributions of  $pO_2$  and  $sO_2$ . The following relation allows to calculate the oxygen concentration in blood  $c_{O_2}$ .

$$c_{O_2} = 1.39 \cdot Hb \cdot \frac{sO_2}{100} + 0.00314 \cdot pO_2 \cdot 7.5 \quad (2.1)$$

with  $Hb$  being the hemoglobin concentration in g/dL,  $sO_2$  in %,  $pO_2$  in kPa. The coefficients  $1.39 \text{ mL O}_2/\text{g Hb}$  is the binding capacity of oxygen to hemoglobin,  $0.00314 \text{ mL O}_2/\text{dL/mmHg}$  the solubility coefficient of oxygen in plasma and  $7.5 \text{ mmHg/kPa}$  to convert kPa to mmHg. The unit of oxygen concentration in blood  $c_{O_2}$  is  $\text{mL O}_2/\text{dL}$ .

### 2.3.2 Liver oxygen uptake rate

The oxygen update rate  $OUR$  of the liver is calculated by applying a mass balance around the liver. This allows to define

$$OUR = (\dot{v}_{O_2,HA} + \dot{v}_{O_2,PV} - \dot{v}_{O_2,VC}) / (m_{liver} \cdot 10) \quad (2.2)$$

where  $\dot{v}_{O_2,i}$  are the fluxes of oxygen in the three in- and outputs HA, PV and VC in  $\text{mL O}_2/\text{min}$  and  $m_{liver}$  the mass of the liver in kg. The unit of  $OUR$  is  $\text{mL O}_2/\text{min}/100\text{g liver}$ .

The individual fluxes  $\dot{v}_{O_2,i}$  are calculated according to

$$\dot{v}_{O_2,i} = F_i \cdot c_{O_2,i} \quad (2.3)$$

with  $F_i$  being the flow rate in the respective branch in L/min.

### 2.3.3 Vascular resistance

Unless defined in a different way, the vascular resistance of HA  $R_{HA}$  or PV  $R_{PV}$  are calculated in the following way.

$$\begin{aligned} R_{HA} &= \frac{p_{HA} - p_{VC}}{F_{HA}} \\ R_{PV} &= \frac{p_{PV} - p_{VC}}{F_{PV}} \end{aligned} \tag{2.4}$$

This way suffices for the general analysis, however, in chapter 6, a more detailed analysis is desired, resulting a different way to calculate the vascular resistance. This is described in more detail in the chapter.

# Chapter 3

## Description of the perfusion system

With the start of the project, the three perviously mentioned commercial machines were available. The initial experiments were conducted with the LiverAssist device. Incremental changes were applied to the system, leading to increasing complexity. At some point, the custom machine was developed, with all components fully integrated. In this chapter, the final machine prototype is described in detail.

### 3.1 Overview

The goal of the perfusion machine is to provide physiological conditions to the liver, i.e. to mimic the *in vivo* situation as close as possible. Hence, the benchmark for the perfusion machine is the human body. The complex setup of the human body and the numerous functions it has to ensure working provides a challenging task when replicating those artificially. The next few paragraphs will describe the main functions of the system necessary for a successful long-term perfusion of livers outside of the body and highlight unique properties of the developed perfusion machine.

Figure 3.1 illustrates how the machine replicates the human body and gives an overview of the integrated functions in the system. Figure 3.2 shows an image of the perfusion loop in the machine and the respective components as indicated in figure 3.1. Figure 3.3 shows an image of the entire machine as it stands in the laboratory at the time of writing. In figure 3.4, the detailed technical scheme of the perfusion machine is

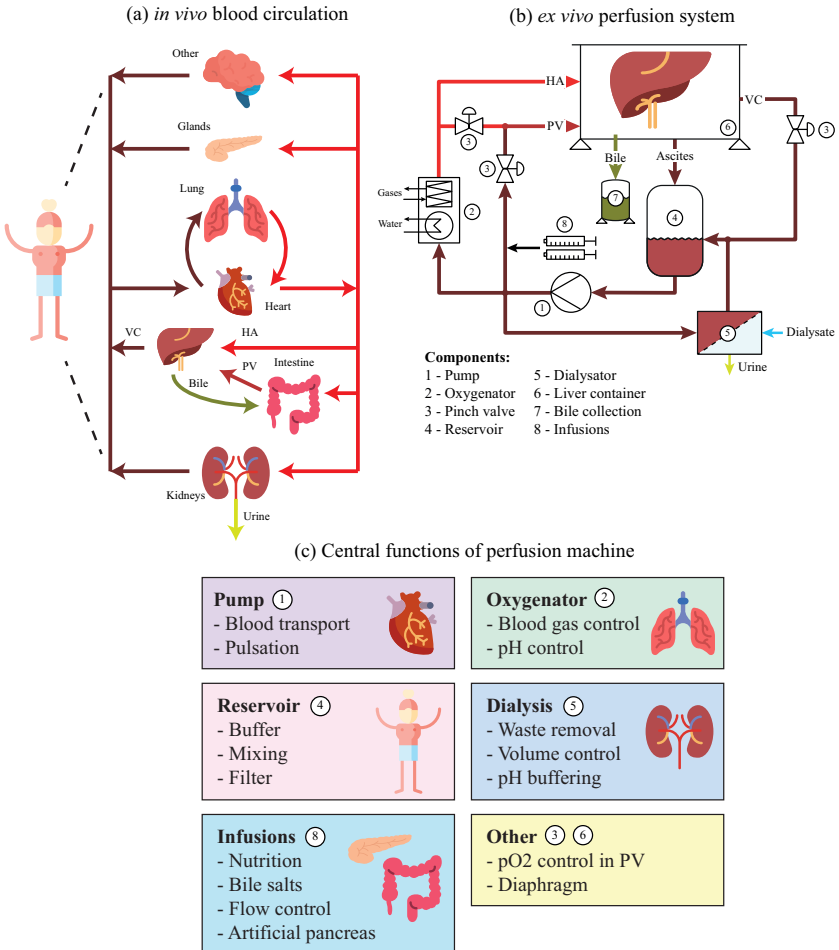
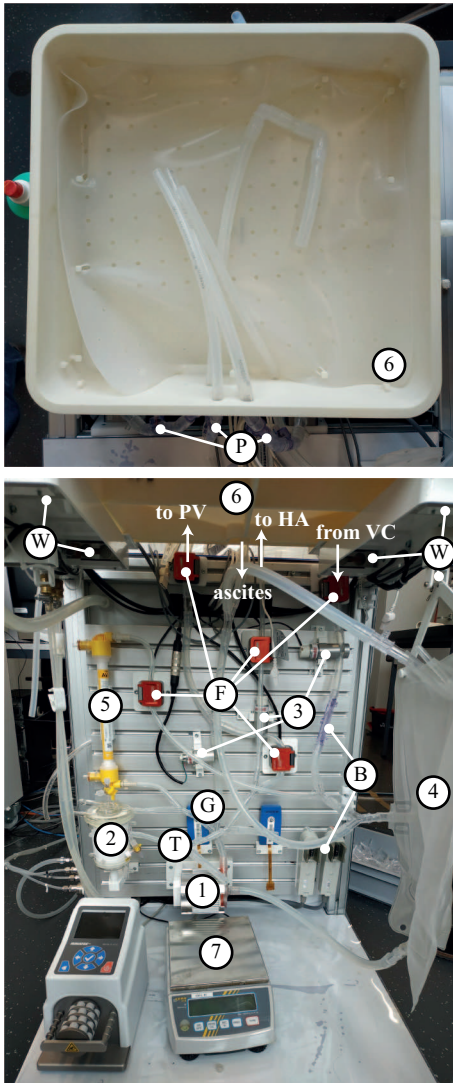


**Figure 3.1:** Simplified illustration of the *in vivo* blood circulatory system (a) and the developed *ex vivo* perfusion system (b). (c) Analogies of the core functions of the *in vivo* system listed with the components and their respective function in the *ex vivo* perfusion system.



**Sensors:**  
 P - Pressure  
 F - Flow  
 T - Temperature  
 B - Blood gas analysis  
 W - Weight  
 G - Glucose

**Components:**  
 1 - Pump  
 2 - Oxygenator  
 3 - Pinch valve  
 4 - Reservoir  
 5 - Dialysator  
 6 - Liver container  
 7 - Bile collection

**Figure 3.2:** Image of the perfusion loop and the liver container with the main components similar to Figure 3.1 indicated.



**Figure 3.3:** Image of the entire machine with liver container, perfusion loop, electronics & control system, Terumo CDI500 and infusion pumps highlighted.

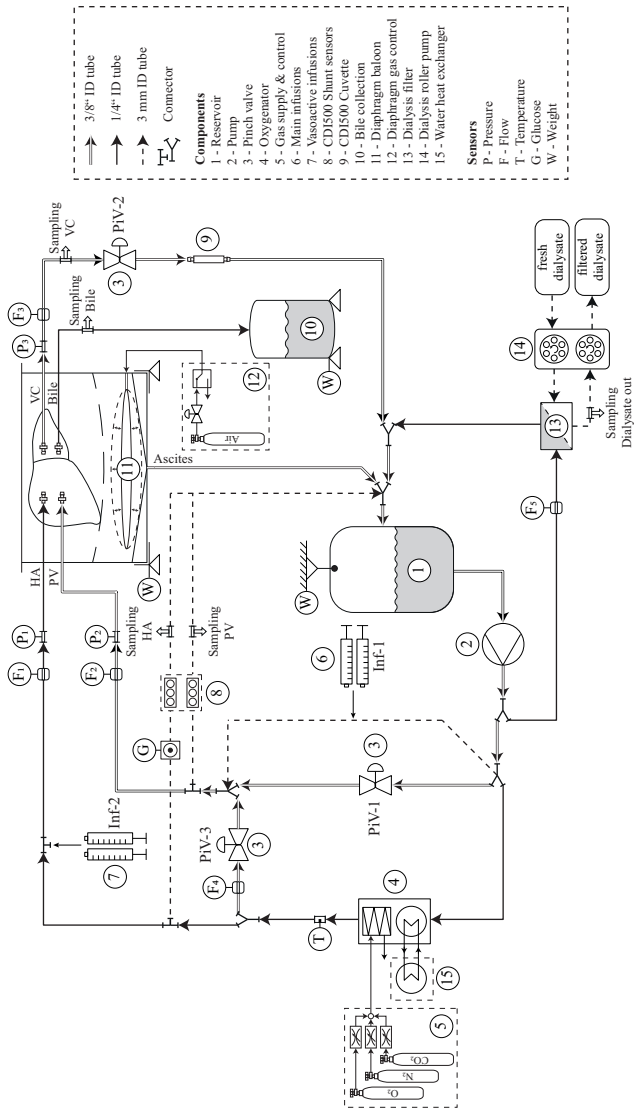


Figure 3.4: Detailed technical scheme of perfusion system.

shown. The system directly mimics central body organs such as the heart, the lung, and the kidneys via a pump, an oxygenator and a dialysis system, respectively. Further integral *in vivo* functions such as nutrition uptake and bile salt recirculation by the intestine, hormonal flow control and pancreatic hormone control are also replicated by various infusions.

## 3.2 Technical details

The system is implemented on a dSpace Microlabbox. In Appendix A.1, an overview of the integrated disposable components, the reusable hardware and the electronic components is listed. The software is programmed in Matlab Simulink which is then compiled and run on the Microlabbox.

## 3.3 Fluiddynamic setup & control

Starting in the heart of the system, the pump provides the necessary means for blood transportation. Given the unique nature of the dual hepatic blood supply, the system was developed to provide physiological pressure and flow conditions at the two liver inlets, hepatic artery (HA) and portal vein (PV). Further, as the PV originates from the intestine, its oxygenation is not at arterial level but already partially deoxygenated. This also had to be considered in the functionality of the machine. With the incentive of minimizing the number of components in contact with the blood, thus minimizing haemolysis and costs, a system with one pump and two pinch valves was designed. These three actuators control either flow or pressure at the HA and PV (see section 3.3.1) and, in combination with the oxygenator, provide physiological oxygen levels in the PV (see section 3.3.1). A pinch valve in the line from the vena cava to the reservoir allows to control the pressure in the vena cava (see section 3.3.3). In addition to the mechanical flow control by the pump and the pinch valves, a biological flow control is also integrated by means of closed-loop infusion of vasoactive substances (see section 3.3.4).



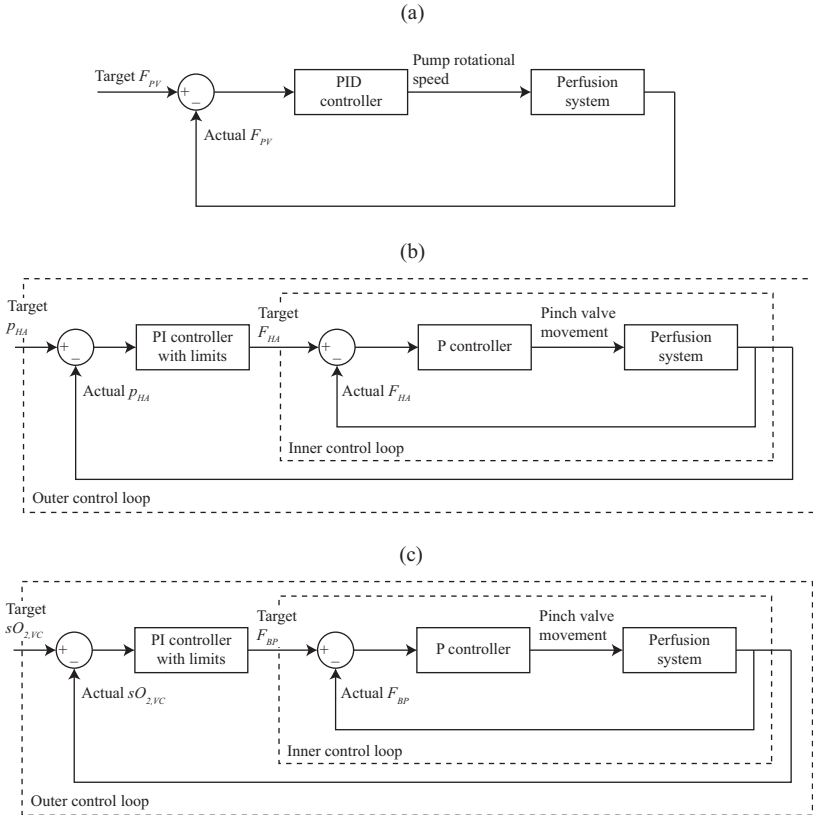


**Figure 3.5:** Control systems of (a) pump, (b) "PV pinch valve" and (c) "bypass pinch valve" controller the basic perfusion control.

### 3.3.1 Basic perfusion

A single pump (Thoratec Centrimag) is used for blood transport. The pump head is bearingless and levitated and driven totally magnetically. This reduces the hemolysis induced by the blood pump and renders it especially suitable for long-term perfusion applications<sup>106</sup>. Pinch valves (Resolution Air, MPPV-8) are used to clamp the tubing, thereby inducing a pressure drop and allowing to control the flow or pressure in those. One pinch valve (PiV-1 in figure 3.4) in the branch from the pump to the PV, from here on referred to as "PV pinch valve", induces a pressure drop, thereby allowing to adjust the flow ratio from the HA to the PV. A second pinch valve (PiV-3 in figure 3.4) is positioned in the line which branches after the oxygenator leading to the PV and is from here on referred to as "bypass pinch valve". This pinch valve allows to control the flow in the bypass (BP) from the HA branch to the PV. Point of this bypass is to elevate the oxygen content of the PV to physiological levels ( $sO_{2,PV} \approx 75 - 85\%$ ). Mixing arterial, oxygen-rich blood from the HA ( $sO_{2,HA} \approx 90 - 100\%$ ) with venous, oxygen-depleted blood from the vein ( $sO_{2,VC} \approx 60 - 70\%$ ) allows to reach any desired concentration in between the two. This leads to a system of three actuators (one pump and two pinch valves) controlling three target flows ( $F_{PV}$ ,  $F_{HA}$ ,  $F_{BP}$ ).

The control system for this is realized as three independent single-input single-output (SISO) systems. Figure 3.5 (a) to (c) give an overview of the three SISO systems. The pump controller (Figure 3.5 (a)) is a PID-controller, controlling the pump rotational speed depending on the PV flow error. Both the pinch valve controllers ((Figure 3.5 (b) and (c)) are cascaded with a PI and a P controller. The inner control controls the steps of the stepper motor to move the pinch valve position depending on the desired flow of the respective pinch valve. In the case of the "PV pinch valve", the flow in the HA is the target of the inner control loop. The outer control loop targets the HA pressure and defines the setpoint of the inner loop. Reason for cascading the two loops is to maintain a target pressure in the HA while keeping the HA flow in a desired range. In normal operation, the target pressure is the mean arterial pressure (MAP) of 65 mmHg with bounds for the flow between 0 and 0.6 L/min. In the case of the "bypass pinch valve", the inner control loop maintains a target bypass flow rate while controlling the pinch valve position by means of

a P controller. The outer control loop targets the oxygen saturation in the VC by varying the BP flow rate setpoint. The explanation for this control strategy is given in section 3.4.2.

### 3.3.2 Pulsation

In addition to its function of basic blood transport, the blood pump is operated in a pulsatile manner, mimicking the blood pulse pressure of the HA closely to the *in vivo* case. There is an ongoing debate whether or not a perfusion pump should be operated in a pulsatile or non-pulsatile manner. On the one hand, some studies have reported beneficial performance of high-risk patients of cardiopulmonary bypass when the perfusion pump was operated in a pulsatile manner<sup>107,108</sup> and other studies have shown such results during kidney perfusion<sup>109</sup>. On the other hand, others have reported no difference between pulsatile and non-pulsatile operation<sup>110</sup>. A recent review concluded on the benefit of pulsatile pump operation during long-term perfusion<sup>111</sup>. For these reasons, experiments were conducted comparing the two operation modes, whose results are described in section 4. In this section, the implementation of the pulsation is described.

In order to realize a pulsation in the HA, the rotational speed of the pump needs to be varied to induce the desired pressure pulse shape. The set point of the PV flow is multiplied by a factor  $K(t)$ , representing the desired pulse shape, thereby yielding a pulsation in the rotational speed of the pump and consequent pulsation of the pressure.

$$F_{PV,SP,puls} = F_{PV,SP} \cdot (1 + K(t)) \quad (3.1)$$

The shape of the implemented pressure pulse is given by superposition of two sine waves, as shown in figure 3.6. This shape was chosen to closely represent the *in vivo* shape<sup>112</sup>. The formula to obtain the specified shape is given by the following relation.

$$K(t) = a_1 \cdot \sin\left(\frac{2\pi}{T_1} \cdot t + \phi_1\right) - a_2 \cdot \sin\left(\frac{2\pi}{T_2} \cdot t + \phi_2\right) \quad (3.2)$$

The following parameters are defined, noting that the parameters of the second sine wave are in relation to the first:  $a_2 = 0.5 \cdot a_1$ ,  $T_2 = 0.5 \cdot T_1$ ,

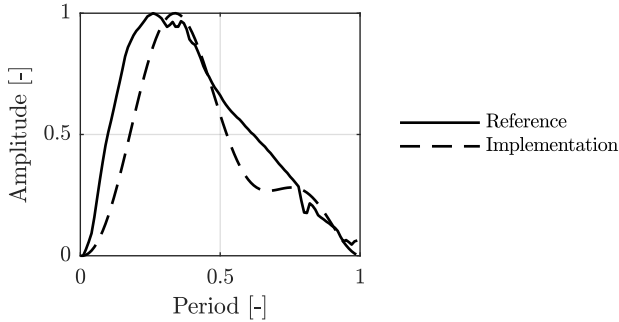


**Figure 3.6:** Comparison of pressure pulse shape in the machine as compared to literature data in abdominal aorta (Reference<sup>112</sup>).

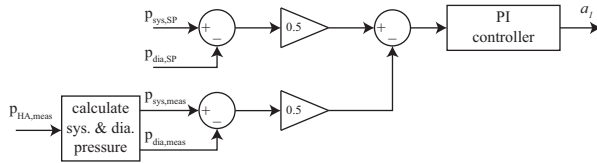


**Figure 3.7:** Illustration of the pressure pulse control.

$\phi_1 = 0$  and  $\phi_2 = 0.75 \cdot \pi$ . The base period  $T_1$  is defined according to the desired pulse frequency, which usually is 60 beats per minute, yielding  $T_1 = 1$  s. The base amplitude  $a_1$  is obtained from a feedback controller, continuously adjusting the amplitude to meet the desired pulse pressure levels. Here, the systolic  $p_{sys}$  and diastolic  $p_{dia}$  pressure are continuously determined from the pressure measurement by calculating the maximal and minimal pressure, respectively, averaged over the last 10 seconds. The difference between the measured systolic and diastolic pressure divided by two is compared to the targeted systolic and diastolic pressure and fed to a PI controller, yield the amplitude of the desired pulse wave, as illustrated in figure 3.7. Usually, systolic and diastolic pressure levels of 80 mmHg and 50 mmHg are targeted. Figure 3.8 shows the rotational speed of the pump and the resulting pressure in the HA, illustrating the function of the pulsation.

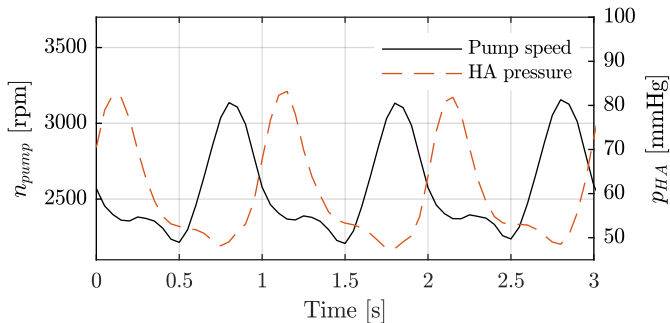


**Figure 3.8:** Figure of pump rotational speed and HA pressure.

### 3.3.3 VC pressure

As described in section 2.2.1, a liver perfusion system can be described as open or closed, depending on the cannulation of the VC. There is an ongoing debate about whether or not to close the perfusion circuit<sup>113</sup>. On the one hand, an open system is easier to implement as there is no need to control the pressure in the outlet line with the blood simply flowing out of the liver into ambient pressure. On the other hand, the additional contact of blood with air in an open system induces further hemolysis which is sought to be minimized during long-term perfusion<sup>114</sup>. However, closing the system requires to either control the pressure at the outlet or poses the risk of veins collapsing, resulting in congestion of the liver sinusoids<sup>60</sup>. Therefore, a closed system was developed where the VC pressure is continuously controlled and adjusted depending on the needs.

In order to control the pressure at the liver outlet, a pinch valve (PiV-2 in figure 3.4) is positioned in the line from the VC to the reservoir. The reservoir, which is at atmospheric pressure level, is positioned approximately 50 cm below the liver. Therefore, in the case of communicating vessels, which is the case if the tubing from the VC to the reservoir is filled with blood, subatmospheric pressure levels would be present directly at the VC if no additional pressure drop was present. The pinch valve in the line allows to induce such an additional pressure drop, thereby allowing the control the outlet pressure at the VC. This is realized by means of a

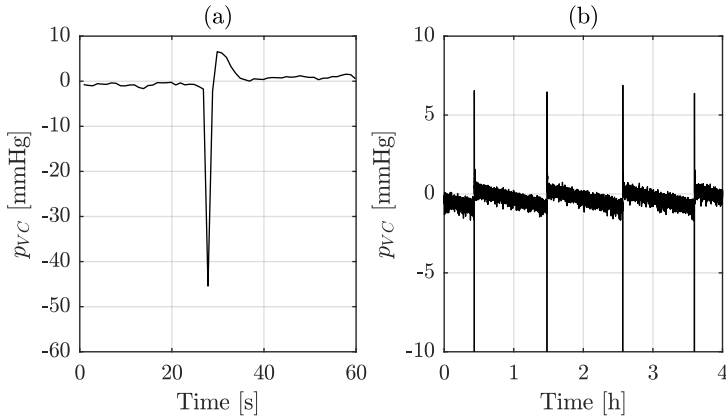


**Figure 3.9:** VC pressure control with detection of collapsing veins. (a) close-up of pressure oscillation which is detected. (b) repeated instances of pressure oscillations approximately every hour.

P controller, similar to the inner control loop of "PV pinch valve" control in figure 3.5 (b). The VC pressure is continuously measured  $p_{VC,meas}$  and compared to the targeted value  $p_{VC,SP}$ . Additionally,  $p_{VC,SP}$  is continuously reduced until a collapsing of the veins is observed and consequently elevated. Reason for this feature is to permanently provide the close to atmospheric pressure at the VC to reduce the resistance for liver outflow and risk for congestion. The VC pressure level has been shown to have a strong influence on HA flow resistance<sup>115</sup>, which is described in more detail in section 6. Kinking of the cannulas or tubes could lead to wrong pressure measurements at the VC and suggest lower pressure levels than which are actually present. By always seeking the collapsing pressure level, one can ensure close to atmospheric pressure at the VC. The collapsing veins are detected by monitoring the pressure in the VC. Upon collapsing of the vessel, there is a sudden decrease in the pressure because there is no outflow from the liver and the communicating vessel to the reservoir creates a suction pressure (see figure 3.9 (a)). The  $p_{VC,SP}$  is continuously reduced by 1 mmHg/h and subsequently elevated

by 1 mmHg upon collapsing of the vessel. Figure 3.9 (b) shows the course of VC pressure during multiple hours, illustrating the collapsing veins at slight subatmospheric pressure every hour.

### 3.3.4 Medicamentous flow control

Adequate perfusion conditions in terms of flow delivered to and pressure present at the liver are an important topic during *ex vivo* liver perfusion<sup>86</sup>. The hepatic circulation is a complex system which is influenced by various extrinsic factors such as hormones, oxygen supply and nutrients and intrinsic factors such as arterial autoregulation and the hepatic arterial buffer response<sup>39</sup>. The flow resistance in the PV is constant and not controlled by the liver and only changes with long-term effects such as liver cirrhosis leading to portal hypertension<sup>116</sup>. The HA, on the other hand, is very variable in its resistance and all of the above mentioned intrinsic and extrinsic factors can theoretically be utilized *ex vivo* to a certain extent to manipulate the hepatic arterial resistance. A big challenge during *ex vivo* liver perfusion remains to maintain physiological perfusion conditions and counteract vasospasm caused by static cold storage prior to perfusion<sup>86</sup>. Therefore, vasodilators are applied to reduce the vascular tension of the HA and provide sufficient perfusate supply to the liver. The use of vasodilators during *ex vivo* liver perfusion was perviously shown to be beneficial for the liver quality<sup>95</sup>. The implementation of these vasodilators is described in this section.

Nitroprussiat (Nitroprussiat Fides, Rottapharm) is infused on demand into the HA branch (⑦ in figure 3.4) to maintain adequate perfusion conditions. Medical infusion pumps (Arcomed syramed  $\mu$ SP6000 and Arcomed volumed  $\mu$ VP7000) are integrated and can be controlled by the system. These allow to infuse at any rate between 0.01 and 999 mL/h at increments of 0.01 mL/h. As the pressure in the HA  $p_{HA}$  is controlled to a constant mean level by the control system described in section 3.3.1, the flow in the HA ( $F_{HA}$ ) varies, depending on the HA flow resistance. Therefore,  $F_{HA}$  is set as the target for the medicamentous flow control. Based on continuous measurements of  $F_{HA}$ , the infusion rate of Nitroprussiat is adjusted by means of a PI controller. Thereby, a lower limit for  $F_{HA}$  is defined below which the infusion of Nitroprussiat is increased. In figure 3.10 (a), an exemplary infusion of Nitroprussiat is shown with

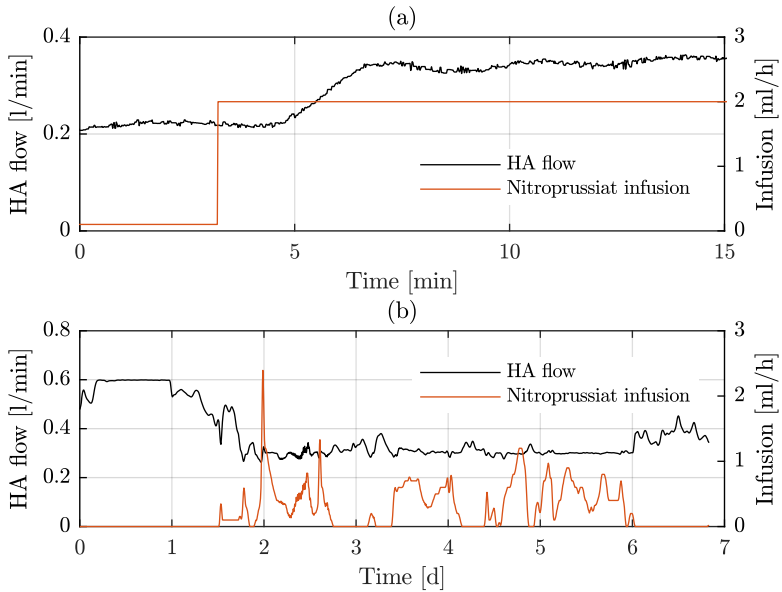


**Figure 3.10:** (a) Exemplary response of  $F_{HA}$  upon a step change of Nitroprussiat infusion. (b) Exemplary course of  $F_{HA}$  and Nitroprussiat infusion during the period of seven day perfusion.

consequent response of  $F_{HA}$ . Figure 3.10 (b) shows the infusion during the course of multiple days of perfusion. One can clearly see the responsiveness of the HA and the ability to maintain the lower limit of  $F_{HA}$ .



## 3.4 Blood physiology

### 3.4.1 Temperature

Temperature is an elementary factor to influence metabolism. Different perfusion technologies are distinguished in their respective perfusate temperature (see figure 1.2) and allows control the metabolic state of the liver. The presented system perfuses organs at normothermic temperatures (34-37°C) and therefore requires a control to maintain adequate perfusate temperatures.

The temperature of the blood is measured by means of an NTC temperature sensor (MBD 2.2K3MBD1, TE Connectivity). This allows to measure the temperature directly in the blood stream. The sensor (Ⓣ in figure 3.4) is positioned directly behind the oxygenator which, next to its function as a gas exchanger, is supplied with water from a heat exchanger (Julabo 461-0606) to control the temperature of the blood. A PI controller is applied which varies the water temperature of the heat exchanger and maintains a target blood temperature. With this configuration, the temperature of the perfusate can be controlled to any level in the desired range between almost 0°C and up to 37°C.

### 3.4.2 Blood gases

*In vivo*, blood gases are closely regulated by the lungs. In particular, oxygen and carbon dioxide concentrations are controlled by respiratory reactions of the lung. Both gases are dissolved in the blood and measured in terms of partial pressures  $pO_2$  and  $pCO_2$ . Oxygen binds to hemoglobin, which increases the amount of oxygen that can be transported in the blood as compared to pure water. Dissolved carbon dioxide is in equilibrium with carbonic acid, leading to an inverse relationship between carbon dioxide concentration in the blood and  $pH$ . An increase of  $pCO_2$  results in a reduction of  $pH$  and vice versa. Therefore, chemosensors in the body react to  $pO_2$ ,  $pCO_2$  and  $pH$ , whereby the response to changes in  $pCO_2$  and  $pH$  is more pronounced as compared to  $pO_2$ . Upon a reduction of  $pO_2$ , the body reacts by increasing respiration to supply more oxygen. Similarly, elevated  $pCO_2$  or reduced  $pH$  levels lead to an enhanced respiration, washing out more  $CO_2$  from the blood.<sup>52</sup>

Although it is obvious that avoidance of prolonged hypoxia is essential during *ex vivo* perfusion, the effects of hyperoxia are less distinct. Studies concerning the consequence of hyperoxia concluded on post-transplantation detrimental effects, such as vasoplegia and posttransplant cholangiopathy<sup>69</sup>.

The *ex vivo* perfusion system controls the blood gases in a analogue way to the *in vivo* respiratory mechanism. A sensor, which continuously measures  $pO_2$  and  $pCO_2$  in the blood (Terumo CDI500 Shunt Sensor), is integrated in a bypass from the HA branch to the venous branch (see ⑧ in figure 3.4). By means of three independent gas supplies (see ⑤ in figure 3.4) and gas flow controller (Bronkhorst), oxygen, nitrogen and carbon dioxide are lead to the oxygenator (Medos hilite 2400 LT). The flow of the three gases can be individually controlled in the range from 0.01 NL/min to 1 NL/min ( $\dot{V}_{O_2}$  and  $\dot{V}_{N_2}$ ) and 0.002 NL/min to 0.2 NL/min ( $\dot{V}_{CO_2}$ ).

In normal operation, no  $CO_2$  is supplied as the liver produces  $CO_2$  and it needs to be removed from the system. During initiation of the system when no liver is connected and in times when the liver barely consumes oxygen, e.g. in the first few minutes of perfusion, additional  $CO_2$  needs to be supplied to maintain physiological  $pCO_2$  levels in the blood.

Oxygen and nitrogen gas supplies are continuously feedback controlled during perfusion. Thereby, the system controls the fraction of oxygen  $FiO_2$  in the supplied gas and the total gas flow rate  $\dot{V}_{gas}$ . The control system is designed in a similar fashion as has been described for blood gas control during extracorporeal heart lung support systems, e.g. during heart or lung transplants<sup>54</sup>. Figure 3.11 depicts the control system for the blood gas control implemented. In case of oxygen (figure 3.11 (a)), a PI controller targets the desired  $pO_2$  level and adjusts the  $FiO_2$  in the gas flow. In case of nitrogen (figure 3.11 (b)), a control cascade is applied. Thereby, the inner loop controls  $pCO_2$  to a desired range by varying  $\dot{V}_{Gas}$ . The outer loop controls  $pH$  to a target level by allowing the setpoint for  $pCO_2$  to alter in the range from 4.5 to 6.5 kPa, to remain in a physiological range. The following two relations describe how the individual gas flows of oxygen and nitrogen are calculated.

$$\begin{aligned}\dot{V}_{O_2} &= FiO_2 \cdot \dot{V}_{gas} \\ \dot{V}_{N_2} &= (1 - FiO_2) \cdot \dot{V}_{gas} - \dot{V}_{CO_2}\end{aligned}\tag{3.3}$$

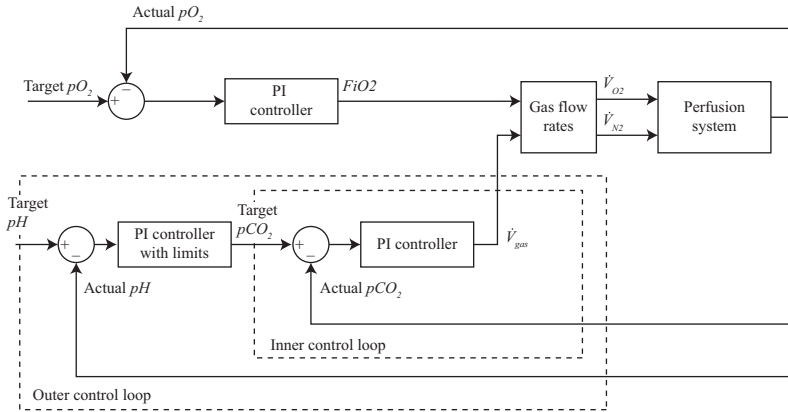


**Figure 3.11:** Control system to control gas flow rates of oxygen and nitrogen to maintain target  $pO_2$  and  $pH$ .

As mentioned above,  $\dot{V}_{CO_2}$  is manually adjusted and usually zero during normal perfusion.

By means of these controllers,  $pO_2$  is maintained at a desired level, usually between 10 and 12 kPa and  $pH$  is targeted to remain at 7.4. Figure 3.12 shows the levels of  $pO_2$  (a),  $pCO_2$  (b) and  $pH$  (c) during the course of seven days of perfusion of an exemplary perfusion experiment.

### PV oxygen saturation

*In vivo*, the PV originates from the intestinal organs and leads to the liver. Part of the oxygen is already consumed and, therefore, the oxygen saturation is lower as compared to the HA. Most available systems provide arterial oxygenation in the PV (see chapter 2.2.1). However, in order to have a system close to physiology, the PV oxygen saturation was controlled to physiologic levels. Further, studies have shown the importance of hypoxia during liver regeneration<sup>117,118</sup>. With the goal of achieving *ex vivo* liver regeneration on the perfusion machine, the ability to control the oxygen content of the PV was mandatory to be able to induce hypoxia.

From a technical point of view, a lower oxygen content in the PV can be

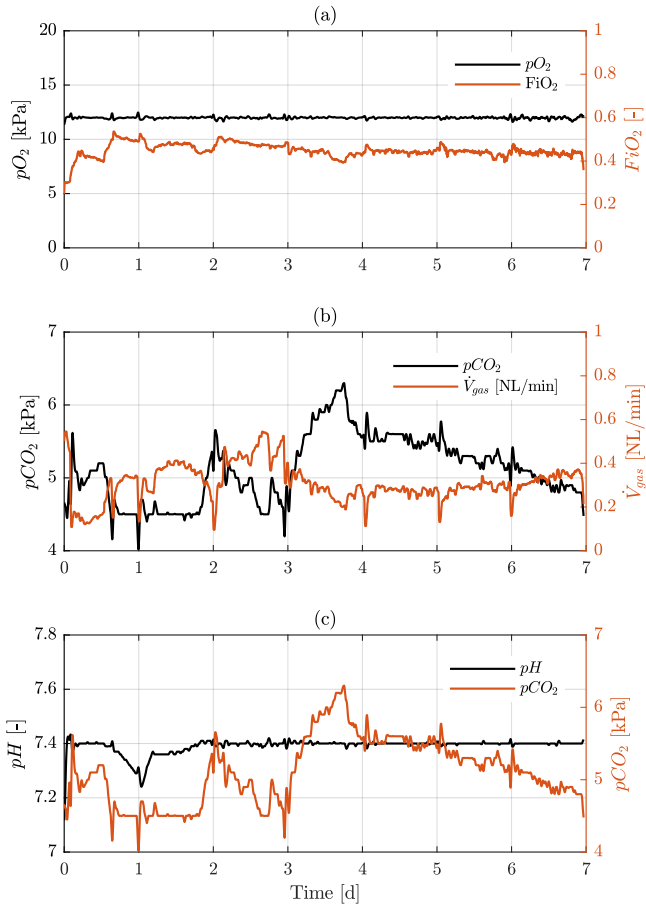


**Figure 3.12:** Exemplary experiment illustrating (a)  $FiO_2$  controller to maintain  $pO_2$  at 12 kPa. (b) Inner loop of  $V_{gas}$  controller maintaining  $pCO_2$  and (c) outer control loop to vary  $pCO_2$  setpoint, targeting  $pH$  of 7.4.

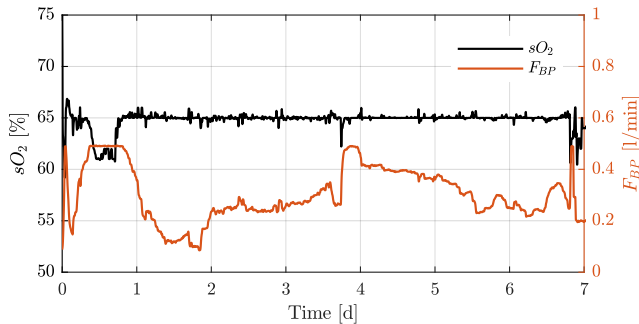


**Figure 3.13:** Control of VC  $sO_2$  to 65% during seven days of perfusion by varying bypass flow rate  $F_{BP}$ , mixing arterial and venous blood.

realized in two ways. Either a second oxygenator for the PV is installed with an individual gas supply to control the oxygen content directly or arterial blood is mixed with venous blood to provide physiologic portal blood<sup>60</sup>. In this case, the oxygen content of the PV was controlled by means of mixing arterial blood with venous oxygen depleted blood. On the one hand, this reduces the costs for each disposable set because a second oxygenator is not required and, also, there is no need for additional gas flow controllers. A single pinch valve in combination with a flow sensor is sufficient for this solution. On the other hand, an oxygenator provides a large surface area which increases the risk of hemolysis which is sought to be minimized during *ex vivo* perfusion. Therefore, a bypass from the HA branch to the PV branch was integrated. A description of the controllers of the bypass is given in section 3.3.1 and illustrated in figure 3.5 (c).

Instead of targeting a desired PV saturation level, the controller maintains the desired VC saturation to 65%. By controlling the VC oxygen saturation, a constant oxygen content in the cells can be maintained. Upon changing oxygen demand, the liver can extract more or less oxygen from the blood<sup>42</sup>. The oxygen saturation in the VC is measured with a cuvette (Terumo CDI500 Cuvette, ⑨ in figure 3.4).

**Table 3.1:** Components and its respective concentration in the dialysate solution.

Component	Concentration	
Sodium $\text{Na}^+$	140	mmol/L
Calcium $\text{Ca}^{2+}$	1.5	mmol/L
Potassium $\text{K}^+$	4	mmol/L
Magnesium $\text{Mg}^{2+}$	0.5	mmol/L
Chlorine $\text{Cl}^-$	109	mmol/L
Bicarbonates $\text{HCO}_3^-$	35	mmol/L
Glucose	5.5	mmol/L
pH	$\approx 7.2$	

### 3.4.3 Dialysis

Up to this point, there is no controllable mean to remove components from the system. A major limitation of many *ex vivo* perfusion systems remains the inability to remove metabolic waste products<sup>8</sup>. *In vivo*, the kidneys function as a mean to remove metabolic waste products, ensure physiological electrolyte balance and maintain blood pH balance. These functions can be replicated *ex vivo* by means of a dialysis system. Most existing perfusion systems (see table 2.1) pass on the integration of a dialysis, as their purpose usually lies on short-term perfusion. However, in order to maintain physiological perfusate conditions during prolonged *ex vivo* perfusion, a dialysis is indispensable.

In this context, a dialysis system was integrated into the perfusion loop. The dialysis unit offers a way to remove components from the perfusion circuit. Its main component is the dialysis filter (Fresenius, Ultraflux AV paed) where a physiological dialysate solution (Fresenius multiBIC, components see table 3.1) flows on the one side and blood flows on the other side of the membrane in a counter current manner (see figure 3.14). The blood equilibrates with the dialysate solution, thereby keeping electrolytes and bicarbonates at a physiological level and removing metabolic waste products. A roller pump (Ismatec Reglo ICC) thereby independently defines the in- and outflow rate of dialysate solution to and from the dialysis filter. Typically, the dialysate flow rate

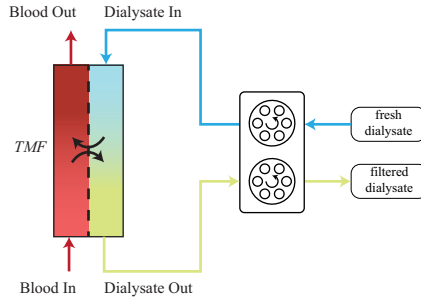


**Figure 3.14:** Illustration of integrated dialysis system consisting of the dialysis filter and a roller pump. Fresh dialysate solution is delivered to the filter and the filtered dialysate is removed.

to the filter is maintained at 200 mL/h.

In addition to its cleaning function of the blood, the exact amount of fluid exchange through the filter can be defined by defining the difference in flow rate of the dialysate solution into and out of the filter, i.e. the transmembrane flow ( $TMF$ ). This gives a manner to control the fluid content of the blood, i.e. the blood plasma, and, hence, control the haematocrit level of the blood. The hematocrit can be kept at a constant level throughout the perfusion duration. The hematocrit control is implemented by means of a PI controller, targeting a desired hematocrit level and varying the  $TMF$  by manipulating the dialysate outflow rate in a range from -50 to 50 mL/h. The hematocrit of the perfusate is continuously measured by means of the cuvette (Terumo CDI500 Cuvette, ⑨ in figure 3.4). Figure 3.15 shows the hematocrit level during seven days of perfusion with the respective dialysate flow rates.

### 3.4.4 Glucose

Physiological blood glucose levels are of utmost importance for successful long-term liver perfusion and eventual *ex vivo* liver regeneration. In the perfusion system, a unique glucose sensor is integrated, which is capable of continuously measuring the blood glucose concentration. Based on this sensor, the control system injects glucagon and insulin interchangeably,

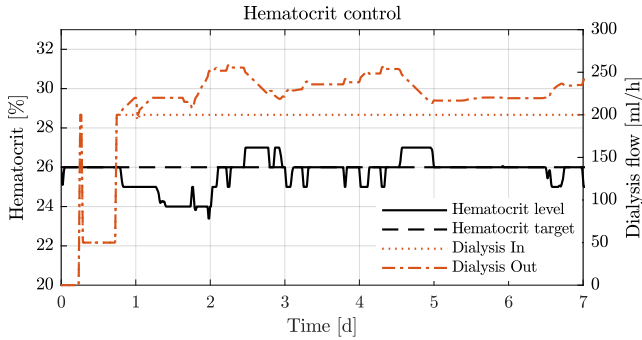


**Figure 3.15:** Hematocrit control during one experiment. Hematocrit was targeted to 26% and dialysate outflow rate controlled to reach the target. Dialysis was primed after approximately 6 h of perfusion and started after 20 h by increasing the dialysate flow rate to 200 mL/h.

similar to the body during fasting and feeding, respectively. In both cases, insulin and glucagon, proportional controllers are implemented, thereby only reacting if the threshold is surpassed. Due to the relevance of the glucose control, a separate chapter was dedicated to this topic. In chapter 5, more details about the glucose sensor and the respective control are elaborated.

### 3.4.5 Infusions

Table 3.2 and table 3.3 summarize the bolus infusions at perfusion start and the continuous infusions during the perfusion, respectively. These were obtained after an extensive literature review<sup>18</sup>. All of these medications are infused into the PV (⑥ in figure 3.4).

Prior to perfusion start, steroids (Solu-Medrol), an antibiotic (Tazobactam) and albumin are supplemented to the perfusate. Albumin is supplied to provide physiological plasma albumin levels and, hence, ensure a physiologic oncotic pressure.

During the perfusion, various infusions are supplied in a continuous manner. Parental nutrition (Nutriflex Special 70/240, Upper bag) supplies



**Table 3.2:** Overview of bolus infusions at perfusion start.

Infusion	Description	Amount
Steroid	Solu-medrol	500 mg
Antibiotic	Tazobactam	2.25 g
Albumin	Human Albumin 20%	200 mL

**Table 3.3:** Overview of continuous infusions during perfusion.

Infusion	Description	Concentration	Rate
<i>Continuous</i>			
Parental nutrition	Nutriflex Special 70/240	Upper Bag	12 mL/h
Bile salts	Taurocholic acid	0.071 g/mL	2 mL/h
Heparin	Heparin-NA (B.Braun Medical AG)	1000 U/mL	0-2 mL/h
Steroid	Solu-medrol	20.83 mg/mL	1 mL/h
Antibiotic	Tazobactam	0.135 g/mL	1 mL/h
<i>Feedback controlled</i>			
Insulin	Actrapid (Novo Nordisk Pharma, Human insulin)	450 U/L	autom.
Glucagon	GlucaGen (Novo Nordisk Pharma, Glucagon)	11 U/L	autom.
Vasodilator	Nitroprussiat Fides, Rottapharm	1 g/L	autom.
Vasoconstrictor	Phenylephrine (Neo-Synephrine HCL, Ospedalia AG)	0.4 g/L	autom.

mainly amino acids to provide basic ingredients for and support liver metabolism. Bile salts (Taurocholic acid) are supplied to support bile production. *In vivo*, 95% of bile salts are recycled by the intestinal tract and returned to the blood stream. As there is no such mechanism in the *ex vivo* system, the bile salts are supplemented. Heparin is supplied to avoid coagulation of the blood which occurs in any extracorporeal blood circulation system. Steroids (Solu-medrol) are supplied due to their anti-inflammatory effect and bile production stimulation, and antibiotics (Tazobactam) to reduce the chance of bacterial infection in the *ex vivo* system. All of these infusions are given at a basal rate. In addition, certain hormones such as insulin or glucagon are supplied in a feedback controlled manner, depending on the liver's metabolism. However, these are described in another chapter of this thesis.

## 3.5 Liver storage

### 3.5.1 Container

In the *ex vivo* perfusion system, the liver is placed inside of a container. Figure 3.16 shows the drawing of one of these containers, from different perspectives: (a) top view, (b) front view, (c) side view with section, and (d) perspective view. Different versions of the liver container were produced where the basic design and concept is very similar and the exact measures vary in a certain range, as described in the figure caption.

The basic design of the liver container is the following. A row of hooks is implemented around the inside of the container on which a silicone mat is hung and spans across the inside of the container. The liver is put on this mat. Four holes are integrated on the front side of the container where the silicone tubes for HA, PV, VC and bile collection are lead through. These can also be seen in figures 3.2 and 3.3. At the bottom of the container is a funnel where ascites fluid is collected and also returned to the blood circulation. In the center of the container, right below the hooks of the mat, is an adapter where the balloon, simulating the diaphragm movement, is connected to. This is described in more detail in section 3.5.2. A lid covers the container to reduce exchange of air and contaminants with the surrounding environment. The entire box as

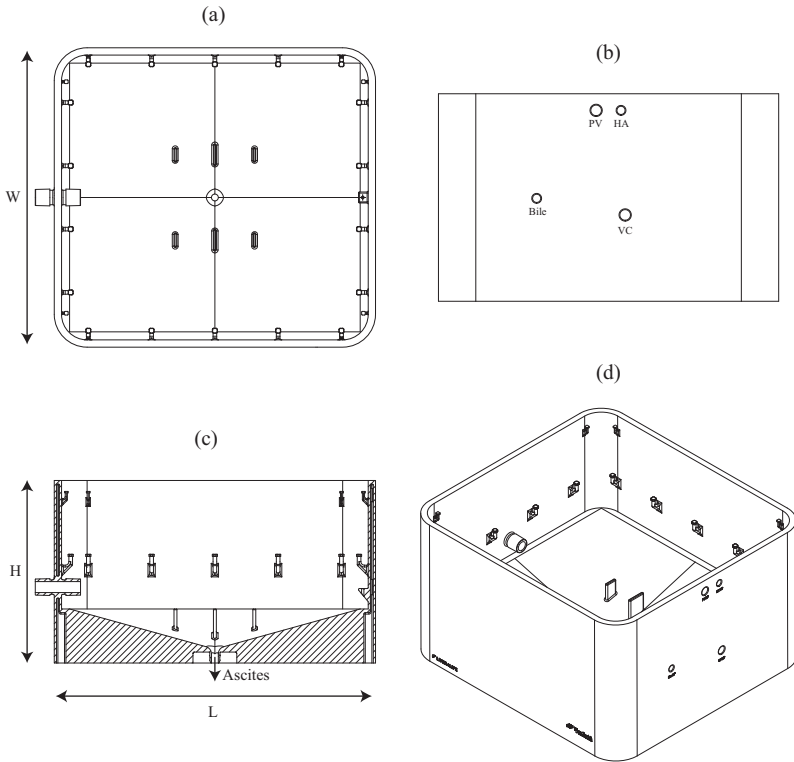


**Figure 3.16:** Drawing of one of the liver containers with approximate measures. (a) top view, (b) front view, (c) side view with section, (d) perspective view. Different versions of liver container were designed. Basic design and concept is very similar, the exact measures vary in a certain range. Length  $L \approx 400$  to  $440$  mm, height  $H \approx 185$  to  $265$  mm, width  $W \approx 380$  to  $410$  mm. The drawings are missing the balloon for the movement, the mat on which the liver lays, the lid of the container, and the liver itself.

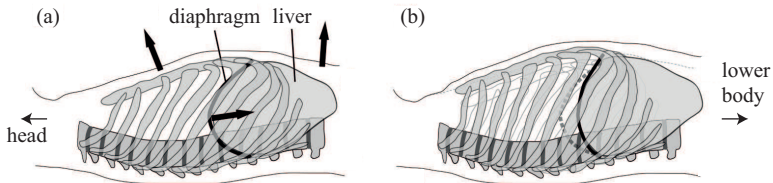


**Figure 3.17:** *In vivo* illustration of liver movement due to respiratory motion. (a) full exhalation position, arrows indicate movement of chest and diaphragm during inhalation. (b) full inhalation position. Image modified from Siebenthal<sup>119</sup>.

shown in figure 3.16 is 3D printed of polyamide (PA 2200) in one piece.

### 3.5.2 Movement

*In vivo*, the liver is positioned below the diaphragm. Through respiratory motion of the lung, it moves in a periodic manner. Figure 3.17 illustrates this *in vivo* movement of the liver where (a) shows the full exhalation position and (b) shows the full inhalation position, with the respective movement effect on the liver.

This movement is replicated *ex vivo* by means of a balloon, positioned below the liver (see figure 3.18). Figure 3.18 (a) illustrates the implementation of the diaphragm in the liver container. Pressurized air is used to inflate the balloon, pushing the center of the liver upwards. With a local, inhomogeneous uplifting of the liver, a massage effect is exerted on the liver. By means of a switching valve (12 in figure 3.4), the pressurized air is lead to and away from the balloon in a periodic manner. In combination with a pressure reduction valve, the inflation volume and frequency can be defined. Figure 3.18 (b) shows an image of the implemented balloon in the container.

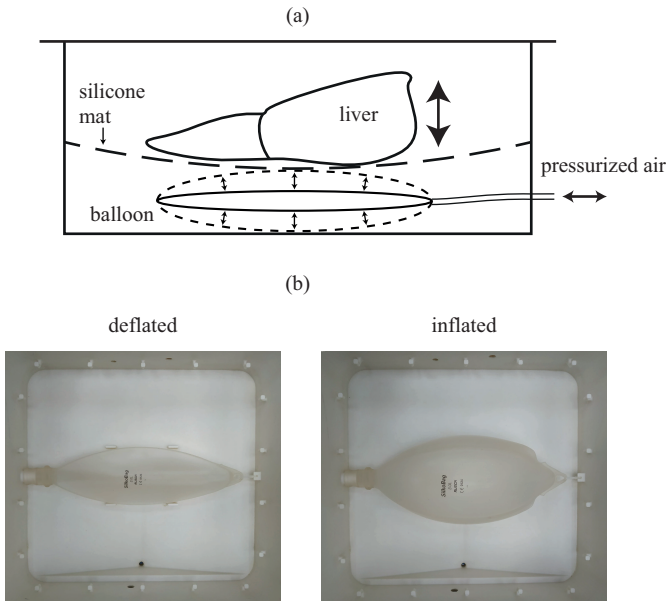


**Figure 3.18:** Illustration of diaphragm simulation. (a) conceptual drawing, (b) image of deflated (left) and inflated (right) balloon in the machine (view from top, mat and liver missing).

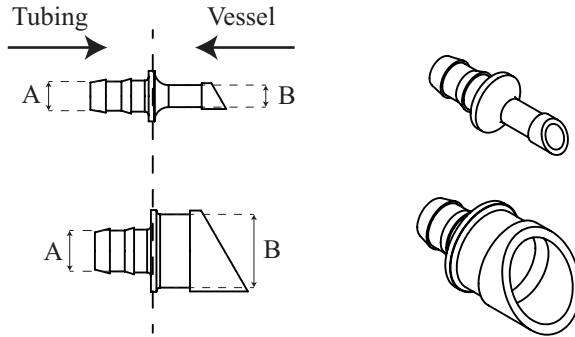


**Figure 3.19:** Drawing of vessel cannulas. Top row shows an example of a 1/4 inch cannula and bottom row of a 3/8 inch cannula. On the left side, the tubing is connected and the inner diameter (ID) of the tube is defined by A. On the right side, the vessel is sutured where the size of the vessel is defined by B.

## 3.6 Further

### 3.6.1 Liver cannulation

The liver vessels need to be connected to the tube set of the perfusion loop. For this purpose, custom cannulas were designed. Figure 3.19 shows two exemplary sets of cannulas which were applied in the loop. On the one side (left side of the cannulas in the figure), the tubes are connected to the cannula and on the right side, the vessels are connected. Thereby, the tubes are simply pushed onto the cannula as done with a standard connector piece and the vessels are sutured to the cannula. The cannulas are hollow in the inside, allowing the blood to freely pass from the tubing to the vessels.

The top row in figure 3.19 shows the smaller size where tubes with an inner diameter (ID) of 1/4 inch can be connected to. These are usually used for the cannulation of the HA and the bile duct. The bottom row shows the larger cannulas to be connected to a 3/8 inch tube which are usually applied for the PV and VC cannulation. The exact choice of

cannulas is always taken during the preparation of the liver when the size of the vessels is determined.

### 3.6.2 Bile mass measurement

As described in chapter 2.1.4, bile production is an important factor to evaluate the liver's function during *ex vivo* liver perfusion. Therefore, a continuous bile mass measurement was implemented into the system. In the current version, a bucket is placed on top of a scale (Kern PCB 10000) and the bile is continuously collected in this bucket. With the density of bile being approximately  $1 \text{ g/mL}^{120}$ , the mass is converted into a volume measurement, which is commonly reported in the literature.

### 3.6.3 Blood and box weight measurement

In order to determine the amount of blood in the system, the weight of the reservoir and the liver container is measured. As the tubes and all other components are always filled with blood and their volume doesn't change during the course of the perfusion, the weight of the container and the blood reservoir allows to calculate the mass of blood in the system. This was especially relevant for the analysis of the study about the hepatic arterial buffer response, which is described in chapter 6.

For this purpose, force sensors (Megatron KM200/50N), which can measure up to 50 N (approx. 5 kg) each, are implemented. In the case of the blood reservoir mass measurement (figure 3.20 (a)), a concept was developed where the blood reservoir is hung below the force sensor. The mounting was realized in a way that the blood reservoir could swing in all directions, resulting in no additional torque on the force sensor. In order to measure the mass of the liver container, the box was positioned on four individual plates, each sitting on top of a force sensor (see figure 3.20 (b)). By positioning the container on four individual plates, the force was induced locally on the force sensors, again avoiding additional torque which would tamper the force measurement.

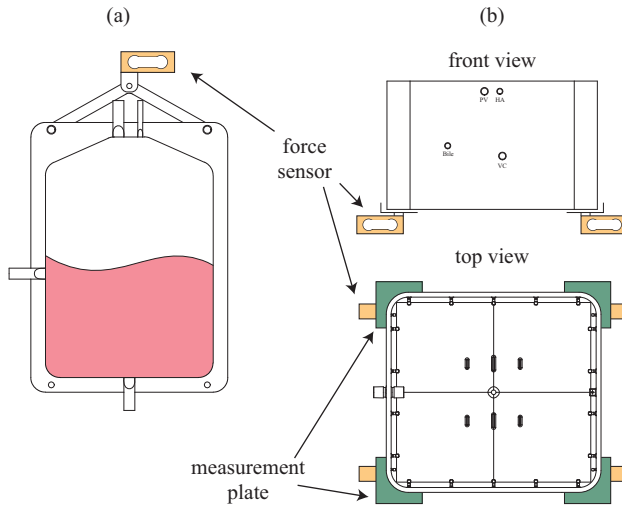


**Figure 3.20:** Illustration of (a) blood reservoir mass measurement and (b) liver container mass measurement. The force sensors are indicated in orange and the plates, where the liver container is resting on, are highlighted in green.



# Chapter 4

## Development of the perfusion system

In this chapter, the development process of the perfusion system is described. In the initial phase of the project, experiments were conducted with a commercially available machine (LiverAssist). A first laboratory prototype was then developed with the knowledge gained from those initial experiments. With the own prototype, experiments were conducted in a systematic manner and incremental changes were added to the system to improve the perfusion. In the following sections, these incremental steps are described and the individual effects on the perfusion shown and discussed. Finally, the quality of the liver is assessed and viability of liver for seven days *ex vivo* presented.

### 4.1 Experimental Procedure

#### 4.1.1 Liver procurement

All the experiments described in this chapter were conducted with pig livers. The livers were harvested from land race pigs in accordance with the Swiss Animal Protection Law and Ordinance. Laparotomy was performed under general anesthesia and sterile conditions. The livers were removed in standardized manner as described previously<sup>121</sup>. After removal from the pig, the livers were put on ice where they remained until connection to the perfusion machine. The age of the pigs was about six months and they weighed between 80 and 100 kg, with an average liver weight of 1.7 kg.

### 4.1.2 Blood collection

For the perfusion experiments, whole blood from the same pig was used. The pigs were exsanguinated and the blood was collected in a sterile bag. Usually, around 2.5 to 3 L of blood was obtained. Prior to priming the system with the blood, it was depleted of leukocytes by filtering it with a leukocyte filter (LeukoGuard BC2).

### 4.1.3 Preparation of the perfusion machine

Prior to connecting the livers to the perfusion machine, the system was prepared in a sterile manner and primed with blood. When the system was primed, the bolus medication was added. The blood was then allowed to circulate for a few minutes, allowing the system to reach the target levels for the blood gas control and temperature and the bolus medication to be thoroughly and homogeneously mixed. Before the livers were connected, they were prepared on the back table, fixing the cannulas to the vessels (HA, PV, VC and bile) and flushing the liver with saline solution.

### 4.1.4 Connection and initial phase

The livers were connected to the perfusion system in the following order. First, the PV was connected and the flow was set to approximately 0.5 L/min. Second, the HA was connected and the pressure was set to the target level of 50/80 mmHg (diastolic/systolic pressure). This commenced the start of perfusion. The flow in the PV was gradually increased to the target level of 1 L/min during the course of 10 minutes. After connecting the HA, the VC was attached and the respective pressure control activated. Lastly, the bile drainage was joined. This entire procedure usually took between 5 to 10 minutes. Afterwards, the liver container was closed and remained sealed until biopsies were taken. All the controllers were activated and the system remained autonomous from this point. In the initial phase, blood samples were taken hourly and, after six hours, only on a daily basis. Figure 4.1 shows an image of a liver connected to the perfusion machine.

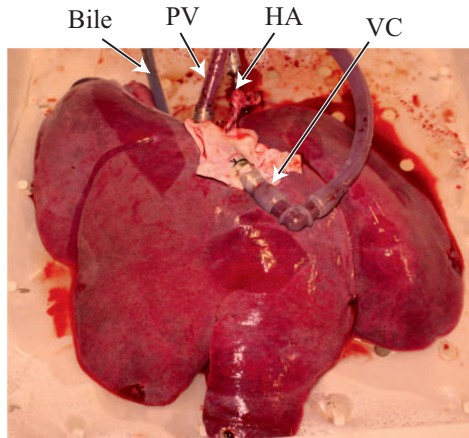


**Figure 4.1:** Image of pig liver connected to machine.

### 4.1.5 General perfusion

From this moment on, the system was running fully autonomous, with the exception of daily routines such as blood and tissue sampling, sensor calibrations and replacing or refilling of the medications. Table 4.1 shows the experimental settings of the main controllers during the perfusion. The controllers were set to the defined target levels unless declared otherwise in the description of the respective experimental groups. Blood was never replaced or added to the system during the course of perfusion, i.e. the same blood that was primed in the beginning was used for the entire duration.

## 4.2 Incremental steps

The initial perfusion protocol was based on the initial literature research<sup>18</sup>. The experimental and machine setup was the same as described in the previous chapter (chapter 3), with certain differences, as highlighted in the following paragraphs. Table 4.2 summarizes the main differences between the different experimental groups. For each experimental group,

**Table 4.1:** Overview of perfusion and controller settings

Parameter	Target Value	Comment
<i>Hemodynamic</i>		
$F_{PV}$	1 L/min	
$F_{HA}$	0.25 – 0.6 L/min	upper and lower limits enforced by vasoactive infusions
$p_{HA}$	80/50 mmHg	(systolic/diastolic)
$p_{VC}$	$\approx 0$ mmHg	results from fluctuation control
<i>Blood physiology</i>		
$T_{Blood}$	34 °C	
$pO_{2,art}$	10 – 12 kPa	
$pCO_{2,art}$	4.5 – 6.5 kPa	results from $pH$ control
$pH_{art}$	7.4	
$sO_{2,VC}$	65 %	
$Glu$	6.5 mmol/L	
$Hct$	25 – 28 %	depending on total blood volume

four livers were perfused.

Briefly, the first group included a hyperglycemic protocol where glucose and insulin were constantly infused at a high rate. In the second group, glucose infusion was manually controlled to obtain normoglycemic levels. In the third group, the operating mode of the pump was switched from non-pulsatile to pulsatile. The fourth group integrated a dialysis unit to the system to provide electrolyte control, waste product removal and hematocrit control. In the last group, the oxygen content of the PV was controlled to physiological levels as compared to the arterial one before.

### 4.2.1 Hyperglycemic group

The first group and, thereby, initial experiments were the "Hyperglycemic" group. In these experiments, the following distinct differences to the final prototype described in chapter 3 were present.

**Table 4.2:** Overview of experimental groups

Group	Glucose infusion	HA pressure	Dialysis	PV O <sub>2</sub> level
1 - Hyperglycemic	hyper	non-pulsatile	no	arterial
2 - Normoglycemic	normo	non-pulsatile	no	arterial
3 - Pulsatile	normo	pulsatile	no	arterial
4 - Dialysis	normo	pulsatile	yes	arterial
5 - Phys.* PV sO <sub>2</sub>	normo	pulsatile	yes	phys*

Notes: \* - physiological

- Glucose and insulin were continuously infused to the system at a rate of 22 mmol/h and 0.9 U/h, respectively
- The HA was operated in a non-pulsatile manner at a pressure level of 65 mmHg
- No dialysis was integrated to the system
- The PV oxygen level was the same as the HA

The choice of the specified glucose and insulin infusion rates was based on the literature review, where hyperglycemic glucose levels (> 10 mmol/L) in combination with insulin infusion rates from 1 to 200 U/L were reported<sup>18</sup>.

Figure 4.2 shows the course of blood glucose (a) and tissue glycogen (b) levels during the course of perfusion with the hyperglycemic protocol (blue circles). One can see that the combination of permanent glucose levels above the physiological limit with constant infusion of insulin leads to continuous storage of glycogen. Only two of four livers survived for longer than four days and one of the two rapidly released glycogen between day four and five which we observed on various occasions and is commonly reported upon organ failure<sup>122</sup>.

### 4.2.2 Normoglycemic group

As a consequence of the elevated glucose levels and consequent deposition of glycogen in the liver tissue, the perfusion protocol was adjusted in the

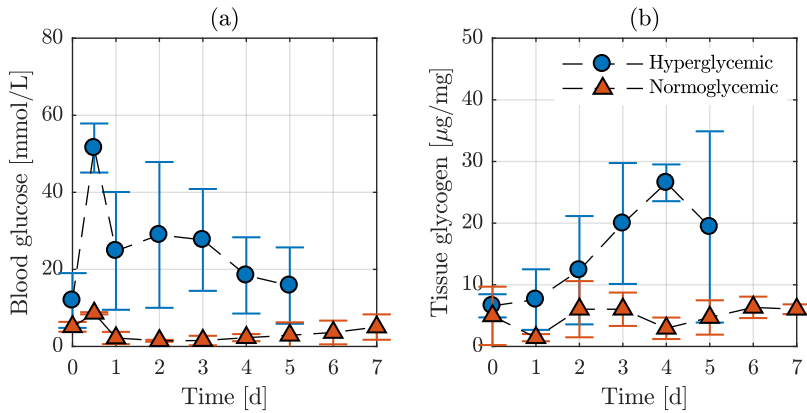


**Figure 4.2:** Course of (a) blood glucose and (b) tissue glycogen with hyperglycemic (blue circles) and normoglycemic (red triangles) protocol. Data reported as mean  $\pm$  sd.

following way.

- Glucose infusion rate was manually adjusted to keep glucose level in physiological band (4 – 10 mmol/L<sup>53</sup>)

The result of this is depictable from figure 4.2. First, glucose levels with the normoglycemic protocol (figure 4.2 (a) - red triangles) are no longer in the hyperglycemic range. Second, tissue glycogen content (figure 4.2 (b)) remain at a steady level with the manually controlled glucose infusion. In both case, a significant difference between the two groups becomes apparent and glycogen deposition could be reduced significantly.

During these experiments, glucose was controlled in a manual fashion. However, this lead to the occasions, e.g. during nights when no staff was present at the machine, that periods of hypoglycemia occurred (see figure 4.3, red circles). Erythrocytes solely rely on glucose as their main energy source and hypoglycemic levels will lead to additional hemolysis<sup>123</sup>. To reduce the risk of hypoglycemia and avoid the necessity of staff to constantly be present at the perfusion machine to manually ensure physiological glucose levels, the automated insulin and glucagon infusion concept was introduced. Thereby, no additional glucose is infused and

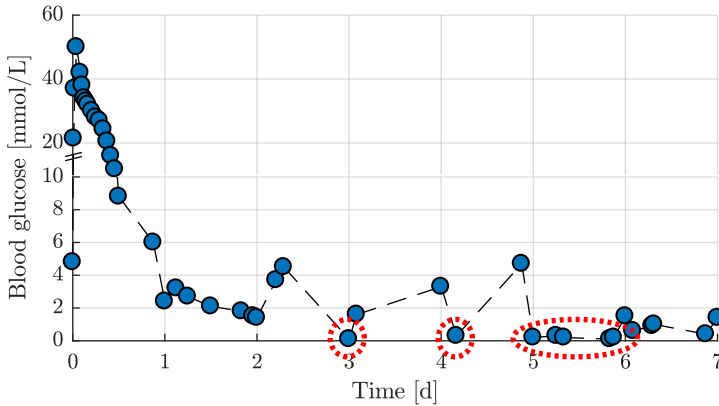


**Figure 4.3:** Course of glucose during one experiment with manual glucose control. Periods of severe hypoglycemia highlighted by red circles.

glucose metabolism is controlled by infusion of insulin and/or glucagon. With the liver's ability to obtain glucose from various pathways such as gluconeogenesis, the synthesis of glucose from amino acids, lactate or glycerol, there is a mean to control the blood glucose level<sup>124</sup>. A sensor is integrated to continuously measure blood glucose levels and provide the basis for the closed loop pancreatic hormone infusion. In chapter 5, the details about this control concept are elaborated.

### 4.2.3 Pulsatile group

In a next step, the perfusion modus of the pump was varied from non-pulsatile to pulsatile. Thereby, the main difference to the previous group is the following.

- Pump operated in a pulsatile manner to obtain HA pressure levels of 50/80 mmHg (diastolic/systolic)

The pulsatile pump operation was realized in the way as described in section 3.3.2. In the field of perfusion, there is a general debate about

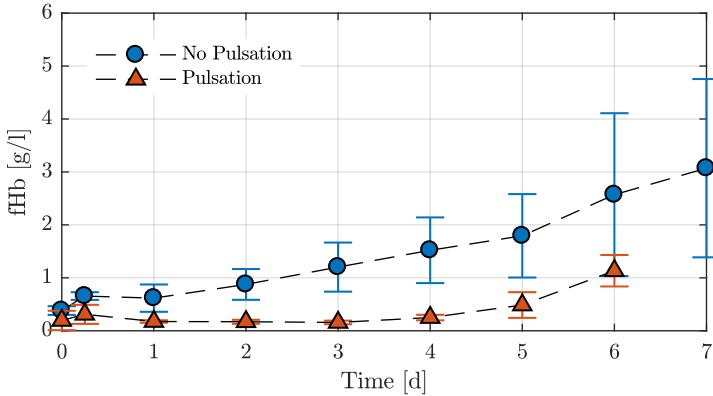


**Figure 4.4:** Free hemoglobin level in blood during the course of perfusion, comparing the non-pulsatile and pulsatile operation of the blood pump, resp. HA pressure. Data reported as mean  $\pm$  sd.

the benefits of pulsation and whether or not to perfuse in a pulsatile or non-pulsatile manner. On the one hand, some studies have reported beneficial performance of high-risk patients of cardiopulmonary bypass when the perfusion pump was operate in a pulsatile manner<sup>107,108</sup> and other studies have shown such results during kidney perfusion<sup>109</sup>. On the other hand, others have reported no difference between pulsatile and non-pulsatile operation<sup>110</sup>. A recent review concluded on the benefit of pulsatile pump operation during long-term perfusion<sup>111</sup>. With no clear consensus being available in literature, the two operation modes were implemented and compared on the perfusion machine.

Figure 4.4 shows the course of free hemoglobin (fHb) during perfusion, comparing the two operation modes. There is a significant difference between the two groups with the free hemoglobin level in the non-pulsatile group being higher, indicating lower hemolysis during pulsatile operation of the pump. Hemolysis is a challenge for all *ex vivo* perfusion systems and a limiting factor for long-term perfusion<sup>80</sup>. Therefore, hemolysis rate is sought to a minimum level. No study could be identified in



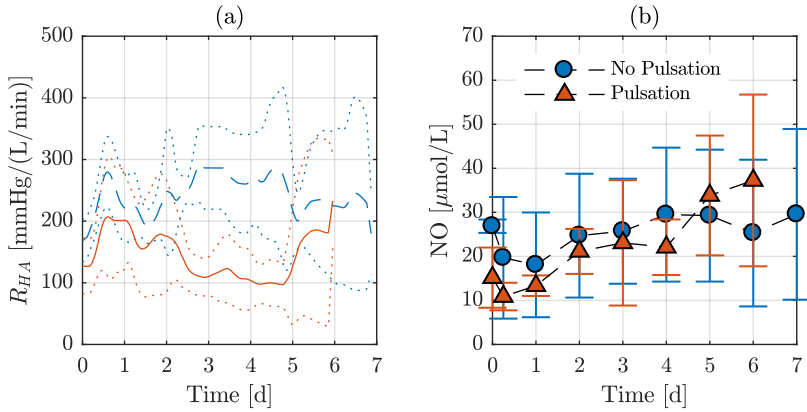


**Figure 4.5:** (a) vascular resistance in HA ( $R_{HA}$ ) and (b) nitric oxide (NO) level in blood during non-pulsatile and pulsatile operation of blood pump. Data reported as mean  $\pm$  sd.

literature where non-pulsatile and pulsatile operation of the pump were compared and a difference in fHb was identified. One study where the pump was operated in a non-pulsatile manner, showed increasing levels of fHb during the course of perfusion<sup>77</sup>. Intuitively, one would conclude on a worse hemolysis rate with pulsatile operation of the pump, as pumps always induce a physical stress on the erythrocytes<sup>113,125</sup>. The pulsation induces additional shear forces and thereby should increase the risk of hemolysis. This may actually be the case regarding the pump itself but in the system including the liver, additional factors come into play. A possible explanation of improved hemolysis rates with pulsatile perfusion could be a better microcirculation. This coincides with the conclusions of a review who stated beneficiary effects of pulsatile perfusion<sup>126</sup>. They postulated "vascular shocks" and pulsatile energy to cause physical displacement of vascular tissue and ensure patency of vascular beds, thereby preventing shunting. This could explain the reduced hemolysis rate with pulsatile perfusion with the erythrocytes not getting "stuck" in the micro-capillaries of the vascular bed. This also overlaps with conclusions from modelling approaches of a different group who showed

benefits of pulsation in complex vascular networks<sup>127</sup>. In addition to improved flow heterogeneity they observed an increased vessel dilation under pulsatile conditions. This leads to a reduced flow resistance as was also observed during our experiments (see figure 4.5 (a)). Contrary to their explanation of nitric oxide (NO) levels to be the cause for the increased vessel dilation, our experiments showed no difference in NO concentration between the two groups (see figure 4.5 (b)). Therefore, a possible explanation for the reduced hemolysis and vascular resistance with pulsatile operation may be the theory of "vascular shocks" and pulsatile energy leading to physical displacement of the vascular tissue.

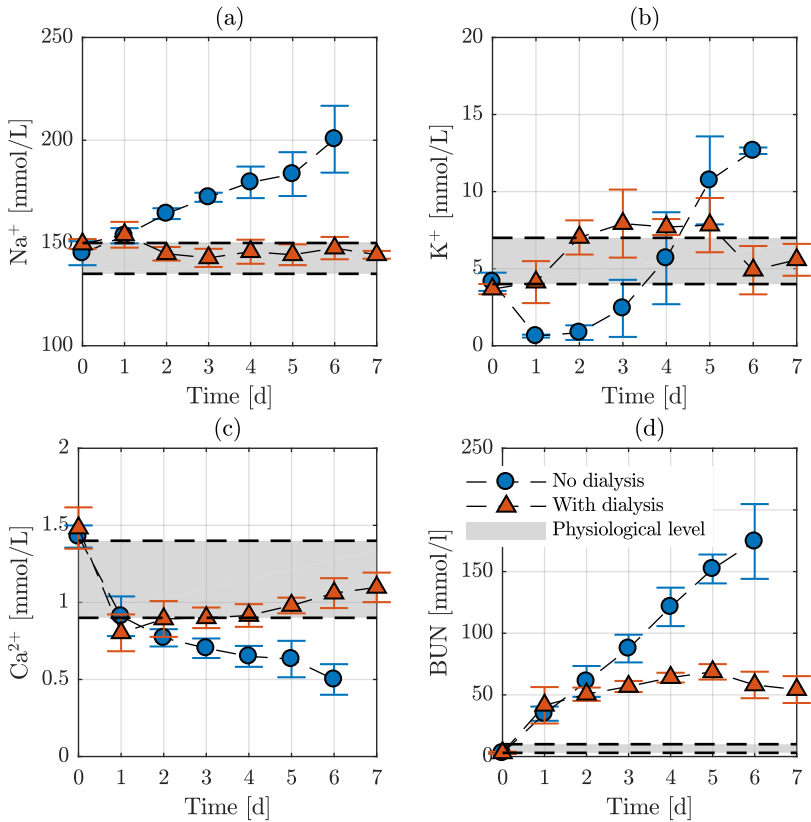
#### 4.2.4 Dialysis group

In a next step, a dialysis system was integrated into the system. A dialysis gives a mean to ensure physiological electrolyte content, remove metabolic waste products from the system and control the fluid content of the blood, i.e. control hematocrit level (see description in section 3.4.3). Therefore, the main difference to the previous group is the following.

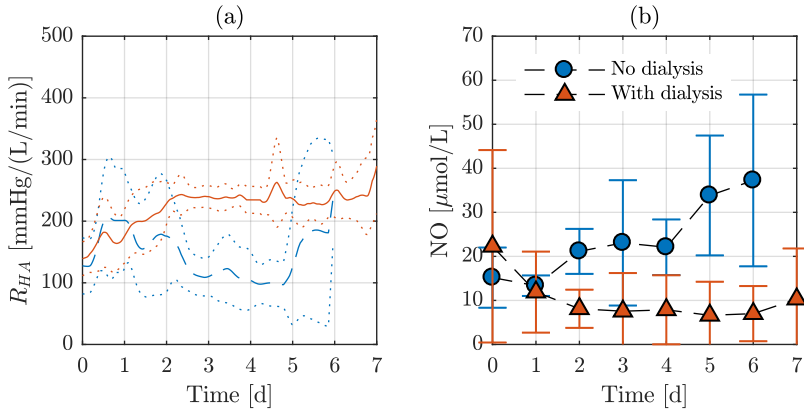
- Integration of a dialysis unit to the system

Figure 4.6 shows the course of the electrolytes sodium (a), potassium (b) and calcium (c), as well as blood urea nitrogen (BUN) (d) during perfusion. One can clearly see the system including the dialysis is able to keep the electrolytes in the physiological band. This was also observed in other systems which integrated dialysis to the perfusion system, although, those systems focused on short-term perfusion<sup>80,82</sup>. Although hypernatremia ( $\text{Na}^+ > 156 \text{ mmol/L}$ ) was shown to not have a negative effect on graft quality upon transplantation<sup>128,129</sup>, it is unclear what kind of influence sodium levels of 200 mmol/L could have. According to the guidelines of the European Association for the Study of the Liver (EASL), sodium levels above 165 mmol/l marks livers as a extended criteria liver with higher risk upon transplantation<sup>130</sup>. In any case, a system closer to physiology should only have beneficial effects as compared to others.

BUN is the final product from amino acid metabolism and usually removed by the kidneys. It was shown in patients with chronic renal failure that elevated levels of urea have deleterious effects<sup>131</sup>. In the present system, the dialysis is capable of removing a certain amount of



**Figure 4.6:** (a) Sodium ( $\text{Na}^+$ ), (b) potassium ( $\text{K}^+$ ), (c) calcium ( $\text{Ca}^{2+}$ ) and (d) blood urea nitrogen (BUN) levels during perfusion with (blue circles) and without dialysis (red triangles). Data reported as mean  $\pm$  sd.



**Figure 4.7:** (a) vascular resistance in HA ( $R_{HA}$ ) and (b) nitric oxide (NO) level in blood during experiments without dialysis and with dialysis. Data reported as mean  $\pm$  sd.

the produced BUN. However, BUN also rises to a non-physiological level and reaches a plateau at approximately 50 mmol/L. At this level, the removal rate of BUN by the dialysis is in equilibrium with its production rate by the liver. A much high dialysate flow rate, than the one applied in the system ( $\dot{V}_{dia} \approx 200 \text{ mL}/\text{h}$ ), would be required to ensure BUN levels within the physiological band. However, the dialysis removes all molecules from the blood which are able to pass through the filter. Therefore, certain molecules are removed which may also be beneficial for the perfusion. It is currently unknown which molecules belong to this group and, therefore, the dialysate flow rate is sought to a minimum. The key is to operate the dialysis at a level where it suffices to ensure physiological blood conditions but at a minimum to remove as few unknown components as possible.

Figure 4.7 (a) shows the vascular resistance of the HA without dialysis (blue) and with dialysis (red). There is a significant difference between the two groups where the dialysis group shows a higher vascular resistance. The assumption is that there are certain components of the blood that are being removed by the dialysis. Figure 4.7 (b) shows the NO level during both experimental sets. One can see that there is a difference between

the two groups and in the dialysis group, there is less NO in the blood. In order to avoid hypoperfusion of the liver, nitroprussiat was infused in a closed loop manner to maintain adequate flow rates in the HA (see details in section 3.3.4). However, one can see in figure 4.7 (a) that the vascular resistance in the group with the dialysis was maintained at a constant level of about 250 mmHg/(L/min) after day two. Reason being that this was the limit where the nitroprussiat infusion was trigger and, therefore, nitroprussiat was constantly infused into the system, resulting in total infusion amounts of about 250 mL during seven days. The following change in perfusion protocol tackled this factor.

### 4.2.5 Physiological PV saturation group

*In vivo*, the PV originates from the intestinal tract which results in a partial deoxygenation and oxygen levels between venous and arterial level ( $sO_{2,PV} \approx 75\% - 85\%$ ). As described in table 2.3 in section 2.2.1, none of the commercial machines and only very few of the research machines control the oxygen level in the PV. Usually, the PV is supplied with the same oxygen content as the HA, leading to hyper oxygenation of the liver. Again, aiming to obtain a close to physiological system, the system was modified in the following way as compared to the previous group.

- Provide physiological oxygen content to the PV by means of mixing venous and arterial blood (for technical details see section 3.4.2)

Figure 4.8 (a) and (b) show the oxygen saturation ( $sO_2$ ) of the PV and VC, respectively, with the arterial ("Arterial PV", blue circles) and venous ("Venous PV", red triangles) oxygen content in the PV. In the case of arterial oxygenation in the PV,  $sO_{2,PV}$  is close to 100%, leading to a high  $sO_{2,VC}$  of around 80%. On the other side, with a controller VC oxygen saturation of approximately 65%, the PV oxygen saturation lies in the range from 75% to 85% depending on the current demand.

Despite lower oxygen delivery to the liver, it is capable of extracting the same amount of oxygen from the blood (see figure 4.8 (c)). There is no significant difference between the two groups in terms of oxygen uptake rate (*OUR*). The *OUR* is calculated as defined in section 2.3.2.

Figure 4.9 (a) shows the vascular resistance of the HA with arterial and venous  $sO_{2,PV}$ . At the first glance, there is no difference in  $R_{HA}$

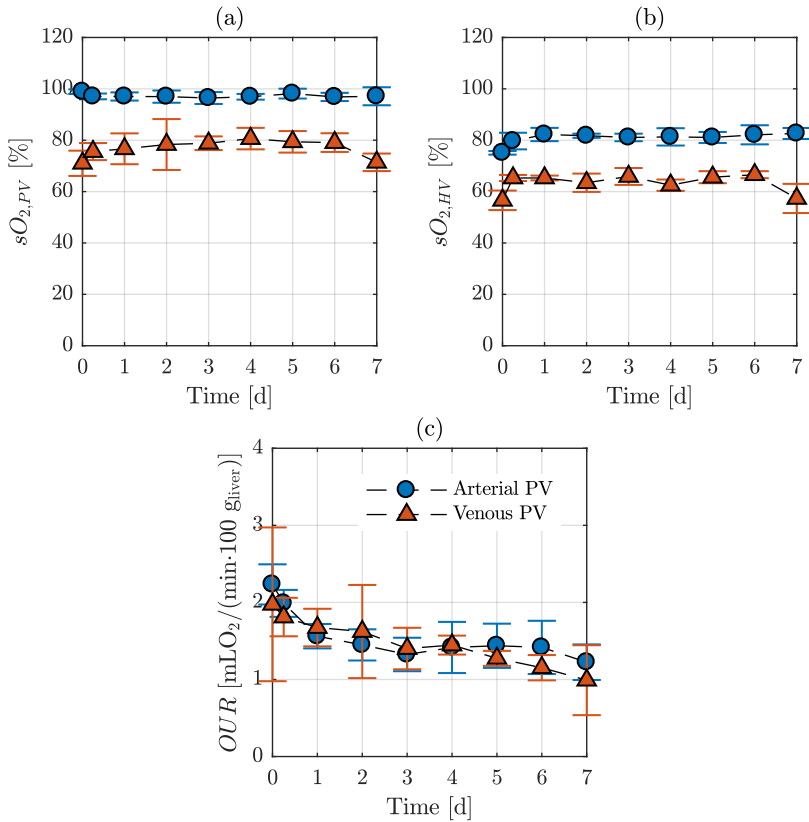


**Figure 4.8:** (a) oxygen saturation ( $sO_2$ ) in PV, (b) oxygen saturation in VC and (c) oxygen uptake rate ( $OUR$ ) of the liver with arterial and venous oxygenation in PV. Data reported as mean  $\pm$  sd.

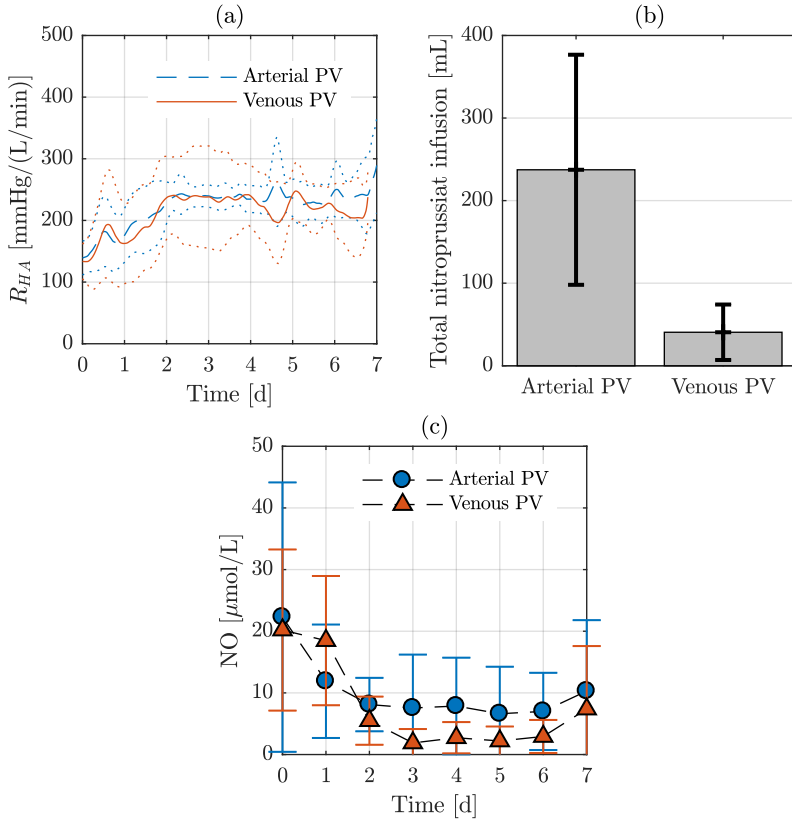


**Figure 4.9:** (a) vascular resistance in HA ( $R_{HA}$ ) and (b) total nitroprussiat infusion and (c) nitric oxide (NO) concentration in blood during perfusion with arterial and venous oxygenation in PV. Data reported as mean  $\pm$  sd.

between the two groups. However, this is only the case because the system counteracts vasoconstriction by infusion of vasodilator nitroprussiat. When looking at the total infusion amount of nitroprussiat during the duration of seven days of perfusion (see figure 4.9 (b)), there is a significant difference between the two groups. On average,  $237 \pm 139$  mL are infused in the "Arterial PV" group as compared to  $41 \pm 34$  mL in the "Venous PV" group. Such a significant lower demand for vasodilator infusion, while maintaining the same  $R_{HA}$ , allows to draw the conclusion about a vasoconstrictive effect in the HA of hyper oxygenation in the PV. This coincides with the observations about hyper oxygenation leading to vasoconstriction in the HA<sup>132,133</sup>. A possible explanation could be NO levels in the blood. NO metabolism was shown to be dependent on oxygen concentration and an increase in oxygen reduces the NO level<sup>134</sup>. Therefore, reducing oxygen level in the blood should lead to a reduction of NO concentration in the blood. Figure 4.9 (c) shows the concentration of NO in the blood in the two groups during perfusion. There is no significant difference between the two groups. However, one needs to consider that the vasodilator nitroprussiat is acting by adding NO to the system. Therefore, reduced infusion amounts of nitroprussiat while maintaining the same NO levels indicates that less NO is metabolized.

### 4.3 Further features

Certain features were included in the machine which were not exclusively evaluated, or integrated during initial development and indicated improved perfusion. These components and functions were integrated based on clinical experience, literature and the desire to obtain a close to physiological system.

For example, VC pressure control was not exclusively elaborated but rather included with the incentive to close the perfusion circuit. It is known that blood contact with air induces additional hemolysis<sup>114</sup> which is sought to a minimum during *ex vivo* perfusion to ensure sufficient blood during the entire duration. However, closing the perfusion loop by cannulating the VC requires that the pressure is controlled. On the one side, too high pressure may lead to outflow obstruction and consequent liver congestion and, on the other side, too low pressure could lead to



collapsing veins and consequent damage of those. For this reason, the feedback control for VC pressure was integrated.

The need to control HA oxygen to physiological levels is also not clear. This decision was also based on the desire to obtain a close to physiological system. While it is obvious that avoidance of prolonged hypoxia is essential during *ex vivo* perfusion, the effects of hyperoxia are less distinct. Studies concerning the consequence of hyperoxia after transplantation concluded on detrimental effects, such as vasoplegia and posttransplant cholangiopathy<sup>69</sup>. Further, hypoxia was shown to have beneficiary effects on liver regeneration<sup>118</sup>. Conversely, with the desire of achieving liver regeneration on the perfusion system, the need to be able to control the oxygen level during perfusion is inevitable.

The artificial diaphragm movement was first integrated during the initial perfusion experiments in an early stage of the development process. A beneficiary effect was observed visually. After seven day perfusion, the liver was evaluated based on positron emission tomography combined with computed tomography (PET-CT) which demonstrated homogeneous metabolism and absence of relevant non-perfused areas on the liver surface in contact with the silicon mat (data not included here). Again, with the intention of obtaining close to physiological conditions, the artificial diaphragm movement was kept in place but the clear positive effect could be evaluated by comparing the system with and without the functionality.

## 4.4 Seven day pig liver perfusion

With the final perfusion protocol, the system is able to keep pig livers alive *ex vivo* for seven days. The data presented in this section was obtained with the final machine and protocol, as described in chapter 3, and is the same as the physiological PV saturation group.

Figure 4.10 shows the flow and pressure of the (a) HA and (b) PV during seven days of perfusion. The system controls HA pressure to a mean arterial pressure (MAP) of 65 mmHg. Depending on the vascular resistance of the HA, the flow is set accordingly. The system allows the HA flow to vary in the range from 0.25 to 0.6 L/min. Usually, we observed vasoplegia during the initial phase of the perfusion with the flow in the HA reaching the upper limit of 0.6 L/min and the system therefore

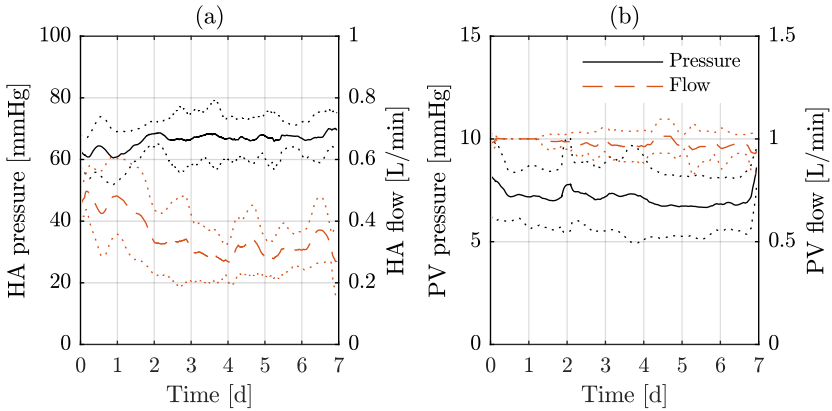


**Figure 4.10:** Flow and pressure in (a) HA (mean pressure) and (b) PV during seven days of perfusion. Data reported as mean  $\pm$  sd.

lowering the HA pressure to slightly lower levels to satisfy the upper bound of 0.6 L/min. As this only occurred in the early phase of perfusion and lasted for few hours, no counter measures in form of vasoconstrictors were taken. On the other hand, the lower limit was enforced by infusion of vasodilators (see section 3.3.4). Usually, flow reduced after perfusion day one or two when the dialysis unit was activated and at some point reached the lower limit. Regarding the PV, it was constantly flow controlled to usually 1 L/min. The pressure in the PV then adjusted accordingly and was not explicitly controlled. The pressure in the PV usually remained at a steady physiological level during the course of perfusion.

Finally, the quality of the liver has to be assessed. As described in section 2.1.4, there are various ways that livers are assessed *in vivo*. However, there is a general debate about whether or not these criteria can also be applied to *ex vivo* perfused livers<sup>19,43,56</sup>. Nonetheless, there are a number of parameters which are generally applied to assess liver function *ex vivo*.

Bile production is a key function of the liver. Figure 4.11 (a) shows the bile production during seven days of perfusion. The average bile pro-

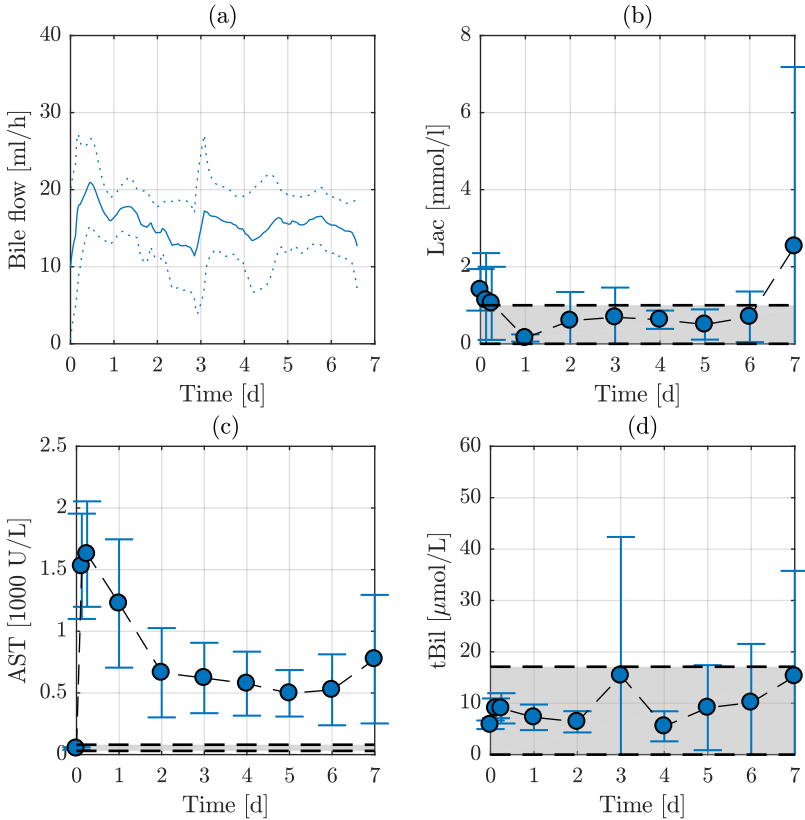


**Figure 4.11:** (a) bile production, (b) blood lactate concentration, (c) aspartate amino transferase (AST) and (d) blood total bilirubin levels as indicators of viable liver function during seven days of perfusion. Data reported as mean  $\pm$  sd with physiological range indicated by the grey area.

duction during the perfusion duration is about 15 mL/h. Bile production is usually reported in *ex vivo* perfusion studies and was also reported as a good marker for liver viability<sup>56,68</sup>. Previous studies of *ex vivo* liver perfusion reported bile flow rates between 5 and 13 mL/h<sup>20,32,82,83</sup>. In the longest previous report of pig liver perfusion of 72 h, bile production ceased after 12-24 h<sup>32</sup>. Bile production has also been criticized by arguing that it can be falsely increased by continuous infusion of bile salts such as taurocholic acid<sup>19</sup>. Bile salt supplementation is commonly applied *ex vivo* as the natural recirculation is not in place. Therefore, not supplementing bile salts leads to reduction of bile production, as about one third of bile production is bile salt dependent<sup>43,44</sup> and could lead to accumulation of waste products such as bilirubin. Therefore, bile production during *ex vivo* liver perfusion can be interpreted in two ways. First, absence of bile production while bile salts are being supplemented would indicate liver failure. Second, existing bile production while supplementing bile salts indicates liver function but needs to be interpreted as one parameter of a group of parameters. In summary, bile production itself is not a guarantee for liver function but its absence is a strong indication for liver failure.

Figure 4.11 (b) shows the lactate level in the blood during seven days of perfusion. After an initial increase of lactate in the first couple of hours after reperfusion, the lactate level drops and usually remains in the physiological range. An initial increase is always observed during *ex vivo* perfusion due to the ischemia time prior to perfusion<sup>102,31</sup>. Lactate is a sensitive indicator of perfusion quality with it being produced upon anaerobic metabolism due to lack of oxygen<sup>135</sup>. Its applicability as a function marker of liver quality however is controversially discussed<sup>43</sup>. Elevated lactate levels are associated with liver dysfunction<sup>61</sup> and lactate clearance may be used as a sign of viability<sup>62</sup>. On the other hand, livers have failed after transplantation despite lactate clearance during NMP<sup>63</sup>. Again, as was the case for bile production, lactate levels cannot be interpreted by itself and need to be considered in combination with a group of parameters.

Figure 4.11 (c) shows the concentration of aspartate aminotransferase (AST) during perfusion. This enzyme, which is usually not or only at minor concentrations present in the blood, is released into the blood stream upon cell injury. Therefore, elevated levels of AST in the blood are a

commonly applied indicator for cell injury and frequently reported during *ex vivo* liver perfusion. In the initial phase of perfusion, a sharp increase is always observed due to ischemia reperfusion injury<sup>60</sup>. Subsequently, AST levels drop and reach a plateau after a few days, as it is removed by the intrinsic immune system of the liver, the Kupffer cells<sup>136</sup>. During liver transplantation, a decline of AST levels is interpreted as a sign of liver function<sup>137</sup>. In other pig liver perfusion experiments with a duration of less than 12 hours, AST levels remained high<sup>82,83</sup>, whereas in experiments lasting longer than 12 hours, AST levels were not reported<sup>32,20</sup>. In transplantation experiments, these usually start to decline after 12-24 hours<sup>68</sup>. Similarly, in human liver transplantation, AST levels peak after 48 hours of liver transplantation, followed by a constant decline<sup>137</sup>. In our experiments, AST usually decline or remained at a plateau until day five or six and subsequently inclined in some cases. However the interpretation of this increase is delicate. Because AST is not hepatocyte specific but also released from RBCs. Thus, some AST increase after day 6 might be due to hemolysis observed afterwards (see figure 4.4). More liver specific ALT is unfortunately not produced by pig hepatocytes but only in human<sup>138</sup>. However, the reason for free hemoglobin increase after day 6 in pig livers unclear.

In figure 4.11 (d), the course of total bilirubin in blood is shown. The liver removes bilirubin from the blood stream and excretes it within the bile. When bile output ceases, bilirubin increase, as observed during previous *ex vivo* perfusion reports<sup>32</sup>. During our experiments, bilirubin concentration in the blood showed to correlate well with other markers of liver function. Physiological bilirubin levels in the blood are another indicator of well liver function.

Figure 4.12 shows the H&E staining of a probe of a liver perfused for seven days. The sample illustrates intact liver structure and cell integrity, further indicating viable liver perfusion up until day seven.

Overall, liver function has to be evaluated as a sum of various parameters. Different approaches are applied by various groups and the real proof of concept remains a transplantation. However, this was not included in this thesis. The data shows that livers can reproducibly be kept viable for seven days and in some cases even up to ten days (data not shown here). An explanation for why some parameters of individual livers start to divert after this duration on the *ex vivo* perfusion system

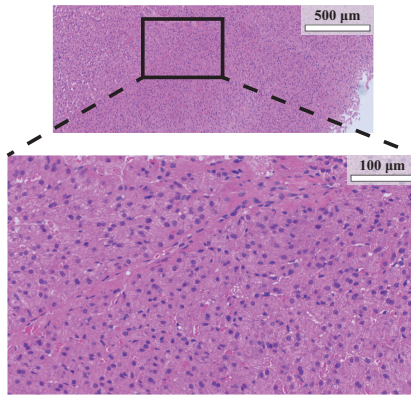


**Figure 4.12:** H&E staining after seven days of perfusion.

is only speculative. On the one hand, as the experiments of the dialysis group show, certain unknown molecules are removed from the system. This may include essential components which are depleted after multiple days of *ex vivo* perfusion. Further, the perfusion system replicates the body from a technical point of view to the best of our knowledge but, again, there could well be essential blood components such as hormones missing, which are not supplemented. Why other organs can not be kept viable *ex vivo* for such a long duration remains an open discussion. There have been hypothesis that there must be a certain hormone essential for *ex vivo* perfusion limiting current perfusion durations<sup>139</sup>. A recent study demonstrated successful *ex vivo* heart perfusion for three days but only in a perfusion loop with cross circulation from an alive sheep<sup>140</sup>. Considering that we were able to perfuse livers in an isolated *ex vivo* system for seven days, leads to the hypothesis that there might be an essential component for long-term *ex vivo* perfusion originating from the liver. If such a molecule could be identified, the door for long-term perfusion of other organs than the liver or even organ banking might be opened.

## 4.5 Conclusion

In this chapter, the development process of the perfusion machine was described. Five major experimental groups were defined and incremental changes from one to the other performed. Thereby, the following main findings were obtained

- Glucose supplementation needs to be controlled to ensure physiological blood glucose and tissue glycogen levels in order to avoid hyperglycemia.
- Pulsatile operation of the pump and thereby HA pressure leads to less hemolysis in the perfused liver.
- Dialysis is essential to ensure physiological electrolyte and hematocrit levels and to remove metabolic waste products. However, dialysis increases the vascular resistance of the HA by removing nitric oxide and possibly other components.
- Physiological oxygen content in the PV reduces the vascular resistance in the PV, leading to a lower demand for vasodilator infusion.

With the final perfusion machine prototype, livers were perfused in a vital state for seven days. Various parameters were assessed in order to evaluate the quality of the liver and demonstrated viable *ex vivo* liver perfusion for seven days. In summary, not a single parameter is able to give a statement about the liver quality but they need to be evaluated in combination. The presented technology may now open the door for novel therapeutic interventions which required a prolonged duration *ex vivo* prior to transplantation.





# Chapter 5

## Glucose control

In this chapter, details about the blood glucose control are elaborated. A glucose sensor is implemented into the circuit, measuring directly in blood, and insulin is delivered directly into the blood in a closed-loop manner based on the glucose sensor measurement. Two controllers were implemented and tested during the perfusion of pig and human livers. A model was developed for its application in a model-based controller. This allows for tight control of blood glucose (BG) and provides a more physiological environment to *ex vivo* perfused livers as compared to currently available perfusion systems.

### 5.1 Introduction

*In vivo*, glucose is a key energy supplier, being tightly controlled mainly by the pancreas, with euglycemic levels of BG lying in the range of 4-10 mmol/L<sup>53</sup>. The liver plays a pivotal role in BG homeostasis, as it is a major storage site of glucose as glycogen. Glycogen might reach up to 10% of the liver's own mass<sup>54</sup>. The liver is one of the main targets of pancreatic hormones controlling glucose metabolism. During fed state with excess glucose in the blood, the pancreas releases insulin to trigger glucose conversion to glycogen in the liver with the help of glucokinase, leading to a decrease in BG concentration. On the other hand, during fasting state, glucagon is released by the pancreas to increase BG level through glycogenolysis, the breakdown of glycogen to glucose, and gluconeogenesis, the synthesis of glucose from amino acids, lactate and glycerol, yielding an increase in BG levels<sup>54</sup>. Glucose is not a primary energy source for hepatocytes giving its place to fatty acids and ketogenic amino acids<sup>55</sup>.

However, erythrocytes, lacking a mitochondria, rely solely on glucose as energy source<sup>123</sup>. Thus avoiding hypoglycemic levels is essential to avoid hemolysis due to lacking glucose, rendering glucose a pivotal ingredient during *ex vivo* perfusion.

Reported *ex vivo* liver perfusion studies include insulin and/or glucose as perfusate additives. Either insulin is infused at a constant rate or adjusted to meet desired BG levels based on periodic, manual glucose measurements. The supplied insulin infusion rates vary greatly across protocols<sup>18</sup>. Further, some groups infuse additional glucose to keep a desired BG level, whose infusion rate is based on manual BG measurements<sup>31,93</sup>. However, no studies could be identified in which insulin and/or glucose were supplied in a closed-loop fashion with an integrated continuous glucose measurement and automated insulin infusion, i.e. an "artificial pancreas" (AP) during *ex vivo* liver perfusion<sup>18</sup>.

## 5.2 Materials & Methods

### 5.2.1 Perfused livers

Pig and human livers were perfused on the developed perfusion machine. The pig livers were harvested and blood was collected in a standardized manner as described in chapter 4. The procedure for the human livers is described in chapter 7. Erythrocytes and blood plasma was mixed to establish the perfusate during the human liver perfusion. The livers included in this chapter are the ones where the glucose sensor was located in the HA.

### 5.2.2 Perfusion machine

The experiments were conducted on the developed perfusion machine as described in chapter 3. Relevant for this chapter is the location of the glucose sensor ( $\textcircled{G}$  in figure 3.4) in the HA branch. This is of importance as the sensor shows a slight dependency on the oxygen content in the blood (see figure 5.3). The oxygen concentration in the HA is controlled to a steady level and eliminates this influence. The pancreatic hormones insulin and glucagon are infused into the PV ( $\textcircled{G}$  in figure 3.4), similar to the hormone release *in vivo*.

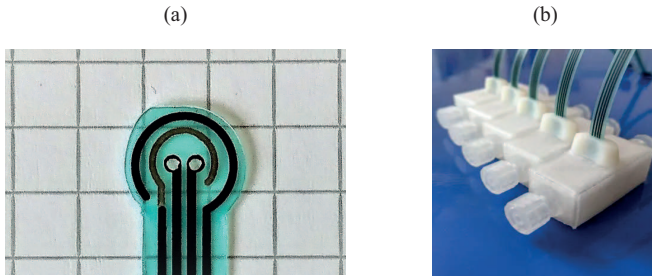


**Figure 5.1:** Image of glucose sensor CITSens Bio Glucose Sensor of C-CIT Sensors AG. (a) close up of electrode, (b) image of flow cells<sup>141</sup>.

### 5.2.3 Continuous glucose measurement

In this study, the CITSens Bio Glucose Sensor of C-CIT Sensors AG was used (see image in figure 5.1). It's a single use sensor developed for the application in the pharmaceutical industry. The measuring range of the sensor is 1-30 mmol/L<sup>141</sup> with a guaranteed operating lifetime of 14 days<sup>142</sup>. The sensor utilizes the enzymatic oxidation of glucose with direct electron transfer from the underlying enzyme  $\beta$ -D-glucose to the electrode<sup>142,143</sup>. The resulting electrical current, which is measured in the sensor, lies in the range from -2000 to 20 nA. This electrical current needs to be calibrated and converted to the glucose value, which correlate in a linear relationship, as described in the following section. As a reference value for the calibration, BG is periodically measured using the ABL90 Flex from Radiometer. During the first couple of hours of liver perfusion, the sensor was calibrated on an hourly basis and thereafter only once per day. The sensor has a measuring period of 20 s.

#### Sensor characteristic

Below 11 mmol/L, the sensor possesses a linear relationship between the BG and the electrical current, according to the manufacturer. The zero point is reproducible<sup>142</sup> and fixes the sensor calibration at 20 nA to 2 mmol/L. Therefore, a single measurement at a level above 2 mmol/L

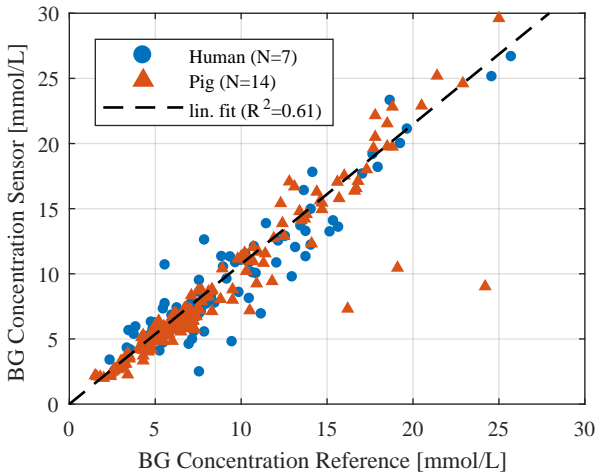


**Figure 5.2:** Sensor glucose reading versus reference glucose reading (Radiometer ABL90 Flex) at time of calibration. The data is distinguished between pig and human liver perfusion experiments.

allows for a calibration of the sensor. The following affine equation describes the behaviour of the sensor:

$$G_S = a \cdot (I_S - I_O) + G_O \quad (5.1)$$

with  $G_S$  and  $I_S$  indicating the glucose concentration, in mmol/L, and electrical current, in nA, of the sensor, respectively,  $G_O = 2$  mmol/L and  $I_O = 20$  nA being the fixed calibration points and  $a$  being the calibration constant in mmol/L/nA. The calibration constant is obtained by storing  $I_S$  at time of sampling and solving for  $a$  with the reference measurement used as  $G_S$ .

According to the manufacturer, the sensor hadn't been tested in blood prior to our experiments. Therefore, in a first step, we show the applicability of the sensor in blood.

In Fig. 5.2, the relation between the sensor BG measurements and the reference BG measurements at the time of calibration is shown. Thereby,

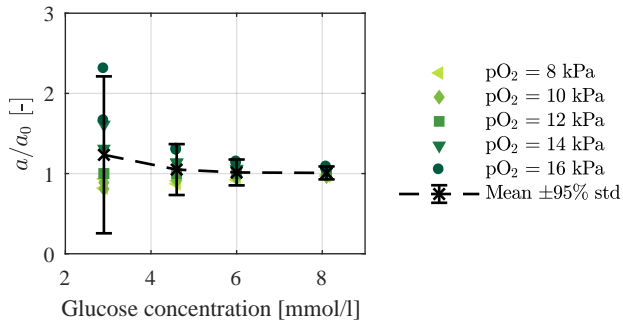


**Figure 5.3:** Influence of partial oxygen tension on glucose sensor. The slope of each sensor measurement,  $a$ , is normalized to the slope at 12 kPa,  $a_0$ , at each glucose level in order to show the effect of  $pO_2$  at different glucose concentrations.

the sensor signal is the glucose value obtained with the calibration constant of the previous calibration. The data includes all the time points of these experiments, when a calibration was performed. The results are distinguished between pig and human liver perfusion experiments. Further, the sensor was allowed to acclimatize for at least one hour in the blood, as was suggested by the manufacturer. Therefore, data points within the first hour were excluded from the analysis. The distinction between pig and human blood showed that there is no significant difference in the sensor's behaviour between the two scenarios. A linear fit to the data yields an  $R^2$  of 61%.

During initial testing of the glucose sensor, we observed an influence of oxygen tension in the blood on the sensor's behaviour. We therefore performed a sensitivity analysis of the sensor slope in dialysate solution (Fresenius Ultraflux AV Paed), where we varied glucose concentration by infusing glucose concentrate and controlled partial oxygen tension to different levels. Fig. 5.3 shows the slope  $a$  of the measurement at different glucose concentrations and  $pO_2$  levels, normalized to the slope  $a_0$  at 12 kPa. It is normalized to 12 kPa because the system controls the arterial  $pO_2$  to this level during perfusion. With decreasing glucose concentration, the influence of  $pO_2$  becomes significant. This could be

due to side reactions happening at the electrode, such as the formation of hydrogen peroxide. These are normally negligible but when the sensor is approaching its lower operating limit (2 mmol/L), it seems to become significant. With increasing glucose concentration, the influence of oxygen reduces and at some point becomes minor. In the lower end of the desired operating range, at around 4 mmol/L, there is still a significant influence which will have an effect on the glucose control if oxygen levels vary. Therefore, we always placed the sensor in the hepatic artery, where oxygen levels are controlled to a steady level. With variations of at most  $\pm 0.5$  kPa of  $pO_2$  in the HA and usual operating levels between 5-7 mmol/L, the influence of oxygen is considered as a minor disturbance and is not directly addressed in the calibration. In addition, we applied an iterative least squares method for the calibration to reduce the effect of falsely calibrated time points, as described in the following section.

### Sensor calibration

Because we observed a variation of the slope  $a$  during the course of the experiments, the sensor had to be calibrated at least once per day. To reduce effects of disturbances during the calibration, we applied an recursive least-squares (RLS) method with exponential forgetting for the calibration<sup>144</sup>. The RLS considers previous calibrations when a new calibration is conducted where a forgetting factor  $\lambda$  determines the weight of previous calibrations. If  $\lambda = 1$ , all previous calibrations are considered equally, whereas with  $\lambda < 1$ , previous calibrations are reduced in weight. The RLS algorithm is defined as follows, which is applied to the slope  $a$  if BG is below 11 mmol/L. The error  $e$  at a calibration step  $k$  is calculated accordingly to

$$e^{(k)} = \underbrace{(G^{(k)} - G_O)}_{y^{(k)}} - \underbrace{(I^{(k)} - I_O)}_{h^{(k)}} \cdot a^{(k)} \quad (5.2)$$

where  $G^{(k)}$  denotes the reference glucose measurement and  $I^{(k)}$  the electrical current of the sensor at that time.

At the most recent calibration  $r$ , the following weighted error  $\epsilon$  is minimized which considers all previous calibrations ( $k = 1, \dots, r - 1$ ) and

the current calibration ( $k = r$ ):

$$\epsilon_{(r)} = \sum_{k=1}^r \lambda^{r-k} \cdot [y_{(k)} - h_{(k)} \cdot a_{(k)}]^2, \quad \lambda < 1 \quad (5.3)$$

In order to reduce computational expenses, the minimization can be rephrased in a recursive way such that only the most recent slope  $a_{(r)}$  and one additional variable  $\Omega_{(r)}$ , which keeps track of past calibrations, need to be stored. Every time a new reference measurement is available, the slope is updated by evaluating

$$a_{(r)} = a_{(r-1)} + \frac{\Omega_{(r-1)} \cdot h_{(r)} \cdot [y_{(r)} - h_{(r)} \cdot a_{(r-1)}]}{\lambda + c_{(r)}} \quad (5.4)$$

$$\Omega_{(r)} = \frac{\Omega_{(r-1)}}{\lambda} \cdot \left[ 1 - \frac{\Omega_{(r-1)} \cdot h_{(r)}^2}{\lambda + c_{(r)}} \right] \quad (5.5)$$

where  $c_{(r)} = \Omega_{(r-1)} \cdot h_{(r)}^2$  to simplify the notation.

When the sensor is calibrated for the first time, the algorithm is initialized by setting

$$a_{(1)} = \frac{y_{(1)}}{h_{(1)}} \quad (5.6)$$

$$\Omega_{(1)} = \frac{1}{h_{(1)}^2} \quad (5.7)$$

The forgetting factor  $\lambda$  was set to 0.25, which was determined retrospectively with an optimization on a set of experiments and yielded an appropriate trade-off between disturbance rejection and signal tracing.

### 5.2.4 System modelling

A mathematical model of the glucose/ insulin metabolism was developed to be applied in a model-based controller. The model comprises two parts; the modelling of the balance of blood glucose and insulin in the perfusion system, and the modelling of the liver metabolism of glucose and insulin. The model is based on the Sorensen model, adapted to the perfusion system<sup>145</sup>.

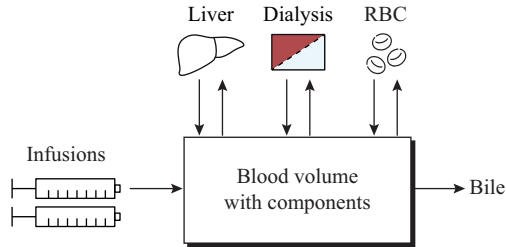


**Figure 5.4:** Mass balance of a component in the blood of the perfusion system.

### System mass balance

If one draws a boundary around the blood in the perfusion system, the inputs and outputs according to Fig. 5.4 would become present for glucose and insulin. Fig. 5.5 shows the cause and effect diagram of the system model, which is described in the following paragraphs.

As indicated in Fig. 5.4, the infusions are a way to directly add components to the system. The liver removes and produces components within the system depending on its metabolism and the dialysis allows to passively add and remove components to and from the system. Constantly produced bile from the liver leaves the system and the red blood cells (RBC) consume glucose. This yields the following mass balance:

$$\begin{aligned}
 \text{Glucose: } V^G \cdot \frac{dG}{dt} &= \dot{G}_{hep} + \dot{G}_{dia} + \dot{G}_{rbc} \\
 \text{Insulin: } V^I \cdot \frac{dI}{dt} &= \dot{I}_{inf} + \dot{I}_{hic} + \dot{I}_{dia}
 \end{aligned} \tag{5.8}$$

where  $G$  and  $I$  denote the glucose and insulin concentration in the blood,  $V^G$  and  $V^I$  total glucose and insulin relevant volume in L, and  $\dot{G}$  and  $\dot{I}$  the in- and output of glucose and insulin due to infusion (*inf*), the net hepatic glucose production (*hep*), the hepatic insulin clearance (*hic*), dialysis (*dia*) and red blood cells (*rbc*), respectively. No glucose is infused directly and, in the healthy state, a negligible amount of glucose is present in the bile<sup>146,57</sup>, leading to their exclusion in the mass balance. Insulin is not consumed by RBCs and, even though insulin was shown to



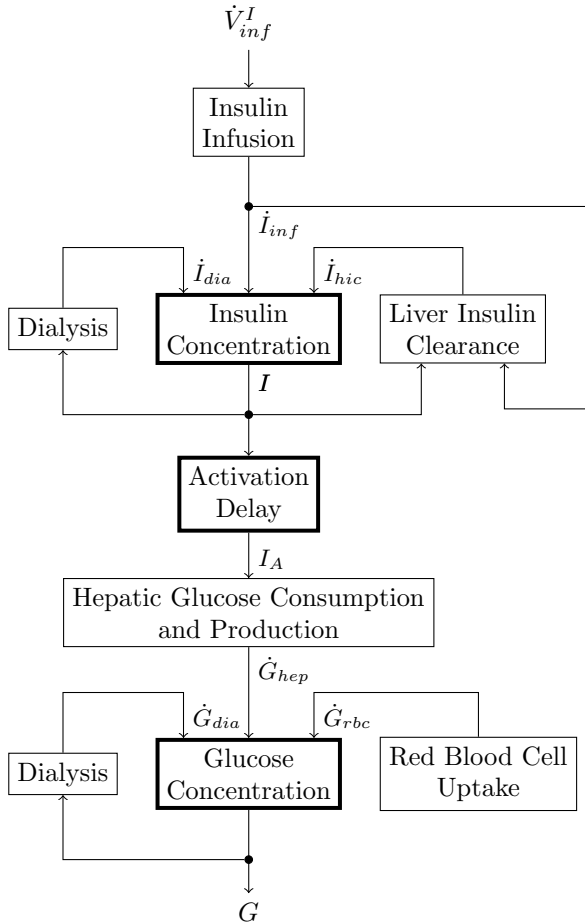


**Figure 5.5:** Cause and effect diagram of the system model.

be in bile<sup>147</sup>, the large difference between blood flow through the liver ( $\sim 1.5$  L/min) and bile production ( $\sim 20$  mL/h) makes the influence of insulin in bile on the system dynamics negligible. Therefore, these two fluxes are excluded for insulin.

In the following, the different terms and fluxes for glucose and insulin mass balances are discussed.

## Glucose

The total glucose relevant volume is distributed in the water content of whole blood and the interstitial fluid of liver tissue<sup>145</sup>. Thereby, 93% of blood plasma is water and 71% of RBC is intercellular water. Further, the RBC water glucose is assumed to equilibrate quickly with plasma glucose, hence, no dynamics are considered here. The interstitial fluid in liver tissue is approximately 0.63 L/kg<sup>145</sup>. This yields the following relation

$$V^G = (0.93 \cdot (1 - f_{Hct}) + 0.71 \cdot f_{Hct}) \cdot V_{blo} + 0.63 \cdot m_{hep} \quad (5.9)$$

where  $f_{Hct}$  is the non-dimensional hematocrit fraction in the blood,  $V_{blo}$  is the total blood volume in L and  $m_{hep}$  the liver mass in kg.

The consumption of glucose by the RBC is considered to be independent of BG and insulin level. Derived from the equations listed in Sorensen<sup>145</sup>, we applied

$$\dot{G}_{rbc} = -25 \text{ } \mu\text{mol}/(\text{min L}) \cdot f_{Hct} \cdot V_{blo} \quad (5.10)$$

The amount of glucose entering or leaving the system via the dialysis depends on the actual concentration of BG. The dialysis filter is a membrane where blood and dialysate solution flow in a counter-current manner. In the perfusion system, the blood flow is much larger as compared to the dialysate flow, making the dialysate side the bottle neck. Hence, the dialysate equilibrates with the blood, leading to the glucose concentration of the dialysate leaving the filter being the same as the glucose concentration of blood entering the filter ( $G_{dia,out} = G$ ). For simplicity, we assume that the volume flow rate of the dialysate entering the filter is equal to the flow rate leaving the filter ( $\dot{V}_{dia,in} = \dot{V}_{dia,out} = \dot{V}_{dia}$ , in L/min). This yields

$$\dot{G}_{dia} = \dot{V}_{dia} \cdot (G_{dia,in} - G) \quad (5.11)$$

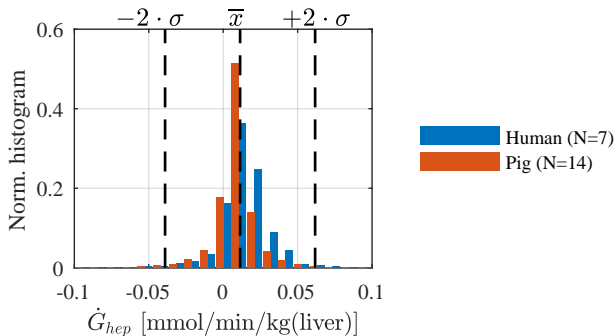


**Figure 5.6:** Normalized histogram of net hepatic glucose production (NHGP). Mean level  $\bar{x}$  with two standard deviations  $\pm 2 \cdot \sigma$  of all experiments are indicated by vertical dashed lines.

with the concentration of glucose in the dialysate entering the filter  $G_{dia,in}$  being 5.5 mmol/L. With BG above this level, the sign of  $\dot{G}_{dia}$  becomes negative, leading to glucose leaving the system.

Models have been developed that consider interpatient variability and contain normalized relations to different basal parameters<sup>145,148,149</sup>. These models, on the one side, decouple the glucose production and consumption and, on the other side, decouple the individual influences of glucose and insulin on glucose metabolism. Although this approach increases the accuracy of the model and allows for the model to be applied with different patients, it requires the basal level of all parameters to be known or to be identified. The approach of this model was to reduce the number of parameters to be measured or identified to have an applicable model for the perfusion machine. Therefore, the hepatic glucose consumption and production are lumped into one function. As compared to the Sorensen model, the following two assumptions are made when formulating the lumped model. First, the production and consumption of glucose are lumped together with only insulin influencing the net production/consumption rate. Second, the BG concentration doesn't influence the glucose production and consumption of the liver directly. Considering that the model is applied to control glucose to a constant level, this assumption seems valid, as BG should only vary

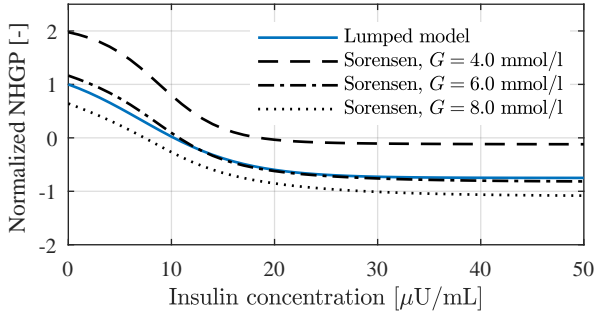


**Figure 5.7:** Comparison of NHGP function used in this model as compared to the Sorensen approach<sup>145</sup>, applied in many models, at different glucose concentrations. The “Lumped model” function is normalized to  $\dot{G}_{hep}^{max}$ . The Sorensen functions are evaluated with the basal levels and normalized with the basal hepatic glucose production.

mildly in the operating condition. The following function represents the net hepatic glucose production (nhgp)  $\dot{G}_{hep}$ .

$$\dot{G}_{hep} = \beta \cdot (\alpha - \tanh[\gamma \cdot (I_A - \delta)]) \quad (5.12)$$

where  $\alpha$ ,  $\beta$ ,  $\gamma$  and  $\delta$  are parameters and  $I_A$  is the active insulin as will be described later in (5.21).

A more intuitive interpretation of the function is obtained by introducing two variables, namely the minimal and maximal net hepatic glucose production rate,  $\dot{G}_{hep}^{max}$  and  $\dot{G}_{hep}^{min}$ . These are defined as

$$\begin{aligned} \dot{G}_{hep}^{max} &:= \dot{G}_{hep}(I_A = 0) = \beta \cdot (\alpha + \tanh[\gamma \cdot \delta]) \\ \dot{G}_{hep}^{min} &:= \dot{G}_{hep}(I_A \rightarrow \infty) = \beta \cdot (\alpha - 1) \end{aligned} \quad (5.13)$$

allowing to rephrase parameters  $\alpha$  and  $\beta$  according to

$$\alpha = \frac{\dot{G}_{hep}^{max} + \dot{G}_{hep}^{min} \cdot \tanh(\gamma \cdot \delta)}{\dot{G}_{hep}^{max} - \dot{G}_{hep}^{min}} \quad (5.14)$$

$$\beta = \frac{\dot{G}_{hep}^{max} - \dot{G}_{hep}^{min}}{1 + \tanh(\gamma \cdot \delta)} \quad (5.15)$$

where  $\alpha$  is unitless and  $\beta$  is in mmol/min/kg(liver).

$\dot{G}_{hep}^{max}$  and  $\dot{G}_{hep}^{min}$  are obtained from analysing the rate of change of glucose in the measurement data. This is realised by solving the glucose mass balance in (5.8) for  $\dot{G}_{hep}$  with the continuous glucose data. Fig. 5.6 shows the normalized histogram of  $\dot{G}_{hep}$ , separated for human and pig experiments. The average  $\dot{G}_{hep}$  lies at  $\bar{x} = 0.01$  mmol/min/kg(liver), with a standard deviation of  $\sigma = 0.025$  mmol/min/kg(liver). We defined  $\dot{G}_{hep}^{max} := \bar{x} + 2 \cdot \sigma$  and  $\dot{G}_{hep}^{min} := \bar{x} - 2 \cdot \sigma$ . In order to define  $\gamma$  and  $\delta$ , we compared the lumped function to the Sorensen function at different BG concentrations. Fig. 5.7 shows the evaluated NHGP of Sorensen<sup>145</sup> at different glucose concentrations, neglecting the contribution of glucagon. The NHGP were normalized to the basal rates, to compare the different models. The individual parameters for the lumped model are defined as  $\dot{G}_{hep}^{min} = -0.04$  mmol/min/kg(liver),  $\dot{G}_{hep}^{max} = 0.06$  mmol/min/kg(liver),  $\gamma = 0.1$  1/(I.U./L) and  $\delta = 7$  I.U./L. The target glucose level usually lies in the range from 5.5 to 6.5 mmol/L, hence, the lumped model covers this range in a satisfying manner. However, as there is some inter-liver variation, the minimum and maximum net hepatic glucose production are multiplied by a factor  $f_{hep}$  which lies in the range of 0.1 to 2. This factor also compensates for variations of the liver's behaviour with time during perfusion. Looking at the relations of  $\alpha$  and  $\beta$ , this allows to directly multiply  $\beta$  by the factor, yielding

$$\hat{\beta} = f_{hep} \cdot \beta \quad (5.16)$$

The effect of this can be interpreted with (5.12). An increase of  $\beta$  leads to a stretch of the curve ‘‘lumped model’’ in Fig. 5.7, whereas a decrease of  $\beta$  results in a squeeze of the curve while the zero-crossing remains the same. This allows for a measure to vary the sensitivity of the liver to insulin.

## Insulin

Unlike glucose, insulin is only distributed in blood plasma, since the RBC membrane is impermeable to insulin<sup>145</sup>. Therefore, the insulin relevant volume is calculated according to

$$V^I = (1 - f_{Hct}) \cdot V_{blo} \quad (5.17)$$

One way for insulin to leave the system is via dialysis as the leaving dialysate equilibrates with the entering blood. In contrast to glucose, no insulin is present in the dialysate solution entering the filter, leaving the following relation

$$\dot{I}_{dia} = -\dot{V}_{dia} \cdot I \quad (5.18)$$

The source of insulin in the system is given by its infusion.

$$\dot{I}_{inf} = I_{inf} \cdot \dot{V}_{inf}^I \quad (5.19)$$

where  $I_{inf}$  denotes the concentration of insulin in the infusion which is normally set to 450 I.U./L in our system and  $\dot{V}_{inf}^I$  is the volume infusion rate of insulin which normally ranges between 0.1 and 5 ml/h.

Hepatic insulin clearance works according to the first pass effect. Of all insulin which passes the liver, a certain fraction is cleared, independent of the concentration<sup>145</sup>. This fraction is denoted as  $f_{hic}$ . Additionally, as the insulin is infused directly into the portal vein and not mixed with the entire blood volume before entering the liver, the infusion is also considered in the first pass effect. This yields

$$\dot{I}_{hic} = -f_{hic} \cdot (f_{Hct} \cdot \dot{V}_{blo} \cdot I + \dot{I}_{inf}) \quad (5.20)$$

where  $f_{hic}$  denotes the hepatic insulin clearance. This parameter is estimated during the course of perfusion and, therefore, allows to consider inter-liver variabilities as well as changing clearance levels during the course of perfusion, as has been observed in previous studies<sup>150</sup>.

Physically, there is a delay between the blood insulin level and the activation of NHGP. Mythreyi et al.<sup>149</sup> proposed a third order system, consisting of three first order lags in series to reproduce this effect in the model. This leads to an actual insulin concentration  $I$  in the blood and

a virtual active insulin concentration  $I_A$ . The activation is formulated by

$$\begin{aligned}\frac{\tau_I}{3} \cdot \frac{dI_{A1}}{dt} &= I - I_{A1} \\ \frac{\tau_I}{3} \cdot \frac{dI_{A2}}{dt} &= I_{A1} - I_{A2} \\ \frac{\tau_I}{3} \cdot \frac{dI_A}{dt} &= I_{A2} - I_A\end{aligned}\tag{5.21}$$

where  $I_{A1}$  and  $I_{A2}$  are intermediate values of active insulin, with no actual physical meaning. A value of 27 min was identified for the time constant  $\tau_I$ .

### 5.2.5 Controller

Two controllers were applied and compared during *ex vivo* liver perfusion. The first controller is a P controller targeting the desired glucose level. For the second controller, a model-based controller was applied. This comprised a state estimator to estimate the hepatic insulin clearance  $f_{hic}$  and the factor  $f_{hep}$  and a linear quadratic regulator (LQR). The model described above was used as a basis for both the state estimator and the controller.

## 5.3 Results

### 5.3.1 Sensor calibration

To evaluate the quality of the calibration procedure, the proposed RLS method is compared to a method where only the last calibration is considered (single value - SV). The difference between the continuous signal and the reference value yielded the calibration error. For each liver, the average error of all calibrations was calculated and is shown in Fig. 5.8. When comparing the individual experiments, the RLS and SV calibration show similar results; in some cases the RLS being superior and in other times the SV showing better behaviour. However, in some cases (Liver 4 and 14), there is a large difference between the two calibration procedures with the RLS showing a lower error. This is due to outliers in the

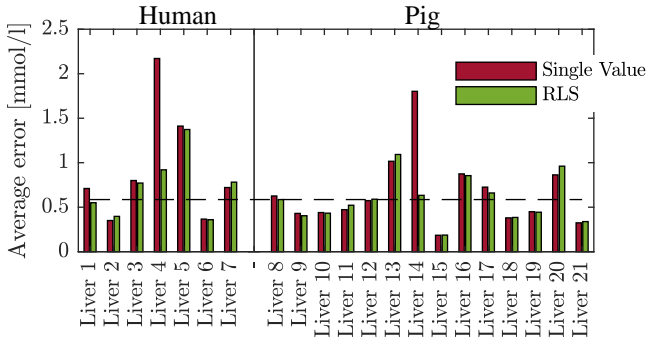


**Figure 5.8:** Comparison of iterative least squares (RLS) and single value calibration procedure. Quality of calibration is quantified with the average error between sensor reading and reference measurement at time of calibration. Horizontal dashed line indicates the average error with the RLS method.

calibration, which could be caused by variations in oxygen concentration at time of calibration or human handling error. In these cases, the RLS shows beneficial behaviour for rejecting outliers, as these false calibration points are only considered partially. The RLS poses a passive method to reduce their influence. The average error of all experiments combined is 0.72 mmol/L and 0.6 mmol/L for the SV and the RLS methods, respectively. This shows an improvement of sensor accuracy with the RLS method. The dashed line in Fig. 5.8 indicates the average error of all experiments of the RLS method (0.6 mmol/l).

### 5.3.2 Model validation

Fig. 5.9 shows the course of glucose comparing the simulations and measurements of BG in four different livers (a to d) upon infusion of insulin. Thereby, no or only basal insulin was infused in advance of the test, ensuring the insulin level in the blood is close to zero. The initial glucose level at time zero was set equal to the measurement value and the only input into the model was the infusion rate of insulin. The insulin clearance  $f_{hic}$  and  $f_{hep}$  are thereby estimated. As can be seen in the four



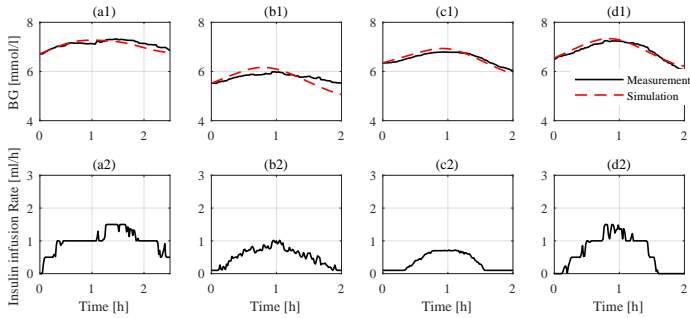


**Figure 5.9:** Comparison of the course of glucose (a1 to d1) upon insulin infusion (a2 to d2) between measurement and simulation output of model with four different livers (Liver 1, 14, 15, and 19 correspond to a, b, c and d, respectively).

exemplary sets, the model is capable of tracking the reaction of glucose upon insulin infusion in the near future with good accuracy. Especially the timing of the model is in good accordance with the measurement whereas the amplitude of the response is not always exact. With the requirement of the model being the predictability of the response to insulin infusion in the near future, this renders the model applicable in a model based control approach.

### 5.3.3 Continuous glucose control

Fig. 5.10 (a) & (c) shows the course of BG during an exemplary perfusion experiment with the administered insulin in Fig. 5.10 (b) & (d) for the case of the P controller and the model based controller, respectively. Due to the inevitable ischemia reperfusion injury (IRI) at the start of the perfusion<sup>151</sup>, BG rises to hyperglycemic levels in the first couple of hours. This phenomena is elaborated in more detail in the discussion. The AP is activated as soon as the sensor has been calibrated at or below 11 mmol/L. Due to the increased uncertainty of the sensor reading at higher glucose levels (see Fig. 5.2 (a) in Materials & Methods), this threshold was applied. Further, the system infused insulin at a constant

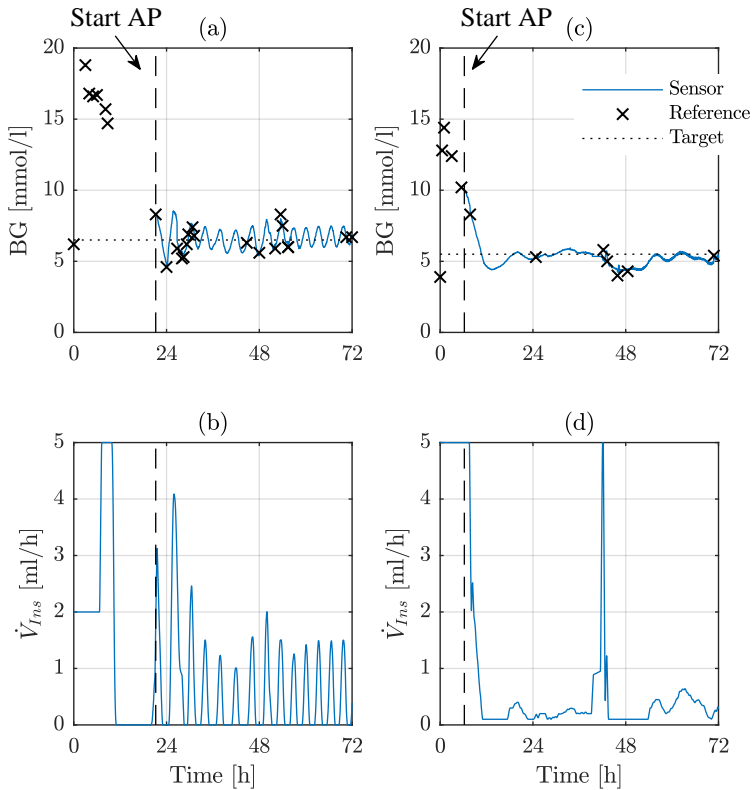


**Figure 5.10:** Example of AP controlling glucose during perfusion. Data from two different experiments with the two controllers shown. (a) & (c) Course of glucose with sensor signal and reference calibrations shown for P controller (a) and model based controller (c), respectively. (b) & (d) insulin infusion adjusted based on current glucose level to reach target for P controller (b) and model based controller (d), respectively.

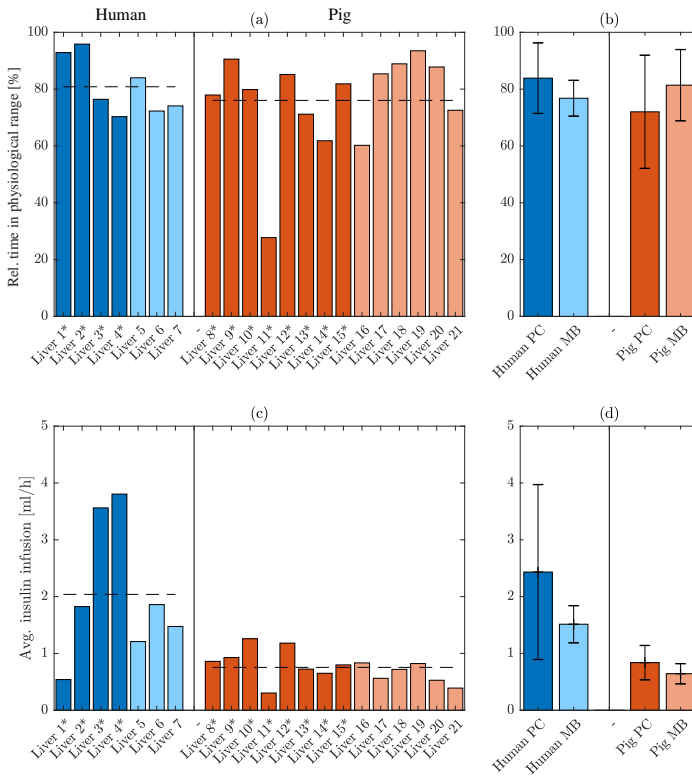


**Figure 5.11:** (a) Time in physiological range relative to the perfusion duration of 96 hours for human and pig livers. The asterisk (\*) in the label of the liver indicates that the P controller (PC) was applied whereas for the others the model based (MB) controller was applied. (b) Average and standard deviation of relative time for human and pig livers with P and MB controllers. (c) Average amount of insulin administered during the course of perfusion. (d) Average and standard deviation of insulin infusion for human and pig livers with P and MB controllers.

rate of 5 mL/h ( $\cong 2.25$  I.U./h) in the initial phase of perfusion to bring down the glucose. This infusion rate also corresponds to the maximum allowed infusion rate of the activated AP. When BG reduces to the physiological range, the AP adjusts the infused insulin to keep the target BG level, usually in the range of 5.5 to 6.5 mmol/L. The most apparent difference between the two controllers is the oscillation of BG and insulin infusion. In the case of the P controller, BG values fluctuate around the target level. Reason being that insulin is only administered to the system if glucose lies above the threshold. With BG value at or below the threshold, no insulin is infused which always leads to the scenario that BG cannot be maintained exactly at the target level. With the selected P value of the controller, this leads to an overshooting and the given oscillation of BG. This is not the case for the model based controller (Fig. 5.10 (c)) where BG is kept at the target level in a steadier manner. The model based controller tries to maintain the specified target level and also administers insulin if BG is at the desired level.

In Fig. 5.11, the percent time within the physiological glucose range (a) & (b) and average insulin infusion (c) & (d) is shown. In Fig. 5.11 (a) & (c), each experiment is illustrated individually with Liver 1 to 7 being human livers and Liver 8 to 21 being pig livers. The asterisk indicates the livers where the P controller (PC) was applied and the ones without with the model based (MB) controller. In Fig. 5.11 (b) & (d), the mean and standard deviation of each controller group is with calculated, with "Human PC" including Liver 1 to 4, "Human MB" including Liver 5 to 7, "Pig PC" including Liver 8 to 15 and "Pig MB" including Liver 16 to 21. The physiological glucose range was defined as 4-10 mmol/L, as reported in literature<sup>53</sup>. The percent time in physiological range is the ratio between the time when BG was inside the physiological range and the perfusion duration of four days. On average, the glucose was kept in the physiological range  $78 \pm 12\%$  and  $76 \pm 17\%$  of the time for human and pig livers, respectively. The initial phase during reperfusion of the livers, when a large amount of glucose is released into the blood by the liver, is one of the main reasons why the time in range is below 100%. However, in some cases, as for example Liver 11, BG dropped to hypoglycemic levels and remained for 24 hours, before elevating to physiological levels again. This can also be seen when looking at the average insulin infusion for this liver, which is lower than all others due to the hypoglycemia. Comparing

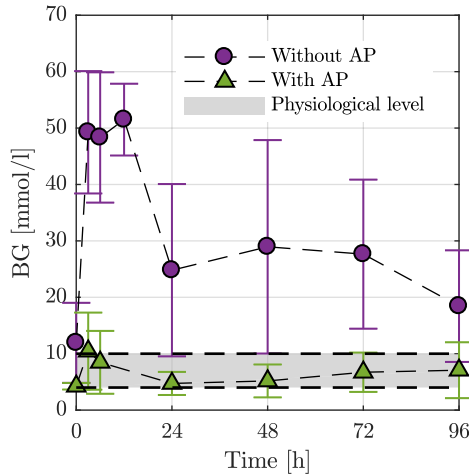


**Figure 5.12:** Blood glucose with and without AP in pig liver perfusion experiments.

the average insulin infusion for each experiment in Fig. 5.11 (b), the human livers required on average 1.8 mL/h whereas the pig livers required 0.9 mL/h. This corresponds to 0.8 I.U./h and 0.4 I.U./h for human and pig, respectively. When comparing the difference in "relative time in physiological range" of the two controller types (Fig. 5.11 (b)), there is no significant difference between the P and MB controller. Similarly, the two controllers show no significant difference in the infused insulin amount (Fig. 5.11 (d)).

### 5.3.4 Effect of AP on perfusion quality

We evaluated the effect of the AP in two experimental sets with pig livers. In these experiments, we varied the type of insulin and glucose supplementation. In the first case, "Without AP", four livers were perfused for multiple days where insulin and glucose was supplied in a constant manner with infusion rates of 0.9 I.U./h and 22 mmol/h, respectively, which was obtained from different protocols<sup>18</sup>. In the second

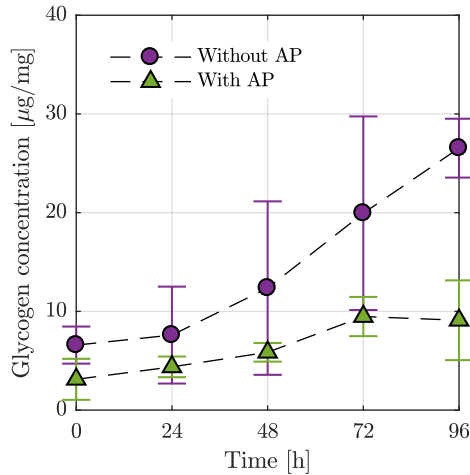


**Figure 5.13:** Glycogen concentration in the liver tissue with and without AP in pig liver perfusion experiments.

case, “With AP”, four livers were perfused while no glucose was infused directly and insulin was controlled in an automated manner by the AP.

Fig. 5.12 shows the course of BG for the two experimental sets. Without the AP, BG levels remain in the hyperglycemic range during the course of the perfusion. With the AP, BG can be maintained in the physiological range for most of the perfusion duration. Both sets show an initial increase of BG due to the IRI. The AP can correct this within approximately half a day to return to physiological levels, whereas BG remains elevated in the case without an AP.

In Fig. 5.13, the liver glycogen content during the course of perfusion is shown for both sets. Without the AP, the excess of glucose and the constant infusion of insulin result in a larger amount of glycogen stored in the liver. With the AP controlling the BG, glycogen content remains lower, but also increases slightly.

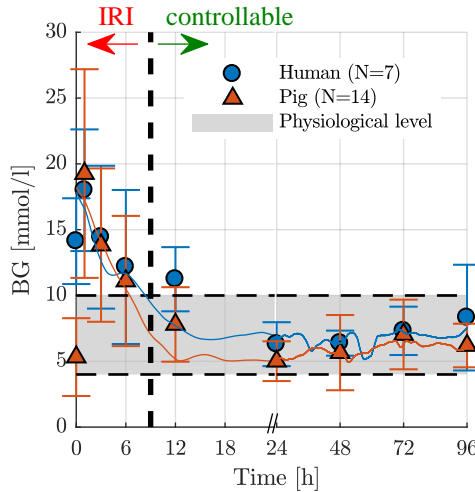


**Figure 5.14:** Blood glucose during 120 hours of perfusion. Note that the resolution of the time axis in the first 24 hours is higher than from 24 to 96 hours. The solid line shows the continuous glucose sensor signal whereas the markers with error bars represent the average value and standard deviation of the reference measurements at the respective times.

### 5.3.5 Course of glucose during perfusion

In Fig. 5.14, the course of glucose of all human and pig livers is shown. The marked points indicate the reference measurement at regular intervals with the solid line being the continuous glucose signal in the respective color. Note that the resolution of the time axis in the first 24 hours is higher than from 24 to 120 hours. When looking at the course of glucose, two phases can be identified. First, glucose is released by the liver due the ischemia reperfusion injury (IRI), leading to a BG increase to hyperglycemic levels, on average peaking at 19 mmol/L within one to two hours. Second, BG subsequently decreases and reaches the physiological range within six to twelve hours. This is the range, where it becomes

controllable for the physiological range and the AP is active, denoting the controllable phase. Further, one can see in Fig. 5.14 that the course of glucose during human and pig livers perfusion is similar.

## 5.4 Discussion

This study is, to the best of our knowledge, the first report of an artificial pancreas integrated into an *ex vivo* liver perfusion machine to continuously control BG in the physiological range for multiple days. The main findings are as follows. First, a sensor to measure glucose in blood for multiple days has been selected and proposed and its application directly in blood shown. Second, two different controllers to maintain glucose concentration in the physiological range were applied and evaluated. Third, we showed the effect of an integrated AP system as compared to no AP present illustrating that glucose can be maintained at physiological levels for multiple days with consequent lower levels of glycogen stored by the liver.

Usually, glucose sensors which are applied in an AP in patients are positioned subcutaneously<sup>152,153,154</sup> or intradermally<sup>155</sup>, with few also measuring directly in blood<sup>156</sup>. The sensor in this perfusion machine measures directly in the blood. It had not been tested in blood before, therefore in a first step, its applicability had to be evaluated. In the target range of 4-10 mmol/L, the sensor behaves in a satisfying manner. With the introduced RLS method for the online sensor calibration, the performance can be enhanced. When the glucose sensor is calibrated in the target range at least once, the slight variation of the sensitivity is handled by the daily calibrations, as can be seen from an average calibration error of 0.6 mmol/L. Further, the goal of the AP is to ensure a steady glucose level. With the glucose ideally only varying slightly in the control range, a sensor variance has only a minor influence on its accuracy. Overall, the sensor is suitable for its application in an artificial pancreas system during *ex vivo* liver perfusion.

Two controllers were implemented and tested during *ex vivo* liver perfusion. The P controller solely operates in a feedback manner and only infuses insulin if BG lies above the threshold. With a sufficiently large P value, this leads to the observed oscillating behaviour. On the other hand, the model based controller also infuses insulin when BG



is at the target level and takes into account how the liver reacts upon insulin infusion. In the end, glucose metabolism in the *ex vivo* system can be modelled but needs to be simplified to be practical. The proposed model adapts existing models in a way that it can be applied in a model based control during *ex vivo* liver perfusion. As there are no predictable disturbances like physical activity or meals, there is no need for model predictive control which considers such, as is done in the state of the art of AP research<sup>157,158</sup>. Despite more details about the underlying system being considered, the two controllers show no significant difference in their ability to keep BG in the physiological range. The main cause for why BG is out of range at some times is the initial period during perfusion of IRI where glucose is released by the liver in an uncontrolled manner. During the rest of perfusion, both controllers can keep BG within the range. With the model based controller, glucose varies in a narrower band as compared to the P controller but the question remains if this is necessary. Possibly, the oscillating behaviour of the P controller provides a more physiologic situation. *In vivo*, BG fluctuates during the day with the various meal intakes and insulin is released by the pancreas in a pulsatile manner rather than continuous, also leading to a reduced risk of insulin resistance<sup>159</sup>. Therefore, it is supposedly non-physiological to constantly infuse insulin as is the case with the model based controller. Concluding, there is no need for a sophisticated model based controller during *ex vivo* perfusion to prevent oscillations of BG. There are few disturbances, such as meals in the case of *in vivo* artificial pancreas systems, and a P controller suffices to ensure physiological glucose levels during NMP.

All livers possessed a certain period at the start of the perfusion, which lasted around 6 to 12 hours, where glucose was in the hyperglycemic range. The explanation is as follows. To increase tolerance to ischemia the liver is flushed with cold preservation solution and cooled down during procurement to reduce metabolism. The subsequent rewarming of the liver when it is reperfused with warm oxygenated blood leads to the inevitable ischemia reperfusion injury (IRI). One symptom of IRI is the uncontrolled release of glucose from the liver to the blood<sup>151</sup>. After the initial increase of glucose upon reperfusion, it declined in all livers to physiological levels within six to twelve hours during our experiments. This coincides with previous observations during *ex vivo* liver perfusion,

where glucose declined within six hours<sup>56,76</sup>. A declining glucose, with parallel infusion of insulin, after the initial rise during NMP is generally considered as a sign of liver function<sup>19</sup>. Further, a lack of declining glucose after IRI has been correlated with elevated lactate levels and lack of bile production and consequently concluded as poor liver function in previous studies<sup>56</sup>. During our experiments, well functioning livers always recovered to physiological glucose levels and were subsequently responsive to insulin.

If no insulin was administered, BG would rise to hyperglycemic levels. A possible explanation for this is the following. The system administers no glucose directly and glucose only enters the system via the dialysis if BG is below 5.5 mmol/L, as this corresponds to the concentration of glucose in the dialysate solution. Therefore, if BG rises above 5.5 mmol/L means that gluconeogenesis, the synthesis of glucose from lactate or amino acids, is occurring in the liver<sup>124</sup>. In the *ex vivo* liver perfusion system, the erythrocytes are the main consumer of glucose as they rely on anaerobic processing of glucose to lactate with the help of the Embden-Meyerhof pathway<sup>123</sup>. Therefore, the main consumption of glucose in our system is by the RBCs as the liver doesn't require glucose as an energy source but mainly acts as a storage buffer<sup>55</sup>. A possible reason for elevating glucose levels when fewer insulin is provided is the gluconeogenesis from the administration of amino acids. As the liver plays a vital role in the protein synthesis, amino acids are supplied into the blood in a constant manner by the system. The liver can utilize these for protein synthesis but also to produce glucose via gluconeogenesis. With the constant infusion of amino acids, the liver synthesises glucose and if no insulin was supplied, this would lead to an increase of BG.

To the best of our knowledge, glucose is not automatically controlled in other *ex vivo* liver perfusion systems. Either insulin is infused in a constant manner<sup>19,101,91</sup> sometimes with additional glucose infusion to avoid hypoglycemia<sup>101</sup>, or adapted to manual BG measurements<sup>31,93</sup>. This leads to a great variation of infused insulin rates, ranging from 1 to 200 I.U./h<sup>18</sup>. On average, our system infused 0.8 I.U./h and 0.4 I.U./h for human and pig, respectively, lying below the lower range of the reported values in literature. Reported BG levels were in hyperglycemic range<sup>31,94</sup> with additional glucose being infused, or it reduced to physiological levels within the first couple of hours<sup>160,91</sup>. Such a high BG accompanied

by constant infusion of insulin should lead to an uptake of glycogen of the liver, as also seen in our data in Fig 5.13. The effect of elevated glycogen content and non-physiological BG levels during perfusion on transplantation outcome remains unclear. However, one needs to consider that the goal of the underlying perfusion machine is to keep livers viable *ex vivo* for multiple days, implying that the blood should be kept as physiologic as possible. Though, we see that the AP only comes into effect after 6 to 12 hours, hence, for short-term perfusion, an AP is not necessarily required. However, glucose monitoring should be initiated from perfusion start since glucose decline might be observed already in earlier phases and can be intercepted, highlighting the importance of glucose monitoring from the start. In the case of long-term perfusion, it would certainly be beneficial to integrate an automated AP to maintain physiologic BG levels, also eliminating the demand for personnel to be constantly present with the machine, thus lower cost and effort for long-term perfusion of livers.

In the developed AP, only insulin is permanently infused and considered in the model as BG usually trended to hyperglycemic levels with its absence. However, an automated infusion of glucagon was always prepared to counteract hypoglycemic levels when it occurred. This happened rarely, since the liver produced glucose by gluconeogenesis in periods of basal insulin injection. Therefore, glucagon was not included in the modelling of the glucose metabolism. Further, a limitation of the model is the simplification of the hepatic glucose production and consumption into one equation with the only dependency of insulin. However, the results obtained with this model are satisfying and work well for the developed controller in the present system.

## 5.5 Conclusion

In this chapter, a method is presented to continuously control blood glucose during *ex vivo* liver perfusion by automated closed loop infusion of insulin. A sensor has been applied and evaluated to continuously measure blood glucose and presents the basis for the controller. Two controllers were implemented and tested, namely a P controller and a model based controller. A model was developed to be applied in the

model based controller. In the end, the P controller suffices to keep blood glucose within the physiological range and potentially provides a more physiological, oscillating situation. The glucose control was developed based on pig liver perfusion experiments and its feasibility with human livers shown. In both cases, blood glucose can be kept in physiological range during most of perfusion duration. This chapter provides the basis to integrate continuous glucose control into an *ex vivo* liver perfusion system and shows its feasibility for long-term perfusion.

## Chapter 6

# Model assisted analysis of the hepatic arterial buffer response during *ex vivo* porcine liver perfusion

In this chapter, hemodynamic studies on the liver were performed. The hepatic arterial buffer response was studied on the *ex vivo* perfusion system and new insights regarding this intrinsic behaviour obtained. The data presented in this chapter was published in a peer reviewed journal<sup>115</sup>.

### 6.1 Introduction

Although the first observation of the intimate relation between hepatic artery (HA) and portal vein (PV) flows was documented in 1911<sup>161</sup>, it took until 1981 when the phenomena was titled hepatic arterial buffer response (HABR)<sup>162</sup>. It describes the reaction of HA flow in response to changes in PV flow. If PV flow is suddenly reduced, HA flow quickly adapts to compensate the reduced PV flow in order to minimize fluctuations of total hepatic flow<sup>163</sup>. On the other hand, the PV shows no response to changes in HA flow<sup>164</sup>, which is why the relationship was named hepatic arterial buffer response. However, observations of a reaction of PV flow upon HA pressure variations have also been reported<sup>165</sup>. Although there is still no clear consensus regarding the underlying mechanism behind HABR<sup>166</sup>, the current main hypothesis relies on the washout of

adenosine<sup>42</sup>. Adenosine, a potent vasodilator, is constantly produced in the space of Mall, the region between the hepatic arteriole, portal venule and bile ductule. According to the washout theory, changes in the PV result in different washout rates of adenosine from the space of Mall. Increased PV flow, which leads to more adenosine being removed from the space of Mall, causes vasoconstriction of the HA due to the vasodilator effect of adenosine on the HA<sup>39</sup>. Although the effect and role of adenosine in HABR is generally accepted, it has been shown that it cannot be the sole mediator of this intimate relation<sup>167168</sup>. Further, the sensory influence on HABR is still in dispute. While studies have shown different behaviours between enervated and denervated rat<sup>169</sup> and pig<sup>170</sup> livers, even showing an inverted response of HABR in the latter case, other studies concluded no neurogenic effect on HABR<sup>171172</sup> while also observing it in transplanted livers<sup>173174</sup>.

In addition to HABR, the liver has an intrinsic regulation mechanism called arterial autoregulation<sup>163</sup>. This describes changes in HA resistance upon changes in HA pressure. If HA pressure increases, HA resistance increases and vice versa. This effect serves to keep total hepatic blood flow constant with changing blood pressures. The current consensus on the underlying mechanism of arterial autoregulation is also attributed to an effect of adenosine. Similar to HABR, a decreased flow in the HA leads to an accumulation of adenosine in the space of Mall and, hence, consequent vasodilation of the HA<sup>175</sup>.

Before the adenosine washout theory regarding HABR emerged, the underlying mechanism was believed to be myogenic<sup>176177</sup>; the response of arteries to contract upon increased transmural pressure or stretch<sup>178</sup>. In addition to HABR and hepatic autoregulation, a third mechanism has been observed: a response of the HA resistance to changing hepatic venous (VC) pressures<sup>179180</sup>. This effect was also reasoned to be of myogenic nature<sup>181</sup>. Of note, *in vivo* studies exploring the effect of vena cava (VC) pressure on HABR have limitations, since they are also affected by the presence of flow from lower extremities and kidneys. Currently, there is no clear consensus regarding a myogenic mechanism in the HA.

The aim of this study was to understand the role of intrahepatic pressures on HA resistance and elucidate its role during HABR in a controlled *ex vivo* setting. For this purpose, flow experiments were conducted on a custom built normothermic *ex vivo* perfusion machine. Due to the

isolation of the liver in the *ex vivo* perfusion machine, influences of blood flow from lower extremities and kidneys are excluded. A simplified hemodynamic model, which splits the liver into three compartments, namely HA, PV and VC, was developed. The model was applied to analyse and interpret the experimental measurements and to relate the resistances of the three compartments.

## 6.2 Materials & Methods

### 6.2.1 Experiments

#### Perfusion machine

The experiments were conducted on the developed perfusion machine. Important for these experiments was that the setup allowed the control of flow or pressure at the HA, PV and VC independently, thereby allowing an investigation of the individual parameters. The force sensors continuously measured the weight of the blood reservoir and of the liver container. This gave feedback about the amount of blood inside the reservoir and, respectively, the liver, which was used to analyze the compliance of the liver.

#### Liver procurement

For the experiments, four land race pigs (mean weight = 102 kg) were used. The experiments were performed in accordance with the Swiss Animal Protection Law and Ordinance. Laparotomy was performed under general anesthesia and sterile conditions. The livers (mean weight = 1.8 kg) and blood (mean volume = 2.95 L) were collected in standardized manner as described previously<sup>121</sup>. Table 6.1 gives an overview of these livers.

**Table 6.1:** Overview of the harvested livers and conducted experiments.

	Liver #	1	2	3	4
$m_{liver}$	kg	2.3	1.7	1.39	1.8
$m_{pig}$	kg	119	108	95	87

## Experimental procedure

During the course of the perfusion, multiple excitation tests were performed, in one of two ways. In one scenario, the PV flow was varied stepwise while keeping HA and VC pressure constant. Such an example is shown in Fig. 6.1. This allowed observing the HA flow changes upon varying PV flow. In the second scenario, the VC pressure was varied while keeping HA pressure and PV flow constant. This allowed to study the HA resistance upon VC pressure changes. Further, HA pressure was always controlled to remain at a constant level to avoid the effect of arterial autoregulation. PV flow and VC pressure were varied from 0.4 L/min to 2 L/min and from  $-4$  mmHg to 10 mmHg, respectively.

### 6.2.2 Data post-processing

The data was analyzed in the following way. As shown in Fig. 6.1, the response of the HA flow upon a stepwise flow change in the PV was approximated by a first order lag element and described by:

$$\frac{F_{HA}(t) - F_{HA,0}}{\Delta F_{HA}} = 1 - e^{-t/\tau} \quad (6.1)$$

where  $F_{HA,0}$  is the flow in the HA before the step in [L/min],  $\Delta F_{HA}$  is the change in HA flow in [L/min] and  $\tau$  is the time constant of the response in [s]. The curve was fitted to the data by estimating  $\Delta F_{HA}$  and  $\tau$ , whereas the starting time  $t_0$  of the step was defined and  $F_{HA,0}$  was set to the value before the step. This yielded an objective analysis of the magnitude and the time constant of the response. Further, the steady state time constant  $\tau_{ss}$  was defined as  $\tau_{ss} = 3 \cdot \tau$  to reflect the time until the response reaches 95% of its maximum value. This method was applied to analyse the measured data in response to applied PV flow and VC pressure variations.

As the goal of HABR was to eliminate fluctuations of total hepatic flow, the buffer capacity ( $BC$ ) of the HA was defined as the ratio of hepatic arterial flow change to PV flow change, i.e.

$$BC = (-100\%) \cdot \frac{\Delta F_{HA}}{\Delta F_{PV}} \quad (6.2)$$



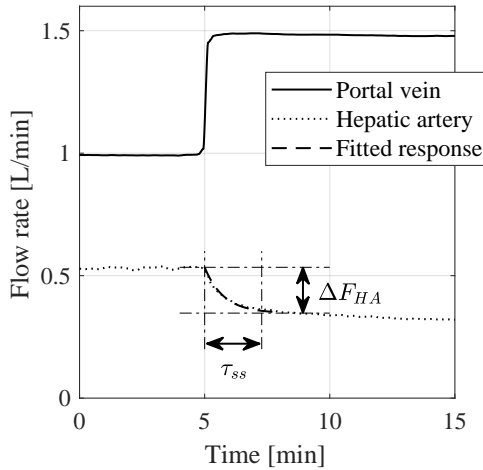


**Figure 6.1:** Example of the imposed PV flow change in liver #1. Step was from 1 L/min to 1.5 L/min and the consequent change of hepatic arterial flow from  $\sim 0.53$  L/min to  $\sim 0.35$  L/min while keeping HA and VC pressure constant. The first order response, change in arterial flow  $\Delta F_{HA} = -0.18$  L/min and steady state time constant  $\tau_{ss} = 137$  s are also illustrated. HA pressure was controlled as described above and VC pressure was controlled to -1 mmHg in this example. The illustrated data was averaged to a 10 seconds period to enhance the readability.

where  $BC$  is in percent. The ratio is multiplied by  $-100$  because of the inverse relationship and the consequent negative sign of  $BC$ . If the HA was capable of buffering the entire change in PV flow, then the buffer capacity was 100%.

### 6.2.3 Hepatic hemodynamic model

#### General model

In order to support the interpretation of the acquired data, a mathematical model was developed. The model is a simplified version of similar models from the literature<sup>182183184</sup>. The model employed an electrical analogy where the pressure drop ( $\Delta p$ ) and blood flow ( $F$ ) were equivalent to the electrical potential ( $U$ ) and current ( $I$ ), respectively. The schematics of the model network is shown in Fig. 6.2 and the respective signal flow chart in Fig. 6.3. The network simplified the circulatory network of the liver into three compartments, namely HA, PV and HV with the junction at the hepatic sinusoids (HS). This yields the following set of equations, which are valid in the steady state scenario.

$$\begin{aligned} p_{HA} - p_{HS} &= F_{HA} \cdot R_{HA} \\ p_{PV} - p_{HS} &= F_{PV} \cdot R_{PV} \\ p_{HS} - p_{VC} &= (F_{HA} + F_{PV}) \cdot R_{HV} \end{aligned} \quad (6.3)$$

with all pressures  $p$  in [mmHg], flows  $F$  in [L/min] and resistances  $R$  in [mmHg/(L/min)].

As the compliance of the liver has been shown to occur solely in the HV<sup>185</sup>, the compliance ( $C_L$ ) was defined to be at the junction of the three branches. Further, previous models have assumed much larger compliance in the HV as compared to PV, leading to the simplification of only considering the compliance in the HV<sup>184</sup>. A linear relationship for compliance of the liver has previously been shown<sup>186</sup> and is commonly applied for venous compliance<sup>187</sup>. Hence, compliance in the model was defined as:

$$C_L = \frac{V_{HV} - V_{HV,0}}{p_{HS} - p_{HS,0}} \quad (6.4)$$

with the volume  $V$  in [L] and compliance  $C_L$  in [L/mmHg].

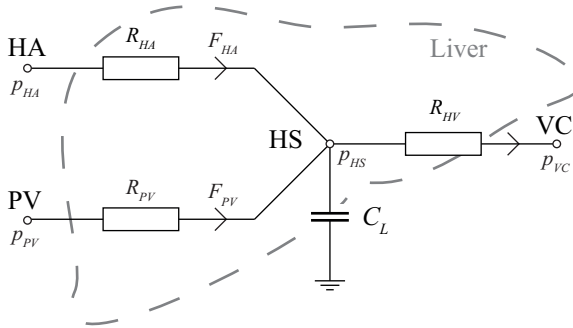


**Figure 6.2:** Illustration of the simplified hepatic model with use of electric analogy. The two entries, HA and PV, the junction in the HS, and the exit of the VC are shown. Three resistances  $R_{HA}$ ,  $R_{PV}$  and  $R_{HV}$  represent the respective branches and a capacity  $C_L$  the hepatic compliance in the hepatic veins.

To obtain the blood volume from the mass measurement, a blood density of  $1060 \text{ kg/m}^3$  was assumed. Due to changing amounts of total blood volume in the system, it was not possible to measure the absolute blood volume inside the liver. Hence, the relative volume changes during liver excitations were measured through measuring the relative volume changes of the blood reservoir. The volume of the reservoir decreases with increasing blood volume in the liver, hence, they were related inversely. Therefore, the following relation applied during a stepwise excitation of the liver

$$\Delta V_{HV} = -1 \cdot \Delta V_{Reservoir} \quad (6.5)$$

### Resistance modeling

The blood was assumed to follow the Hagen-Poiseuille equation in a circular pipe which gives a relation for the flow resistance according to:

$$R = \frac{8\mu l}{\pi r^4} \quad (6.6)$$

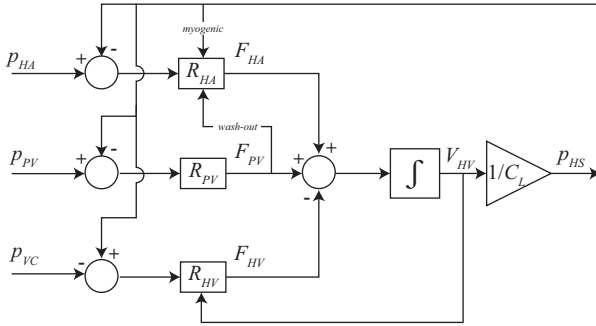


**Figure 6.3:** Signal flow chart of the described model. This illustration highlights the influences of HS pressure and PV flow on HA resistance, described by (6.10) and (6.11), respectively, as well as the HV volume on HV resistance, described by (6.8).

where  $\mu$  is the dynamic viscosity,  $l$  the length of the tube and  $r$  the radius of the tube. The HA, PV and HV branches are comprised of a network of tubes, which the model lumped into a single resistance for each branch. Therefore, there was no single tube length or radius to represent the tube. Further, the volume of a tube was applied ( $V = \pi r^2 l$ ) and it is assumed that the length of the blood vessels is constant ( $l = \text{const.}$ ). When combined with (6.6), this yields the following empirical relation between the flow resistance and the blood volume in the respective branch

$$R \propto \frac{1}{V^2} \quad \rightarrow \quad R = \frac{k_1}{V^2 + k_2 V + k_3} \quad (6.7)$$

where  $k_1$ ,  $k_2$  and  $k_3$  are empirical factors with units [mmHg·L<sup>2</sup>/(L/min)], [L] and [L<sup>2</sup>], respectively. The empirical factors were determined from the measurement data. The PV branch was assumed to have constant resistance as compliance takes place in the hepatic veins<sup>185186</sup>. Therefore,

(6.7) only applied to HV:

$$R_{PV} = \text{const.}$$

$$R_{HV} = \frac{k_{1,HV}}{V_{HV}^2 + k_{2,HV} \cdot V_{HV} + k_{3,HV}} \quad (6.8)$$

with  $k_{1,HV}$ ,  $k_{2,HV}$  and  $k_{3,HV}$  being the empirical factors of the HV, as described above.

Finally, the goal of the model was to obtain the resistance of the HA upon PV flow and VC pressure changes. Observations of the myogenic response of the HA resistance due to changing VC pressure have been reported to be due to changing hepatic sinusoidal pressure levels resulting in a myogenic response of the terminal arterioles<sup>181</sup>. As changes in PV flow also result in varying HS pressures, this effect needs to be considered to correctly analyze the effect of HABR. Here, the goal was to obtain a relationship between the PV flow and HA resistance, where the effect of the HS pressure on HA resistance is considered, i.e. the effect of changing washout rates and myogenic mechanisms need to be decoupled. The assumption was made, that the total HA resistance can be represented by the product of a baseline resistance and two individual factors:

$$R_{HA} = R_{HA,0} \cdot K_{myo} \cdot K_{wo} \quad (6.9)$$

where  $R_{HA,0}$  is the basal HA resistance,  $K_{wo}$  is the dimensionless factor of varying washout rates in the PV, i.e. the influence of changing PV flow rates, and  $K_{myo}$  is the dimensionless factor of changing myogenic responses in the HA, i.e. the effect of HS pressure.

To determine  $K_{myo}$ , the influence of varying HS pressure needs to be known. It can be obtained by solely varying VC pressure, thus varying HS pressure, while keeping all other inputs constant. Comprehensive models have been developed studying the myogenic mechanism in vessels<sup>188</sup>, however, in this paper, a simplified approach was applied. The relationship between hepatic venous pressure and arterial resistance was assumed to be linear, as was shown previously<sup>181</sup>, and was defined as follows

$$K_{myo} = f(p_{HS}) = a \cdot (p_{HS} - p_{HS,0}) + 1 \quad (6.10)$$

with  $a$  and  $p_{HS,0}$  being constants of units [1/mmHg] and [mmHg], respectively. With this function known, the influence of PV flow can then

be calculated and the dependency of HA resistance on PV flow were determined

$$K_{wo} = \frac{R_{HA}}{R_{HA,0}} \cdot \frac{1}{K_{myo}} = \frac{\widehat{R}_{HA}}{K_{myo}} = f(F_{PV}) \quad (6.11)$$

where  $\widehat{R}_{HA}$  is the normalized HA resistance.

By these means, the isolated effect of varying portal venous flow without changes in hepatic sinusoidal pressure can be determined.

### Model identification

Before the proposed model was used for the interpretation of the data, the missing model parameters were identified. This was achieved by fitting the model to the data of the VC pressure variations because, as described above, only VC pressure was varied while keeping HA pressure and PV flow constant. This enabled the identification of the PV resistance in (6.3), the hepatic compliance in (6.4), the relation between HV resistance and HV volume in (6.8) and especially the relation between HA resistance and HS pressure in (6.10). With the identified parameters, the model was applied to the PV flow variations to decouple the effect of washout and myogenic effects.

### Constraints

To estimate the parameters, the following constraints were used. First, the relation of hepatic venous resistance and hepatic blood volume (see (6.8)) was defined to have a negative slope for the given data points. Reason being that with an increasing volume, the radius of the vessels increase, leading to a decrease of resistance. Therefore, a decreasing slope resembles the physiological behaviour.

$$\frac{dR_{HV}}{dV_{HV}} < 0 \quad (6.12)$$

Second, to avoid the denominator of  $R_{HV}$  in (6.8) to become zero, which would lead to a singularity, the denominator was defined to have no real solutions for all volumes. Therefore, when applying the quadratic formula

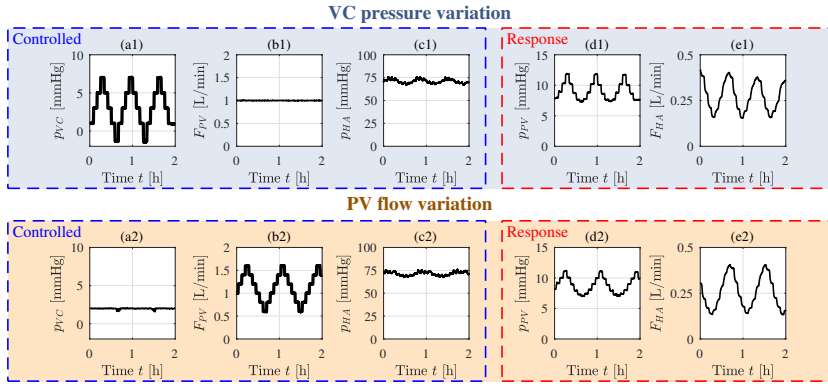


**Figure 6.4:** Exemplary series of Liver #3 showing the effects of varying VC pressure (a1) or PV flow (b2), while keeping HA pressure constant (c1) & (c2), on PV pressure (d1) & (d2) and HA flow (e1) & (e2). During the first 2 hours of the test cycle, VC pressure was varied while all other input parameters were kept constant, whereas afterwards, PV flow was varied while keeping all other parameters constant. The resulting magnitude of HA flow and PV pressure changes are in a similar range for both cases. The illustrated data was averaged over 10 second periods to enhance the clarity of the data.

to the denominator of (6.8) and defining the term in the square root of the quadratic formula to be negative to avoid any real solution to exist, we obtain the following relation.

$$k_{2,HV}^2 - 4 \cdot k_{3,HV} < 0 \quad (6.13)$$

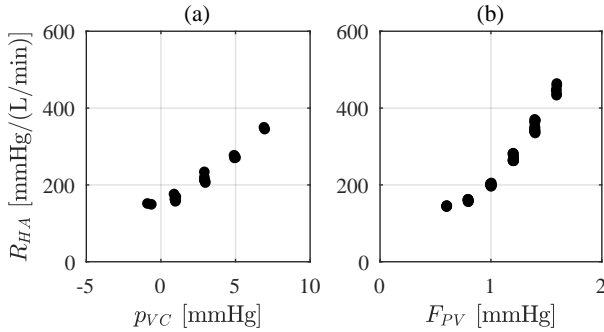


**Figure 6.5:** Exemplary series of Liver #3 of VC pressure and PV flow step changes performed on liver consecutively while keeping all other inputs constant. This example illustrates the isolated effect of varying VC pressure (a) or PV flow (b) on HA resistance, respectively.

## 6.3 Results

### 6.3.1 Observations

In Fig. 6.4, two subsequent VC pressure and PV flow variation cycles are shown. Initially, the VC pressure was varied stepwise (Fig. 6.4 (a1)) while keeping PV flow (Fig. 6.4 (b1)) and HA pressure constant (Fig. 6.4 (c1)). The resulting effect on PV pressure (Fig. 6.4 (d1)) and HA flow (Fig. 6.4 (e1)) is obvious. An increasing VC pressure caused a proportional increase of PV pressure and an inversely proportional decrease in HA flow. As PV flow was kept constant during these test cycles, the increasing PV pressure resulted from elevated HS pressure. Further, HA flow was reduced with increasing PV pressure, while, again, PV flow was kept constant. In the subsequent test cycle, PV flow (Fig. 6.4 (b2)) was varied while keeping VC pressure (Fig. 6.4 (a2)) and HA pressure (Fig. 6.4 (c2)) steady. This is shown on the right side of the dashed line in Fig. 6.4. Again, both PV pressure (Fig. 6.4 (d2)) and HA flow (Fig. 6.4 (e2)) varied in a similar magnitude as before during the VC test cycles. In Fig. 6.5, the resulting HA resistance ( $R_{HA}$ ) was quantified for the



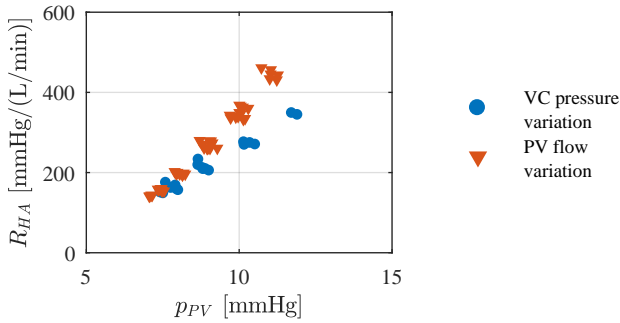


**Figure 6.6:** Relation between PV pressure ( $p_{PV}$ ) and HA resistance ( $R_{HA}$ ) upon variation of PV flow and VC pressure. The shown data points are from the same exemplary sequence of Liver #3 as shown in Fig. 6.4 and Fig. 6.5.

two cases described above. Fig. 6.5 (a) and (b) show the resulting HA resistance upon VC pressure and PV flow variations, respectively. Taking the PV flow at 1 L/min as reference, an increase of 60% yielded a 2.5 fold increase of HA resistance while reducing the PV flow by 50%, yielded a reduction of HA resistance of 40%. Similarly, varying the vena cava pressure from -1 mmHg to 7 mmHg influenced the HA resistance from 150 mmHg/(L/min) to 350 mmHg/(L/min). It becomes apparent that both, VC pressure and PV flow, strongly influenced the HA resistance.

Fig. 6.6 shows the relation between the HA resistance and the respective resulting PV pressures for the two cases. PV pressure does not relate linearly to intrahepatic pressure upon a change in PV flow, as varying PV flow results in different pressure drops from the PV to the HS. This is different for the case of VC pressure variations, as varying PV pressure are only due to changing intrahepatic pressure levels, as flow and resistance in PV stay constant in this scenario. Keeping this in mind, two things become apparent. First, there seems to be a linear relation between PV pressure and HA resistance due to VC pressure variations. This also indicated a linear relation between HA resistance and HS pressure. This is in line with previous studies<sup>181</sup> and justifies the assumption of linearity in (6.10). Second, the change in HA resistance was larger in the case

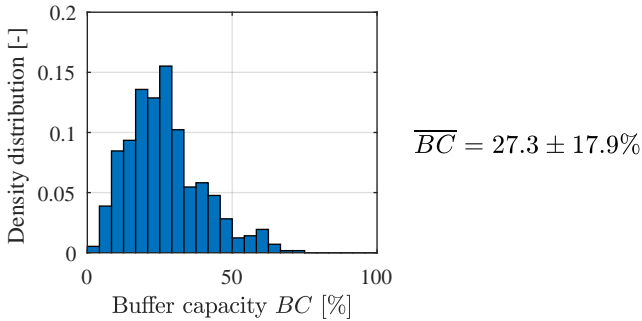
**Table 6.2:** Literature data regarding buffer capacity of HA in various animals.

Source	Animal	$BC$
Lautt et al. <sup>189</sup>	cat	44%
Ezzat et al. <sup>175</sup>	cat	25%
Troisi et al. <sup>190</sup>	human	11%
Henderson et al. <sup>173</sup>	human	9%
Schenk et al. <sup>191</sup>	human	27%
Aoki et al. <sup>192</sup>	human	34%
Jakob et al. <sup>193</sup>	pig	25%
Ayuse et al. <sup>164</sup>	pig	29%

of PV flow variations as compared to VC pressure variations, also in accordance with previous observations<sup>177</sup>. This is most likely due to an overlay of the two effects, namely the myogenic response and washout of adenosine. The different washout rates of adenosine as PV flow varies causes further constriction or dilation of the HA. However, with changing PV flows, intrahepatic pressure also varies and the two effects should be considered in a combined manner. Using the model, a relationship according to (6.9) is sought to decouple these two effects and allow for a better interpretation of the data, as described in the following chapter.

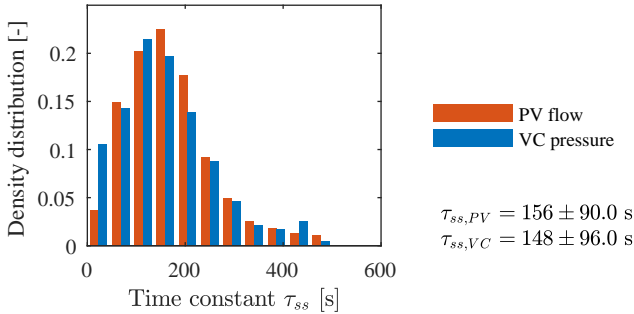
### 6.3.2 Buffer capacity and time constants

Fig. 6.7 shows the distribution of the HABR buffer capacity  $BC$  of all investigated livers. The density distribution includes all the PV flow step changes that were performed with the four livers, which amounts to 567 steps in total. The average buffer capacity  $\overline{BC}$  was 27%, with samples ranging from close to 0 to about 75%. In literature, a large range of data can be found regarding the  $BC$  of the HA (see Table 6.2). Looking at the data from pigs<sup>164,193</sup>, the results are very similar to the ones obtained in our experiments. Two things can be concluded from this comparison. On the one hand, HABR truly seems to be mediated by intrinsic mechanisms of the liver, as opposed to external influences such as nerve stimulus. This has been reported before and is again confirmed by this observation. On



**Figure 6.7:** Distribution of HABR buffer capacity  $BC$ ; capacity of HA flow to compensate for PV flow changes, as described in (6.2). Distribution includes all step tests from all livers, in total 567 steps.

the other hand, the magnitude of HABR of the *ex vivo* perfused liver is of similar magnitude as measured *in vivo*, implying an intact mechanism and functionality despite the *ex vivo* environment. This does support the validity of comparing *ex vivo* and *in vivo* results. Fig. 6.8 shows the distribution of the time constants of the first order responses of HA flow due to VC pressure and PV flow variations according to (6.1) for all test cycles and livers combined. On average, the time to reach 95% of change in HA flow due to changing VC pressure was 148 s, whereas, the time to obtain 95% change in HA flow due to PV flow variations was 156 s. Considering the close match of dynamic behaviour of the responses, this suggests the underlying mechanism during the two scenarios to be similar and supports the proposed model. In literature, the time constants are not reported and the reaction time of HABR is stated as immediate<sup>194</sup>. Considering that the measurements in these reports are performed at time intervals of several minutes, a time constant of 156 s can be considered as immediate.



**Figure 6.8:** Distribution of time constants  $\tau_{ss}$  of HA resistance response due to varying PV flow (blue) or VC pressure (red). Data includes all experimental data points from all livers.  $\tau_{ss}$  indicates the time for 95% of the response to occur.

### 6.3.3 Model identification

As described above, the model is identified by means of the VC pressure variation experiments. Fig. 6.9 shows the obtained compliance of the livers according to (6.3) with the corresponding linear fits for each experiment. The results are in accordance with each other with an average obtained compliance of  $C_L = 6.0 \pm 0.12$  mL/(mmHg·100 g). Liver 2 lies above the other three livers which can be explained as follows. Due to some data points of liver 2 in  $R_{HV} - V_{HV}$  (see Fig. 6.10) outlying, the system estimates a lower slope for  $R_{HV} - V_{HV}$  of liver 2, thereby shifting the data to higher volumes. The important factor in this analysis is the compliance  $C_L$ , which is given by the slope of the lines in Fig. 6.9, and it is very similar for all four investigated livers. In literature, a lower compliance of 2.4-3.0 mL/(mmHg·100 g) was reported in cats<sup>195,186</sup>, 2.0 mL/(mmHg·100 g) in dogs<sup>185</sup> and 2.5-3.3 mL/(mmHg·100 g) in pigs<sup>196</sup>. The obtained compliance in our experiment is approximately two-fold of previously reported data. Livers have shown to behave differently upon denervation<sup>39</sup> with a reduced compliance upon nerve stimuli<sup>197</sup>. A possible reason for the enhanced compliance during our experiments may therefore be the denervation of the livers on the *ex vivo* perfusion

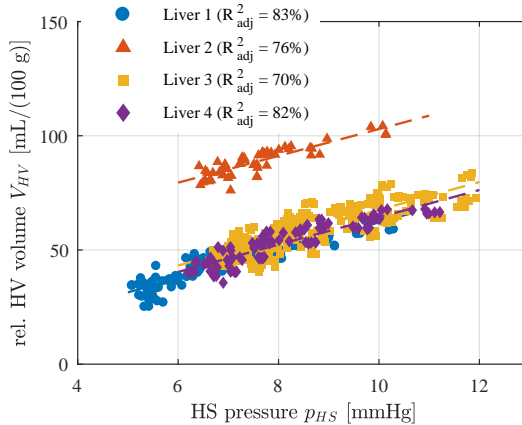


**Figure 6.9:** Hepatic compliance. Results shown with fitted linear model according to (6.3) corrected to the respective liver weights (see Table 6.1).  $R_{adj}^2$  of linear fit is shown. The resulting compliance  $C_L$  are 6.1, 5.9, 6.1, and 6.0 mL/(mmHg·100 g liver), for livers 1 to 4, respectively.

machine. Further, a hepatic blood volume of 8.2 mL/(kg body weight) at  $p_{PV} = 8$  mmHg was reported in cats<sup>186</sup> which is in a similar range to the model results at  $p_{HS} = 8$  mmHg of 10.9 mL/(kg body weight).

Fig. 6.10 shows the obtained relation between HV resistance and HV volume as proposed by the model (6.8). The model can fit the proposed equation with an acceptable accuracy. Again, liver 2 poses an exception with a low  $R_{adj}^2$  of 27% which again can be explained by the outliers in the data set.

For all the livers, the resistance in the PV is fitted to be zero. Even though this is not physical, it provides further insights. First, previous studies have reported a much smaller resistance in the PV than in the HV ( $R_{PV} \ll R_{HV}$ ). In fact, 90% of the total pressure drop from PV to VC was reported to occur across the HV<sup>3940</sup>. Hence, the model underestimates the resistance in the PV, however, qualitatively correctly describes that the main resistance is due to the HV. Second, this suggests

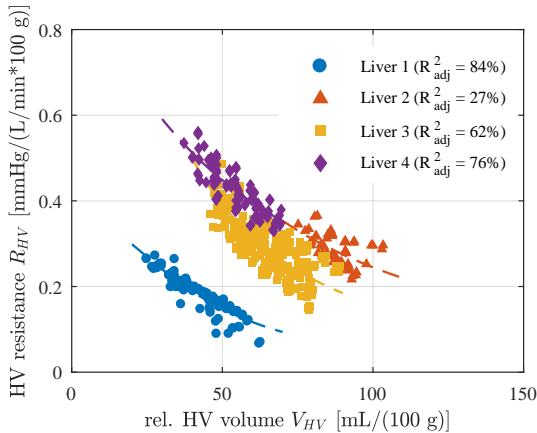


**Figure 6.10:** Model results of relation between HV resistance  $R_{HV}$  and hepatic blood volume  $V_{HV}$ . The resulting coefficients of (6.8) for livers 1 to 4 are, respectively, for  $k_{1,HV}$ : 615, 7803, 3006, 1080 mmHg/(L/min·100 g)/(mL/100 g),  $k_{2,HV}$ : 0, 157, 75, 210 mL/100 g,  $k_{3,HV}$ : 1660, 6178, 1418, 1106 (mL/100 g)<sup>2</sup>.

that the model could be further simplified and the PV branch could be directly lead into the HS, without an additional resistance. Such a model would admit an analytical solution as HS pressure is assumed to be the same as PV.

Finally, the goal of the VC pressure variations was to obtain a relation between the HA resistance and HS pressure as described in (6.10). Fig. 6.11 shows this obtained relationship between HA resistance and HS pressure. The linear fit according to (6.10) is plotted with the data, the respective linear constants are listed in Table 6.3. The linear relation between  $R_{HA}$  and  $p_{HS}$  shows a reasonable  $R^2_{adj}$  for all livers, indicating that the linear assumption is plausible. The slope for all of the four livers is in a similar range with an average value of 0.26 1/mmHg and a standard deviation of 0.06 1/mmHg. The fact that the linear fits do not go through the origin can be neglected due to the following reason.

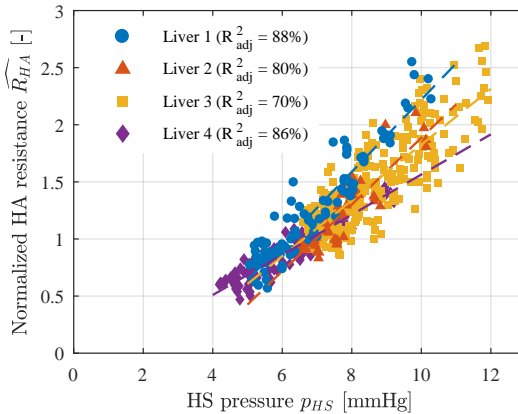


**Figure 6.11:** Influence of HS pressure on HA resistance. Data points obtained from isolated VC pressure variations. Resulting HA resistance versus HS pressure relationship with respective linear fits and adjusted  $R^2$  shown in plot. This represents the influence of HS pressure on HA resistance, i.e.  $K_{myo}$ . The resulting linear coefficients are listed in Table 6.3.

As the manipulation of HS pressure is realised by variation of VC pressure, the HS pressure is limited by the minimum level of VC pressure which was always reached at slight sub-atmospheric pressure in the VC ( $< 0$  mmHg) due to collapsing of the veins. The collapsing sets the lower limit of the attainable VC pressure. Further reducing the VC pressure only resulted in more frequent collapsing of the veins, increased the risk of vessel damage and was therefore avoided. Hence, the entire range of the investigated relation between HS pressure and HA resistance can be seen as linear.

### 6.3.4 Model assisted data analysis

Finally, the identified relations for (6.3), (6.8) and (6.10) in the previous chapter are applied to the PV flow variation data sets. The goal is to decouple the influence of HS pressure, i.e. the myogenic effect, and PV

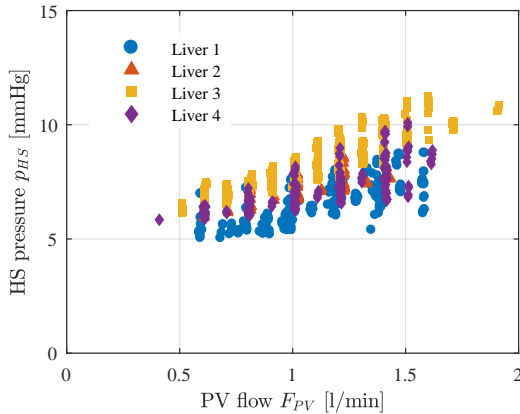


**Figure 6.12:** Relation between HS pressure  $p_{HS}$  and PV flow  $F_{PV}$ . Data points obtained from PV flow variations. A clear correlation between increasing PV flow and increasing HS pressure is observable. The myogenic effect due to the elevated HS pressure needs to be considered for the analysis of the PV flow variations.

flow, i.e. the washout effect, on HA resistance.

In Fig. 6.12, the relation between the HS pressure and PV flow is shown. For all livers, a positive relation between HS pressure and PV flow can be observed. This increase in HS pressure leads to the previously identified increase in HA resistance due to the myogenic response. This is then used to consider the myogenic effect during PV flow changes, as follows.

In Fig. 6.13, the left side of the plots shows the relation between normalized HA resistance and PV flow. In all four livers, a clear correlation is observable, as to be expected due to the known effect of HABR. However, both effects, the myogenic and washout, are contributing to the HA resistance. As shown in Fig. 6.12, a varying PV flow inherently also varies HS pressure and, therefore, the influence of HS pressure on HA resistance, i.e. the myogenic contribution, needs to be considered and deducted as



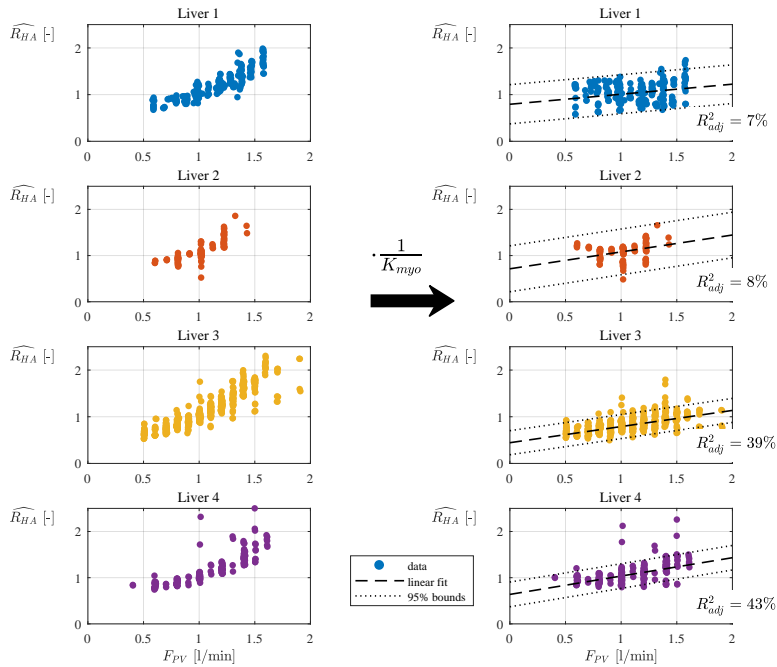


**Figure 6.13:** Left: Normalized HA resistance ( $\widehat{R}_{HA}$ ) versus PV flow ( $F_{PV}$ ). Right: Isolated effect of PV flow on HA resistance by considering the effect of elevated HS pressures on HA resistance. This is realized by evaluating HS pressure at each data point with the obtained  $R_{HA} - p_{HS}$  relationship from (6.10) and correcting accordingly. Linear fit to data and 95% confidence interval shown in graph.

**Table 6.3:** Coefficients for the linear relationship of  $K_{myo}$ 

Liver #	$a$ [1/mmHg]	$p_{HS,0}$ [mmHg]
1	0.32	6.1
2	0.29	7.0
3	0.24	6.6
4	0.18	6.8

described in (6.11). This yields the isolated influence of washout effects in the PV on HA resistance, i.e. the sole effect of adenosine washout in the PV. On the right side of Fig. 6.13, the contribution of HS pressure to the HA resistance change is considered by dividing the results of the left side by  $K_{myo}$ , obtained from the isolated VC pressure experiments. Thereby, the HS pressure at each data point is determined and, according to (6.8) with the obtained parameters in section 6.3.3, the effect on HA resistance evaluated, yielding  $K_{myo}$  for each liver. The isolated data points are then shown on the right side of Fig. 6.13 for each liver which corresponds to  $K_{wo}$  as proposed in (6.11).

When comparing right and left side of Fig. 6.13 for each liver, it becomes apparent that the sole influence of PV flow on HA resistance is less when the myogenic effect of HS pressure elevations are considered, as expected. However, there is still an influence of PV flow on HA resistance, i.e. the washout effect seems to also be present. This suggests an overlaying effect of myogenic contractions in the HA and washout of adenosine in the PV. These conclusions are in accordance with results that do not suggest an exclusive role of the washout theory in HABR<sup>167</sup>. For all livers, there seems to be a mild increase of  $R_{HA}$  with PV flow. This is supported by a linear fit as shown in the figures. However, due to the large variance of the data, the resulting  $R^2$  are indeed very low. On average, a total occlusion of the PV from 1 L/min to 0 L/min, would yield a 33% reduction in HA resistance, considering purely the washout of adenosine.

## 6.4 Discussion

In this study, we have analyzed the effect of VC pressure and PV flow on HA resistance in a controlled *ex vivo* normothermic perfusion machine. The controlled environment allowed for a isolated study of the liver hemodynamics, excluding the influence of other *in vivo* factors. Thereby, we present three main findings.

First, we showed that HABR could be reproduced in the *ex vivo* environment, indicating that the liver can maintain its physiological hemodynamic behaviour. HABR was unimpaired, as the buffer capacity *BC* lies in a similar range as compared to *in vivo* studies<sup>164,193</sup>. This offered an *ex vivo* platform on which HABR could be extensively studied, avoiding influences of other *in vivo* disturbances. The dynamic behaviour of HABR was also quantified. *In vivo* studies normally measured the hemodynamic reactions of the liver in intervals of multiple minutes, which lead to the conclusion of an immediate reaction of the HA upon PV flow changes<sup>194</sup>. With an average reaction time of around 2.5 minutes obtained in our experiments, this is in line with previous observations.

Second, we showed that VC pressure strongly influences HA resistance. The reaction of HA resistance upon elevated VC pressure is well beyond a passive milieu. An influence of elevated venous pressures on HA resistance was previously concluded to be due to a myogenic reaction of terminal arterioles upon elevated sinusoidal pressure<sup>181</sup>. We also applied the myogenic hypothesis to explain the dependency of HA resistance upon VC pressure. Assuming that the VC pressure relates to sinusoidal pressure through a simplified hemodynamic model, we quantified the relation between HA resistance and HS pressure. The relation showed a clear linear behaviour, similar to previous observations<sup>181</sup>.

Third, HABR is mediated by a combined myogenic and washout mechanism. As a change in PV flow inherently also leads to a variation of HS pressure and we clearly observed a dependency of HA resistance on HS pressure, a portion of the PV flow influence on HA resistance must be triggered in the same way as due to VC pressure variations, i.e. myogenic. Therefore, the quantified myogenic response was considered when varying the PV flow. There was still a dependency of HA resistance upon PV flow when the myogenic part was deducted, yielding the isolated effect of adenosine washout. This lead us to our final conclusion that HABR is

mediated by an overlaying effect of adenosine washout and a myogenic reaction.

Currently, the main hypothesis regarding HABR relies on the washout theory of adenosine<sup>198</sup>, however, a recent review has shown that other mediators are also considered<sup>42</sup>. Hydrogen sulfide ( $H_2S$ ) has been shown to play a major role in HABR, as  $H_2S$  donor infusion increased  $BC$  and  $H_2S$  production enzyme inhibitor reduced  $BC$ <sup>168</sup>. Further,  $H_2S$  was shown to decrease the myogenic response in cerebral arterioles<sup>199</sup> and reduce myogenic tone in rats<sup>200</sup>. Hence, the acting mechanism of  $H_2S$  in the liver may be through the myogenic response of the terminal arterioles, which is weakened by the presence of  $H_2S$ . Interestingly, although a myogenic mechanism inside the liver had been observed previously on multiple occasions<sup>177179180181</sup>, also linking its role to HABR<sup>176177181201</sup>, its relevance for HA resistance remains unmentioned in contemporary literature regarding hepatic circulation<sup>4239</sup>. The most recent mentions of an influence of VC pressure levels on HA resistance are in relation with positive end-expiratory pressure (PEEP) studies<sup>180202</sup>. In one study, the central venous pressure (CVP), i.e. VC pressure, was varied by means of PEEP<sup>180</sup>. An increased VC pressure lead to a decrease of PV flow, however, a reaction of the HA was absent even though expected due to HABR. The authors reasoned an opposing effect of reduced HA resistance with reduced PV flow and increased HA resistance with elevated VC pressure. This complies with the observations in our study. As a main player in HABR is the HS pressure, which is increased in their study, a reduction in PV flow cannot surpass this influence on HA resistance. The authors were exposed to further *in vivo* effects of different organs, unable to vary the individual in- and outflow parameters of the liver independent from each other. In another study, authors reported a reduction of HA flow upon elevated VC pressure levels during hypothermic machine perfusion<sup>165</sup>. Further, they reported an alternating increase and decrease of HA and PV flow upon VC obstruction. We did not observe such a phenomena during our experiments, likely caused by the difference in perfusion settings. On the one hand, our experiments were conducted in normothermic as opposed to their hypothermic conditions, where different mechanisms may contribute to these effects. On the other hand, the authors operated PV in a pressure controlled manner as opposed to a flow controlled PV in our scenario. With a flow controlled PV, a

flow reduction is inherently excluded, however, we observed increased PV pressure levels with elevated VC pressure. This compensates the elevated sinusoidal pressure to maintain the desired flow. In yet another study, a myogenic cause of HABR was argued to be due to the correlation of PV pressure and the buffer response<sup>177</sup>. This argument was questioned as PV flow also changes linearly with PV pressure, hence, attributing the buffer response to PV flow instead of PV pressure<sup>198</sup>. Again, the study was restricted to the *in vivo* system, as it didn't allow for the independent control of all in- and outputs of the liver. In the case of our experiments, we were able to vary PV pressure while keeping PV flow constant, showing a clear correlation between PV pressure, resp. HS pressure, and HA resistance. This shows an advantage of the *ex vivo* analysis of the liver hemodynamics, as influences of other organs and *in vivo* factors are excluded.

We do not propose an exclusive role of myogenic mechanism during HABR, as it has already been shown that adenosine washout rate plays a major role in HABR<sup>203</sup>. However, our results suggest there are most likely overlaying effects of myogenic and washout mechanisms. The fact that we propose an overlaying effect coincides with previous studies which accept adenosine as a mediator of HABR but question its exclusive role<sup>167</sup>. Another study observed a stronger effect of HABR as compared to HA autoregulation, suggesting a more potent stimulator for HABR than for autoregulation<sup>164</sup>, implying multiple effects to take place simultaneously during HABR.

Recently, *ex vivo* normothermic liver perfusion gained a lot of interest in the field of transplantation<sup>204205</sup>. A crucial factor during *ex vivo* liver perfusion is the maintenance of adequate pressure and flow levels in the liver<sup>18</sup>. Next to applying vasoactive substances to artificially elevate or reduce HA resistance<sup>86</sup>, HABR could be utilized as a hemodynamic control mechanism. Thereby, the PV flow could be allowed to vary in a certain range to use its influence on HA resistance and reduce demand for externally supplied vasoactive substances. Further, for long-term *ex vivo* liver perfusion, a closed system, i.e. cannulation of the VC, is of importance due to enhanced hemolysis rates occurring upon contact of the blood with air<sup>114</sup>. A closed system avoids air contact, however, requires for the control of VC pressure. As this study demonstrates, VC pressure plays an important role in the hemodynamics of the liver.

Therefore, a sound understanding of VC pressure influence on the HA resistance is important for viable *ex vivo* perfusion of livers.

The paper has some limitations. First of all, this study was performed on livers perfused in an *ex vivo* environment. The livers might indeed behave differently as compared to the *in vivo* situation. Even though the comparison of the *BC* suggests that the HABR was unimpaired, there may be differences that were not accounted for. Second, the model simplified the liver hemodynamics to an extent that it could be applied with an acceptable accuracy. However, this could lead to certain physiological effects being neglected. Further, this paper doesn't deliver any molecular evidence regarding the underlying mechanism of HABR, resp. venous pressure influence on HA resistance. We focus on hemodynamic measurements and apply underlying concepts, which were gathered from literature. However, the given hemodynamic data from our experiments and previously proposed concepts lead us to our conclusions. The strong evidence of a correlation between VC pressure and HA resistance levels, well beyond a passive milieu, while keeping PV flow constant, renders a sole washout theory during HABR unlikely.

## 6.5 Conclusion

To the best of our knowledge, this study is the first to extensively investigate the relationship between HA resistance, PV flow and VC pressure in a defined *ex vivo* perfusion system. This setup allowed for an isolated investigation of the liver hemodynamics without side effects of further organs or hormonal influences and lead us to propose the following conclusions. First, a clear correlation between VC pressure and HA resistance is present, which is concluded to be due to myogenic effects of intrahepatic pressure on the HA. Second, we have shown that HABR is unimpaired during our *ex vivo* studies, with the buffer capacity *BC* being in a similar range as compared to *in vivo* studies. Third, based on the conclusions of the intrahepatic pressure influence on HA resistance, an overlaying mechanism of washout and myogenic effects have been proposed and quantified for HABR. With the growing interest in *ex vivo* liver perfusion, these findings may render useful for finding an optimal adjustment of the perfusion settings. Last, this study demonstrates

---

how the developed perfusion system can be applied to test hypotheses regarding hepatic physiology in an isolated, controlled environment.





# Chapter 7

## Human liver perfusion

In this chapter, the data from perfusion of human livers is presented. These livers were declined for transplantation by all transplant centres in Switzerland and would have been discarded. These livers were accepted for research, put on the perfusion machine and perfused for up to one week. Purpose of this study was to evaluate the system, which was developed based on pig livers, with human livers, determine relevant differences and, in the end, obtain a system which can potentially be transferred to a clinical application. Important to note is the fact that, due to the nature of their origin, the quality of these livers was very heterogeneous. Due to the high degree of heterogeneity, the results from this study function primarily as a proof of concept of the developed perfusion system with human livers and show the application possibilities of such a technology.

### 7.1 Experimental procedure

#### 7.1.1 Source of organs

The human livers were declined for transplantation by all transplant centers in Switzerland. With the approval of the ethics committee (study protocol 2017-000412) and the informed consent from the next of kin of the deceased, these livers were taken for research within the project. Ten human livers were obtained and included in this chapter. The tables in appendix A.2 summarize the perfused human livers.

### 7.1.2 Perfusion system

For the perfusion of the human livers, the final perfusion system, as described in chapter 3, was applied. In general, the system is the same as for the pig livers with only a few differences in the perfusion protocol. These are as follows.

- Vasoactive medication: Flolan (Epoprostenol, GlaxoSmithKline) was supplied as vasodilator medication instead of nitroprussiat. The concentration was set to 4  $\mu\text{g}/\text{mL}$ .
- Concentration of glucagon infusion set to 111 U/L

### 7.1.3 Perfusion procedure

As perfusate, four or five erythrocyte concentrations (EC) and three or four fresh frozen plasmas (FFP) were mixed and added to the system. This amounted to above 2.2 L of perfusate. Albumin was added to reach a concentration of  $> 20$  g/L prior to perfusion start. Due to elevated lactate levels in the ECs and disturbed electrolyte levels, the dialysis was operated at a high rate ( $> 1000$  mL/h) prior to connecting the livers, to wash out lactate and thereby reducing acidosis and correcting sodium. When  $pH$  of greater 7.1 was obtained, the livers were connected. As the livers clear lactate within a few hours,  $pH$  reach physiological levels without the additional need of a buffer such as bicarbonates ( $\text{HCO}_3^-$ ). Important to mention was not to correct  $pH$  to physiological levels (7.4) by means of bicarbonates because this induces the risk of ending up in alkalosis when the liver clears lactate, which cannot easily be reverted. Further, hematocrit was corrected to 27-30% prior to perfusion start by means of dialysis.

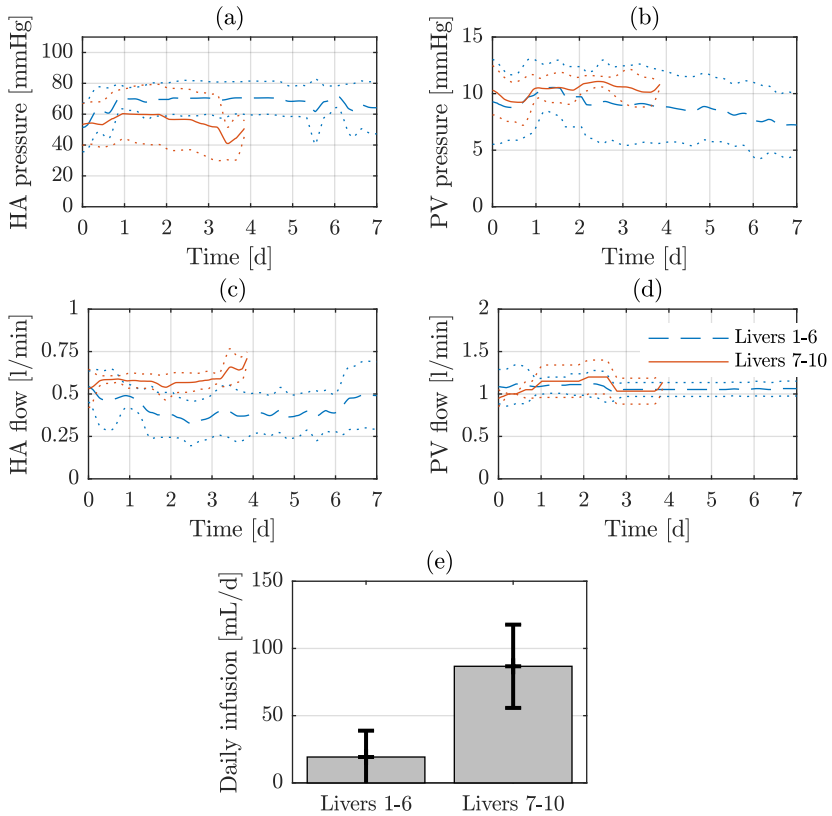
## 7.2 Results

The quality of the obtained livers was very heterogeneous. As mentioned above, all of the perfused livers were discarded for transplantation in by all transplant centers in Switzerland. In some case, the livers performed well and showed actually a stable performance during seven days of perfusion. Others, on the other hand, performed poorly and perfusion

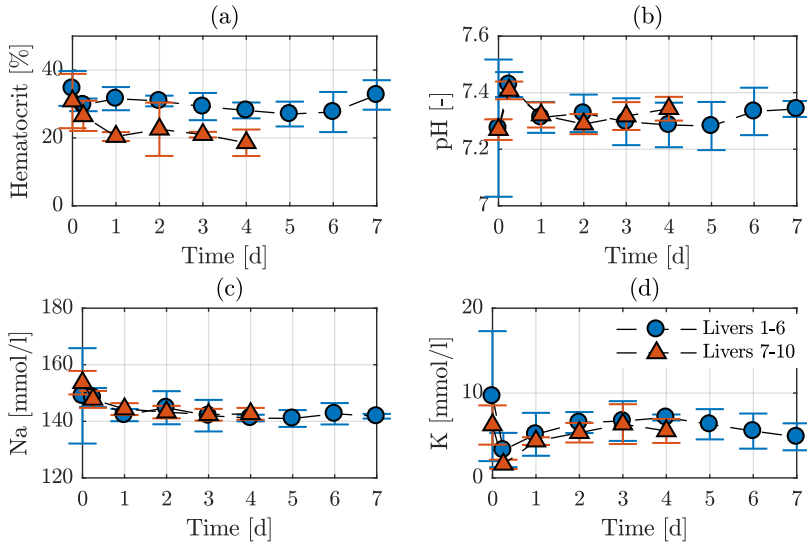
had to be terminated mostly after four days. Therefore, the perfused livers were divided into two groups. The first group ("Livers 1-6") were the ones that reached seven days of perfusion in a good quality. The second group ("Livers 7-10") were the ones that only reached four days of perfusion.

Figure 7.1 shows the pressure in HA (a) and PV (b) as well as the flow in the HA (c) and PV (d) during the course of perfusion of the ten livers. The livers are grouped as described above. In case of livers 1-6, the course of HA flow and pressure is similar to the case of pig livers. After an initial vasoplegia, which is counteracted by infusion of vasoconstrictor phenylephrine, HA pressure reaches the mean target level of 65 mmHg and the flow in HA varies between 0.25 and 0.5 L/min. In the case of the poor performing livers (livers 7-10), even a substantial infusion of vasoconstrictor (see figure 7.1 (e)) cannot counteract the vasoplegia, resulting in HA pressure levels below the desired target of 65 mmHg while HA flow is limited at 0.6 L/min. The perfusion settings in the PV show no difference between the two groups. In figure 7.1 (e), the average daily infusion amount of phenylephrine during perfusion of both groups is illustrated. As can be seen, there is a significant difference between the two groups. As mentioned above, the poor performing livers were unresponsive to vasoconstrictor infusion and the system infused at the limit of the controller. In some cases of the well performing livers, one could observe an increase in demand for vasoconstrictor towards the end of perfusion, indicating that these started to fail as well.

Figure 7.2 shows key components in the perfusate which are maintained by the perfusion system. Figure 7.2 (a) shows the hematocrit during the course of perfusion. As described previously, the system controls the hematocrit level by means of the dialysis and defining the amount of fluid which is added to or removed from the perfusate via the dialysate filter. In the case of livers 1-6, the level can mostly be maintained in the desired range between 25 and 30%. However, for livers 7-10 this was not possible. Despite adding the same amount of perfusate at start of perfusion, the volume quickly reduced after initiation of perfusion and could no longer be controlled to the desired level. The hematocrit had to be maintained around 20% to ensure sufficient amount of blood such that the pump wouldn't suck any air. In figure 7.2 (b), the arterial  $pH$  level is illustrated. Here, one can see the  $pH$  level to be maintained



**Figure 7.1:** Perfusion settings: pressure in HA (a) and PV (b) and flow in HA (c) and PV (d) during perfusion. (e) Average daily infusion amount of phenylephrine during perfusion for both groups. Data reported as mean  $\pm$  sd.



**Figure 7.2:** Perfusate quality: (a) hematocrit, (b) arterial pH, (c) sodium and (d) potassium levels in the perfusate during perfusion. Data reported as mean  $\pm$  sd.

close to the physiological level of 7.4 in both groups. Similarly, sodium (Figure 7.2 (c)) and potassium (Figure 7.2 (d)) are passively controlled to the physiological levels by means of the dialysis in the case of both groups.

In figure 7.3, various parameters allowing to judge the metabolic function of the liver are illustrated. Regarding oxygen consumption (figure 7.3 (a)), lactate clearance (figure 7.3 (b)) and urea production (figure 7.3 (c)), the livers performed similar in both groups. The main difference between the two groups are in the bile production (figure 7.3 (d)), bilirubin concentration in the perfusate (figure 7.3 (e)) and factor V synthesis of the liver (figure 7.3 (f)). Of the well performing livers, all livers produced bile, whereas, of the poor performing livers, only one liver produced bile but only to a minor extent. This also correlates with total bilirubin concentration in the blood, as bilirubin is mainly excreted

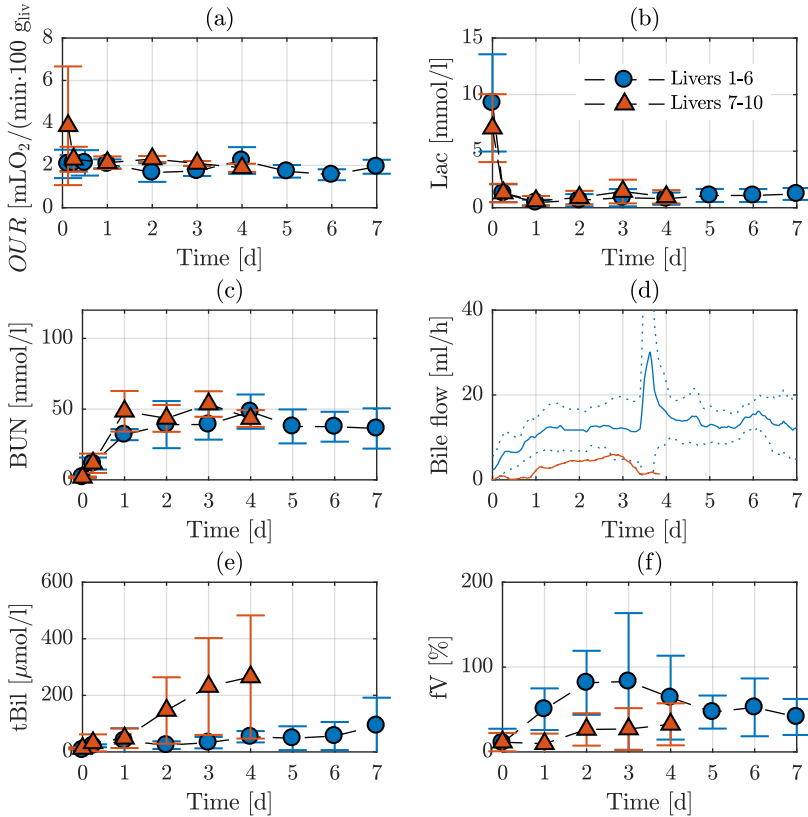


**Figure 7.3:** Metabolic function: (a) oxygen uptake rate ( $OUR$ ) and (d) bile production of the liver, (b) lactate, (c) urea, (e) total bilirubin and (f) factor V (fV) levels in the perfusate during perfusion. Data reported as mean  $\pm$  sd.

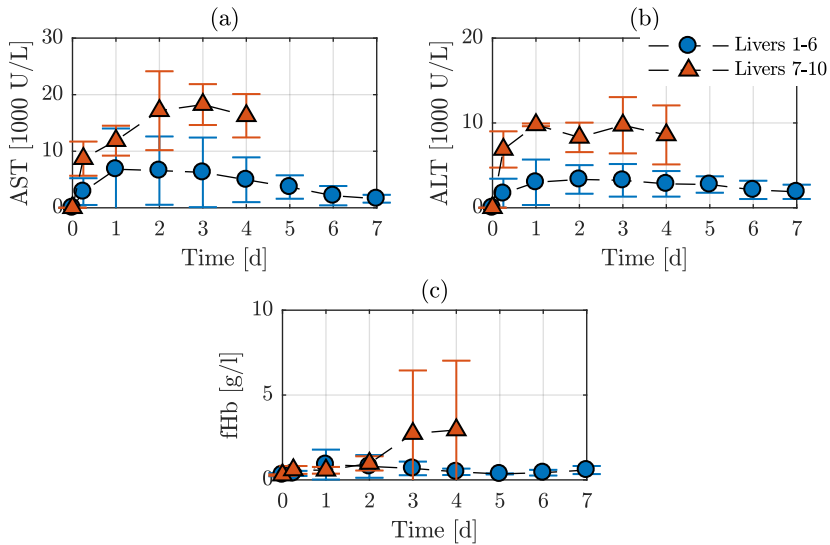


**Figure 7.4:** Damage markers: (a) Aspartate aminotransferase (AST), (b) alanine aminotransferase (ALT) and (c) free hemoglobin (fHb) concentration in the perfusate. Data reported as mean  $\pm$  sd.

from the system in the bile. With absence of bile production by the liver, bilirubin accumulates in the blood leading to a significant difference between the two groups. Factor V (fV) is an important coagulation factor synthesized by the liver with a relatively short half-life time of 20 h. Therefore, its presence allows to assess the liver's metabolic activity and protein synthesising function during *ex vivo* perfusion. On average, the well functioning livers show a higher level of factor V activity as compared to the poorly functioning livers. The second group, remains close to zero and the fV deficiency range ( $fV < 30\%$ )<sup>206</sup>.

In figure 7.4, parameters associated with liver or RBC damage are summarized. Figure 7.4 (a) and (b) show the concentration of transaminases aspartate aminotransferase (AST) and alanine aminotransferase (ALT) in the perfusate, respectively. In both cases, the group of livers 1-6

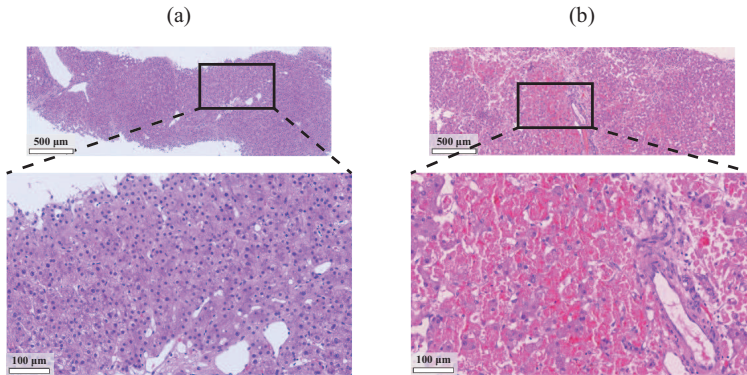


**Figure 7.5:** H&E staining on (a) day seven of perfusion of one of the well functioning livers (Livers 1-6) and (b) day four of perfusion of one of the poorly functioning livers (Livers 7-10).

show a lower increase as compared to livers 7-10, indicating less damage occurring within the liver during perfusion. In case of free hemoglobin (Figure 7.4 (c)), all livers show a similar course, with the exception of one, where on day three and four high levels of free hemoglobin were observed. This indicates low hemolysis occurring during the perfusion. All the livers that lasted for seven days, showed few to no hemolysis. Overall, the well functioning livers showed no increase of damage markers after the initial reperfusion injury.

In figure 7.5, H&E stained biopsy probes of one liver from group livers 1-6 (a) and group livers 7-10 (b) are illustrated. The liver of group livers 1-6 shows an intact integrity up until day seven. The one from group livers 7-10 on the other hand, show confluent cell death and missing hepatocytes, illustrating loss of liver integrity.

### 7.3 Discussion

The study with human livers demonstrates that the perfusion system can keep severely injured human livers, which were discarded by all transplant centers in Switzerland, alive and functioning *ex vivo* for up



to one week. The machine was developed based on pig livers, similar in size and architecture to human livers, and showed to also be applicable with the latter. By mimicking conditions closely to the *in vivo* system, the machine can keep human livers viable. Despite highly heterogeneous quality of the perfused human livers, six of ten livers performed well for up to seven days.

The perfusion of the livers was evaluated based on various parameters. On the one hand, the hemodynamic characteristics were analyzed. In healthy state, the flow in the HA varied between 0.25 and 0.5 L/min while pressure was controlled to a mean level of 65 mmHg. Upon constriction or dilation of vessels, vasoactive medication was infused, leading to a response in the livers. This was not the case for poorly performing livers which suffered from severe vasoplegia that could not be counteracted by means of vasoconstrictors. This was observed throughout all perfused livers, also in case of the well performing livers when a few started to perform poorly. Vasoplegia is also observed in patients in the clinic and occurs in various shock states, e.g. during ischemia-reperfusion after cardiac arrest<sup>207</sup>. Also, post-transplantation of livers, vasoplegia is considered as harmful<sup>69</sup>. This correlates with our observation of vasoplegia in poorly performing livers.

The main difference in the metabolic function of the livers with respect to bile production and factor V synthesis. Bile flow is generally accepted as an indicator for healthy liver function and usually reported during *ex vivo* liver perfusion<sup>70,71,94</sup>. An accumulation of bilirubin, as is the case for poorly performing livers, in the perfusate in absence of bile production is logical as bilirubin is mainly removed by the bile. Further, a difference in the groups is also observable in the case of the damage markers AST and ALT. The increase of both is larger in livers 7-10, indicating a more substantial amount of cell damage in the beginning but also during perfusion. AST is clinically accepted as an indicator for graft function after transplantation<sup>208,209</sup>. A reduction of those enzymes within the perfusate indicates reduced ongoing damage and suggests a recovery from IRI during *ex vivo* perfusion.

Overall, when looking at all of the above mentioned parameters, livers 1-6 showed well function for seven days of perfusion. Factor V activity reduces from the peak at around day 2 or 3 to slightly lower levels. However, factor V interpretation needs to be used with caution with the

highly heparinized *ex vivo* perfusion system. Again, this shows that *in vivo* parameters can not always be translated one to one to the *ex vivo* system. In the end, this allows to draw the conclusion that these livers can indeed be kept healthy for up seven days. Nonetheless, a clear proof of concept that these livers are indeed viable and fully functioning is only given upon transplantation back into a patient. Currently, a clear viability criteria during *ex vivo* perfusion is still missing<sup>19</sup>. Only with successful transplantations, certain parameter could be isolated to create a prediction criteria about transplant outcome. Such a criteria would greatly enhance the benefit of *ex vivo* liver perfusion and contribute to the overall outcome of transplantation.

Such a technology may now open the door for novel therapeutic strategies and allow to assign more organs to patients. On the one hand, as this study with human livers has shown, certain livers, that are currently discarded, illustrated viable function on the perfusion machine and may actually have been transplanted. Hence, the perfusion system could actually allow to evaluate such borderline organs prior to transplantation and allow the transplant surgeon to make a data based transplant decision. This would allow for a more certain decision for transplantation and ultimately more organs to be transplanted. On the other hand, being able to keep livers healthy outside of the body for multiple days, allows for a time window to apply therapeutic interventions prior to transplantation<sup>3</sup>. Such therapies include improving graft quality due to e.g. steatosis or adjusting the organ graft to acclimatize to the recipient<sup>210</sup>.

# Chapter 8

## Conclusions & Outlook

### 8.1 Conclusions

In this doctoral thesis, an *ex vivo* liver perfusion system has been developed which is capable of keeping pig and human livers viable and healthy outside of the body for up to a week. This technology could greatly benefit the transplant society by allowing to store organs for longer periods, evaluate or improve organ quality prior to transplantation or even regenerate such outside of the body. By these means, more organs could be brought to transplantation, ultimately allowing to treat and cure more patients.

#### **Chapter 3 - Description of the perfusion system**

In this chapter, the perfusion system and its functionalities are described. Goal of the perfusion system is to mimic core body functions thereby providing an environment close to the *in vivo* conditions. This includes central organs such as the heart, lung, kidneys, and pancreas but also more subtle imitations like the diaphragm movement, partial oxygen delivery in the portal vein and a closed perfusion circuit. The functional implementation of all these components is described in detail.

#### **Chapter 4 - Perfusion system development**

The perfusion system was developed based on pig liver perfusion experiments. In a stepwise fashion, various settings and components were changed in the system, showing the individual benefits on the liver quality. In summary, the main changes with respect to the initial perfusion

protocol were the following. First, glucose and pancreatic hormones need to be kept in physiological range to avoid hyperglycemia. Secondly, pulsatile operation of the pump and, thereby, HA pressure leads to less hemolysis in the perfused liver. Thirdly, dialysis is essential to ensure physiological electrolyte and hematocrit levels, and to remove metabolic waste products. However, dialysis increases the vascular resistance of the HA by removing nitric oxide and possibly other components. Fourthly, the physiological oxygen content in the PV reduces the vascular resistance in the PV, leading to a lower demand for vasodilator infusion. With the final perfusion system, pig livers were perfused for up to seven days while maintaining them functional and healthy.

### **Chapter 5 - Glucose control**

The developed perfusion system mimics essential body functions in order to keep the blood in a physiological range. This includes the pancreas to control the glucose level in the perfusate. For this purpose, an "artificial pancreas" was integrated into the system.

The artificial pancreas comprises of a glucose sensor to continuously measure the glucose concentration in the perfusate. This sensor had not been applied in blood before and was therefore evaluated in a first step. With a working glucose measurement, two controllers were implemented and tested. A P controller showed to be sufficient for its application in the perfusion system to ensure physiological glucose concentrations during the perfusion duration. Its applicability was shown both in pig and human perfusion experiments and rendered feasible in both cases. The introduced concept can easily be integrated into other perfusion systems to ensure physiological perfusate glucose concentrations.

### **Chapter 6 - Hepatic arterial buffer response**

The configuration of the perfusion system allows the three hemodynamic in- and outputs of the liver to be independently controlled. This provided a platform to individually vary the settings at the respective branches HA, PV and VC and observe the resulting response of HA resistance. A detailed understanding of the mechanisms influencing the HA resistance is of importance in order to ensure physiological perfusion settings *ex*

*vivo.*

With four perfused pig livers, the hepatic arterial buffer response (HABR) was studied on the perfusion system. The intrinsic mechanism describes the response of HA resistance upon varying PV flow conditions. Thereby, HA resistance is proportional the PV flow, i.e. an increase of PV flow leads to an increase in HA resistance and vice versa. In addition, an influence of VC pressure on the HA resistance was identified on the perfusion system. The latter relation remains unmentioned in contemporary literature regarding hepatic circulation, although it had been observed and described before. This lead to further investigations and the proposal of its role also during HABR. The underlying mechanism of VC pressure influence on HA resistance was previously described to be of myogenic nature. Increasing VC pressure levels consequently lead to increasing hepatic sinusoidal pressure levels which cause a myogenic response of the hepatic arterioles. Similarly, varying PV flow and thereby pressure conditions, leads to changes in the intrahepatic sinusoidal pressure and thereby also a myogenic response of the hepatic arterioles. This influence was quantified and by means of a model considered during PV flow variations, showing indeed, that there is also a myogenic effect taking place during HABR.

Concluding, there are two main findings in this chapter, which depend on each other. First, VC pressure has a strong influence on HA resistance, presumably through a myogenic response. Secondly, this myogenic effect must also be present during PV flow variations, as these also lead to changes of intrahepatic pressure, hence causing a myogenic response in the hepatic arterioles.

## **Chapter 7 - Human liver perfusion**

The developed system was evaluated with discarded human livers. These livers were discarded for transplantation by all transplant centers in Switzerland. Despite the presumably poor quality of these organs, six of ten perfused livers performed well and could be kept viable for up to seven days. First of all, this allowed to show that the system, which was developed with pig livers, could also be applied with human livers with only minor changes. Secondly, this gave an impression of the possibilities of the developed system. All of the perfused livers were discarded

because they are assumed to be of too poor quality for transplantation. Perfusion on the machine showed that some of these livers were actually of good quality, at least as could be judged to the best of our knowledge at that time. Clear proof of functionality can only be obtained with transplantation of such a perfused liver. Nonetheless, this shows the potential of evaluating such organs on the *ex vivo* perfusion system prior to transplantation. One may even be able to rescue such organs by applying therapeutic interventions and by going one step further, as is the long term vision of the project, regenerate organs *ex vivo*.

## 8.2 Outlook

The tools and system developed within this thesis provide a solid basis for future investigations in this exciting field. The paragraphs below provide an outline for possible studies that may be carried out in future work.

### Liver perfusion studies

The perfusion machine provides an optimal platform to perform isolated studies on the liver, as was done e.g. in the case of the hepatic arterial buffer response in chapter 6.

The hepatic circulation is a complex system with various influences and the HA resistance is responsive to various triggers. The proposed relations can be used and applied to quantify the contribution of HABR and VC pressure upon HA resistance. Further influences such as the influence of nitroprussiat and phenylephrine, which are applied in the system to manipulate the HA resistance to a certain extent, can be quantified. This may allow to obtain a model which describes the HA resistance dependencies in detail. Such a model may be applied to further enhance the controllers in the perfusion system.

Further studies regarding some components of the system should be undertaken. During the development phase, a close to physiological system was sought. This led to the decision of closing the perfusion loop and cannulating the VC. Based on previous reports, avoiding additional air contact of the perfusate is expected to reduce the hemolysis rate<sup>114</sup>. Nonetheless, experiments could be conducted comparing an open and a closed system with respect to hemolysis and overall perfusion quality.

The effect of the artificial diaphragm should be further evaluated. A potential benefit of its integration was observed during the initial perfusion experiments but should be confirmed on the final machine. The merit of the diaphragm could be evaluated based on visual analysis of the liver surface, near-surface biopsy probes or CT scans of the liver with and without the artificial diaphragm movement.

The setting of a target MAP of 65 mmHg was chosen based on internal discussions with experienced perfusionists and cardiologists and is in align with international guidelines applied during septic shocks<sup>211</sup>. However, as our literature review has shown, the defined settings during *ex vivo* perfusion vary greatly<sup>18</sup>. Further, the target of 65 mmHg has also recently been questioned in the intensive care community<sup>212</sup>. Therefore, experiments with different MAP levels could be conducted to determine an optimal setting during *ex vivo* liver perfusion.

### **Transplantation & evaluation criteria**

The experiments performed within the scope of this thesis were conducted on the perfusion system and the livers were evaluated based on criteria which are commonly applied in the clinical setting. These comprise parameters indicating about liver metabolic function, such as bile production, lactate clearance, coagulation factor synthesis and others, but also cell injury markers, such as transaminase levels in the perfusate. These are commonly accepted and reported during *ex vivo* liver perfusion but, in the end, the only proof of liver function is given by transplanting a perfused liver back into a patient. Within the scope of the project, three transplantations of pig livers after one week perfusion back into a pig were conducted, but had to be stopped after three hours of reperfusion. Such experiments should be repeated to evaluate the health of the perfused livers after one week perfusion.

With transplantation of the perfused livers, an evaluation criteria for the perfused livers could be elaborated. For this purpose, it is important to have a defined labelling criteria such as transplantation outcome. Before a solid statement about the liver's quality is available, evaluation criteria based on perfusion course need to be applied with caution.

### **Liver regeneration**

The developed system provides a framework for systematic experiments to study *ex vivo* liver regeneration. This was the initial incentive of the project and still remains the primary goal. With the given perfusion system, approaches such as ALPPS (Associating Liver Partition and Portal vein ligation for Staged hepatectomy)<sup>213</sup> on the system, hypoxia driven or accelerated liver regeneration<sup>117,118</sup>, hepatic growth factors, and many others can be tested and ultimately, the key for liver regeneration isolated. Achieving *ex vivo* liver regeneration would in the end provide more organs to patients and allow to treat patients who would nowadays not obtain an organ due to long waiting times.

### **Adaption to other organs**

The machine was developed for the perfusion of livers but could also be applied to other organs. This could include hearts, lungs, kidneys or others. In preliminary experiments, which are not included in this thesis, experiments with pig hearts were conducted. The perfusion loop was adjusted accordingly and with only a minor effort, hearts could be perfused for a couple of hours with the Langendorff perfusion setting. The system could be adjusted to perfuse hearts through the heart chambers instead of reversed through the aorta (like in Langendorff) to evaluate their performance. Studying other organs or potentially perfusing those in parallel on the system may allow to identify essential molecules or hormones for long-term perfusion and ultimately enable current utopian visions, such as organ banking.



# A Appendix

## A.1 Machine components

**Table A.1:** Machine components - disposable components which are in contact with blood.

Component	Product Name	Product Company
Blood pump	Centrimag	Thoractec
Pressure Sensor	PRESS-S-025, PRESS-S-038	PendoTECH
Glucose sensor	CITens Bio Glucose	C-CIT Sensors AG
Oxygenator	MEDOS HILITE 2400LT	Medos Medizintechnik AG
Dialysis Filter	Ultraflux AV paed	Fresenius
Online blood gas sensors	CDI500 Shunt sensor, CDI500 Cuvette	Terumo
Artificial Diaphragm - Balloon	SilkoBag 3L	Rüsch
Tubing	Raumedic EDC-Silikon 1/4" or 3/8" ID	Raumedic
Tubing connectors	assorted sizes	Medos Medizintechnik AG
Cannulas	custom-made	41mechanik AG
Blood reservoir	custom-made	HMT Medizintechnik GmbH
Liver container	custom-made, 3D printed	Sculpteo

**Table A.2:** Machine components - peripheral or electronic components which are not in contact with blood.

Component	Product Name	Product Company
<i>Peripheral components</i>		
Artificial Diaphragm - Pressure regulator	Pressure regulator Type DRL	H.Lüdi + Co. AG
Artificial Diaphragm - 3 Port valve	VT307E-5DZ1-02F-Q	SMC Schweiz AG
Gas flow meter O <sub>2</sub> ,N <sub>2</sub> ,CO <sub>2</sub>	F-201CV-2K0-RAD-33-V	Bronkhorst
Heat exchanger blood	461-0606 Kälte-Umwälzthermostat F12-MA	Julabo
Pinchvalve	MPPV-8	Resolution Air
Blood flow sensor	SONOFLOW CO.56/080 & CO.56/120	Sonotec
Temperature sensor	MBD 2.2K3MBD1	TE Connectivity
Infusion pumps	Volumed uVP7000, Syramed uSP6000	Arcomed
Online blood gas monitoring	CDI500	Terumo
Force sensors	KM200/50N	Megatron
<i>Electronic Hardware</i>		
Microlabbox	Microlabbox	dSpace
RS232 to Ethernet Converter	NETCOM+ 813	Vision System
Pinchvalve stepper drive	DRV-1	Resolution Air
Temperature sensor acquisition	D5451	DGH Corp
Pressure sensor amplification	Labjack T7-PRO	Labjack

## A.2 Overview human livers

**Table A.3:** Overview of human livers 1 – 6

Livers	1	2	3	4	5	6
Donor age	48	81	73	54	31	78
Cause of death	CVA	Trauma	CVA	CVA	Anoxia	Anoxia
DBD/DCD	DBD	DCD	DBD	DBD	DCD	DCD
Reason for declining	fibrosis	mitochon. injury	cirrhosis	fibrosis	mitochon. injury	Amyloidosis
HOPE	No	Yes	No	No	Yes	Yes
Functional WI (min)	n.a.	26	n.a.	n.a.	30	19
Asystolic WI (min)	n.a.	19	n.a.	n.a.	20	14
Total cold storage (min)	360	572	360	330	597	510
Liver weight start/end (kg)	2.1/1.5	1.8/1.1	2.3/1.6	2.5/ 1.8	3.2/2.1	1.8/1.3

*Notes:* n.a. – not available, CVA – cerebrovascular accident, DBD – donation after brain death, DCD – donation after cardiac death, HOPE – hypothermic oxygenated perfusion

**Table A.4:** Overview of human livers 7 – 10

Livers	7	8	9	10
Donor age	43	70	53	69
Cause of death	Anoxia	Trauma	CVA	CVA
DBD/DCD	DCD	DCD	DCD	DCD
Reason for declining	mitochon. injury	poor flushout	mitochon. injury	mitochon. injury
HOPE	Yes	No	Yes	Yes
Functional WI (min)	36	25	20	29
Asystolic WI (min)	23	16	15	15
Total cold storage (min)	496	250	280	643
Liver weight start/end (kg)	1.8/1.3	1.5/1.3	1.6/-	2.6/-

*Notes:* n.a. – not available, CVA – cerebrovascular accident, DBD – donation after brain death, DCD – donation after cardiac death, HOPE – hypothermic oxygenated perfusion



# Bibliography

- [1] T E Starzl et al. “Homotransplantation of the Liver in Humans”. In: *Surg Gynecol Obstet.* 117.May 1963 (1963), pp. 659–676.
- [2] S. A. Fayek et al. “The Current State of Liver Transplantation in the United States: Perspective From American Society of Transplant Surgeons (ASTS) Scientific Studies Committee and Endorsed by ASTS Council”. In: *American Journal of Transplantation* 16.11 (2016), pp. 3093–3104.
- [3] Sebastian Giwa et al. “The promise of organ and tissue preservation to transform medicine”. In: *Nature Biotechnology* 35.6 (2017), pp. 530–542.
- [4] Philipp Dutkowski et al. “Challenges to liver transplantation and strategies to improve outcomes”. In: *Gastroenterology* 148.2 (2015), pp. 307–323.
- [5] Yuri L Boteon, Simon C Afford, and Hynek Mergental. “Pushing the Limits: Machine Preservation of the Liver as a Tool to Recondition High-Risk Grafts”. In: *Current Transplantation Reports* (Mar. 2018).
- [6] Andrew M. Cameron et al. “Optimal utilization of donor grafts with extended criteria: A single-center experience in over 1000 liver transplants”. In: *Annals of Surgery* 243.6 (2006), pp. 748–753.
- [7] Laura C. Burlage et al. “Oxygenated hypothermic machine perfusion after static cold storage improves endothelial function of extended criteria donor livers”. In: *Hpb* 19.6 (2017), pp. 538–546.
- [8] Meghan Pinezich and Gordana Vunjak-Novakovic. “Bioengineering approaches to organ preservation ex vivo”. In: *Experimental Biology and Medicine* (2019), p. 153537021983449.

- [9] Clifford Akateh et al. “Normothermic Ex-vivo Liver Perfusion and the Clinical Implications for Liver Transplantation”. In: *Journal of Clinical and Translational Hepatology* 6.3 (June 2018), pp. 1–7.
- [10] Philipp Dutkowski et al. “Evolving Trends in Machine Perfusion for Liver Transplantation”. In: *Gastroenterology* in press (2019).
- [11] Beatriz Domínguez-Gil and Rafael Matesanz. *Newsletter Transplant - International figures on donation and transplantation 2016*. Tech. rep. 2016, pp. 1–22.
- [12] Carlos Jiménez-Romero et al. “Using old liver grafts for liver transplantation: Where are the limits?” In: *World Journal of Gastroenterology* 20.31 (2014), pp. 10691–10702.
- [13] Philipp Dutkowski et al. “First comparison of hypothermic oxygenated perfusion versus static cold storage of human donation after cardiac death liver transplants”. In: *Annals of Surgery* 262.5 (2015), pp. 764–771.
- [14] A. S. Barbas et al. “Ex-vivo liver perfusion for organ preservation: Recent advances in the field”. In: *Transplantation Reviews* 30.3 (2016), pp. 154–160.
- [15] Qiang Liu et al. “Assessing warm ischemic injury of pig livers at hypothermic machine perfusion”. In: *Journal of Surgical Research* 186.1 (Jan. 2014), pp. 379–389.
- [16] Diethard Monbaliu et al. “Preserving the morphology and evaluating the quality of liver grafts by hypothermic machine perfusion: A proof-of-concept study using discarded human livers”. In: *Liver Transplantation* 18.12 (2012), pp. 1495–1507.
- [17] Amelia J. Hessheimer and Constantino Fondevila. “Liver perfusion devices”. In: *Current Opinion in Organ Transplantation* 22.2 (Apr. 2017), pp. 105–111.
- [18] Dilmurodjon Eshmuminov et al. “Perfusion settings and additives in liver normothermic machine perfusion with red blood cells as oxygen carrier. A systematic review of human and porcine perfusion protocols”. In: *Transplant International* 31.9 (Sept. 2018), pp. 956–969.



- [19] Babak Banan et al. “Development of a normothermic extracorporeal liver perfusion system toward improving viability and function of human extended criteria donor livers”. In: *Liver Transplantation* 22.7 (July 2016), pp. 979–993.
- [20] S. D. St Peter et al. “Extended preservation of non-heart-beating donor livers with normothermic machine perfusion”. In: *British Journal of Surgery* 89.5 (May 2002), pp. 609–616.
- [21] Ahmed Nassar et al. “Impact of Temperature on Porcine Liver Machine Perfusion From Donors After Cardiac Death”. In: *Artificial Organs* 40.10 (2016), pp. 999–1008.
- [22] Pierre Alain Clavien et al. “Can immunosuppression be stopped after liver transplantation?” In: *The Lancet Gastroenterology and Hepatology* 2.7 (2017), pp. 531–537.
- [23] Dirk Van Raemdonck et al. “Machine perfusion in organ transplantation: A tool for ex-vivo graft conditioning with mesenchymal stem cells?” In: *Current Opinion in Organ Transplantation* 18.1 (2013), pp. 24–33.
- [24] Alyssa Ward et al. “Social, economic, and policy implications of organ preservation advances”. In: *Current Opinion in Organ Transplantation* 23.3 (June 2018), pp. 336–346.
- [25] Satoru Todo et al. “A pilot study of operational tolerance with a regulatory T-cell-based cell therapy in living donor liver transplantation”. In: *Hepatology* 64.2 (2016), pp. 632–643.
- [26] Sandy Feng. “Spontaneous and induced tolerance for liver transplant recipients”. In: *Current Opinion in Organ Transplantation* 21.1 (2016), pp. 53–58.
- [27] Joseph Leventhal et al. “Tolerance Induction in HLA Disparate Living Donor Kidney Transplantation by Donor Stem Cell Infusion”. In: *Transplantation Journal* 95.1 (Jan. 2013), pp. 169–176.

- [28] Dilmurodjon Eshmuminov et al. “Rapid liver volume increase induced by associating liver partition with portal vein ligation for staged hepatectomy (ALPPS): Is it edema, steatosis, or true proliferation?” In: *Surgery (United States)* 161.6 (2017), pp. 1549–1552.
- [29] Andreas A. Schnitzbauer et al. “Right Portal Vein Ligation Combined With In Situ Splitting Induces Rapid Left Lateral Liver Lobe Hypertrophy Enabling 2-Stage Extended Right Hepatic Resection in Small-for-Size Settings”. In: *Annals of Surgery* 255.3 (Mar. 2012), pp. 405–414.
- [30] D. Eshmuminov et al. “Meta-analysis of associating liver partition with portal vein ligation and portal vein occlusion for two-stage hepatectomy”. In: *British Journal of Surgery* 103.13 (2016), pp. 1768–1782.
- [31] Thomas Vogel et al. “The 24-hour normothermic machine perfusion of discarded human liver grafts”. In: *Liver Transplantation* 23.2 (2017), pp. 207–220.
- [32] Andrew J Butler et al. “Successful extracorporeal porcine liver perfusion for 72 hr.” In: *Transplantation* 73.8 (2002), pp. 1212–8.
- [33] Takaaki Kobayashi et al. “Comparison of bile chemistry between humans, baboons, and pigs: implications for clinical and experimental liver xenotransplantation.” In: *Laboratory animal science* 48.2 (1998), pp. 197–200.
- [34] M.T. Vilei et al. “Comparison of Pig, Human and Rat Hepatocytes as a Source of Liver Specific Metabolic Functions in Culture Systems - Implications for Use in Bioartificial Liver Devices”. In: *The International Journal of Artificial Organs* 24.6 (June 2001), pp. 392–396.
- [35] American Cancer Society Inc. *Chemotherapy for Liver Cancer*.
- [36] OpenStax College. *Anatomy & Physiology*. Houston, 2017.
- [37] Anne M Gilroy et al. *Atlas of Anatomy*. 2nd ed. Thieme, 2012, p. 694.

- [38] Ute Frevert et al. “Intravital Observation of Plasmodium berghei Sporozoite Infection of the Liver”. In: *PLoS Biology* 3.6 (May 2005). Ed. by Thomas Egwang, e192.
- [39] W. Wayne Lauth. *Hepatic Circulation*. Vol. 1. 1. Hoboken, NJ, USA: John Wiley & Sons, Inc., Jan. 2009, pp. 1–174.
- [40] W. Wayne Lauth and C V Greenway. “Conceptual review of the hepatic vascular bed.” In: *Hepatology (Baltimore, Md.)* 7.5 (1987), pp. 952–963.
- [41] C V Greenway and R D Stark. “Hepatic vascular bed.” In: *Physiological reviews* 51.1 (Jan. 1971), pp. 23–65.
- [42] Christian Eipel, Kerstin Abshagen, and Brigitte Vollmar. “Regulation of hepatic blood flow: The hepatic arterial buffer response revisited”. In: *World Journal of Gastroenterology* 16.48 (2010), pp. 6046–6057.
- [43] Christopher J E Watson and Ina Jochmans. “From “Gut Feeling” to Objectivity: Machine Preservation of the Liver as a Tool to Assess Organ Viability”. In: *Current Transplantation Reports* 5.1 (Mar. 2018), pp. 72–81.
- [44] Alejandro Esteller. “Physiology of bile secretion”. In: *World Journal of Gastroenterology* 14.37 (2008), p. 5641.
- [45] James L. Boyer. “Bile Formation and Secretion”. In: *Comprehensive Physiology*. Vol. 3. 3. Hoboken, NJ, USA: John Wiley & Sons, Inc., July 2013, pp. 1035–1078.
- [46] Arthur C. Guyton and John E. Hall. *Textbook of Medical Physiology*. 2006.
- [47] Lisette T. Hoekstra et al. “Physiological and biochemical basis of clinical liver function tests: A review”. In: *Annals of Surgery* 257.1 (2013), pp. 27–36.
- [48] T. W. R. Hansen. “Core Concepts: Bilirubin Metabolism”. In: *NeoReviews* 11.6 (June 2010), e316–e322.
- [49] William H. Crosby. “The metabolism of hemoglobin and bile pigment in hemolytic disease”. In: *The American Journal of Medicine* 18.1 (Jan. 1955), pp. 112–122.

- [50] Giancarlo Maria Liumbruno et al. “Recommendations for the use of albumin and immunoglobulins”. In: *Blood Transfusion* 7.3 (2009), pp. 216–234.
- [51] J. N. HUANG and M. A. KOERPER. “Factor V deficiency: a concise review”. In: *Haemophilia* 14.6 (Oct. 2008), pp. 1164–1169.
- [52] Stefan Silbernagl and Agamemnon Despopoulos. *Color Atlas of Physiology*. 7th ed. Thieme, 2015.
- [53] Francis J. Doyle et al. “Closed-loop artificial pancreas systems: Engineering the algorithms”. In: *Diabetes Care* 37.5 (2014), pp. 1191–1197. arXiv: [arXiv:1011.1669v3](https://arxiv.org/abs/1011.1669v3).
- [54] Steffen Leonhardt and Marian Walter. *Medizintechnische Systeme*. Ed. by Steffen Leonhardt and Marian Walter. Berlin, Heidelberg: Springer Berlin Heidelberg, 2016.
- [55] JM Berg, JL Tymoczko, and L Stryer. “Each Organ Has a Unique Metabolic Profile”. In: *Biochemistry. 5th edition*. New York, 2002. Chap. 30.2.
- [56] Michael E. Sutton et al. “Criteria for Viability Assessment of Discarded Human Donor Livers during Ex Vivo Normothermic Machine Perfusion”. In: *PLoS ONE* 9.11 (Nov. 2014). Ed. by Déla Golshayan, e110642.
- [57] Christopher J.E. E. Watson et al. “Observations on the ex situ perfusion of livers for transplantation”. In: *American Journal of Transplantation* 18.8 (Feb. 2018), pp. 2005–2020.
- [58] Cornelia J. Verhoeven et al. “Biomarkers to assess graft quality during conventional and machine preservation in liver transplantation”. In: *Journal of Hepatology* 61.3 (2014), pp. 672–684.
- [59] Reena Ravikumar, Henri Leuvenink, and Peter J. Friend. “Normothermic liver preservation: A new paradigm?” In: *Transplant International* 28.6 (2015), pp. 690–699.
- [60] Francesca Maione et al. *Porcine Isolated Liver Perfusion for the Study of Ischemia Reperfusion Injury: A Systematic Review*. Vol. 102. 7. 2018, pp. 1039–1049.

- [61] Sarah A. Sterling, Michael A. Puskarich, and Alan E. Jones. “The effect of liver disease on lactate normalization in severe sepsis and septic shock: a cohort study”. In: *Clinical and Experimental Emergency Medicine* 2.4 (Dec. 2015), pp. 197–202.
- [62] Richard W. Laing, Hynek Mergental, and Darius F. Mirza. “Normothermic ex-situ liver preservation: The new gold standard”. In: *Current Opinion in Organ Transplantation* 22.3 (2017), pp. 274–280.
- [63] Mariusz Bral et al. “A ‘Back-to-base’ Experience of Human Normothermic Ex Situ Liver Perfusion: Does the chill kill?” In: *American Journal of Transplantation* 06 (2018).
- [64] M. U. Boehnert et al. “Normothermic Acellular Ex Vivo Liver Perfusion Reduces Liver and Bile Duct Injury of Pig Livers Retrieved After Cardiac Death”. In: *American Journal of Transplantation* 13.6 (June 2013), pp. 1441–1449.
- [65] Shawn D. Peter et al. “Hepatic control of perfusate homeostasis during normothermic extracorporeal preservation”. In: *Transplantation Proceedings* 35.4 (2003), pp. 1587–1590.
- [66] P Reverdiau-Moalic et al. “Comparative study of porcine and human blood coagulation systems: possible relevance in xenotransplantation.” In: *Transplantation proceedings* 28.2 (Apr. 1996), pp. 643–4.
- [67] Ivan Linares-Cervantes et al. “Predictor Parameters of Liver Viability During Porcine Normothermic Ex-Situ Liver Perfusion in a Model of Liver Transplantation with Marginal Grafts”. In: *American Journal of Transplantation* (2019), ajt.15395.
- [68] Jens Brockmann et al. “Normothermic Perfusion A New Paradigm for Organ Preservation”. In: *Annals of Surgery* 250.1 (July 2009), pp. 1–6.
- [69] Christopher J.E. Watson et al. “Normothermic perfusion in the assessment and preservation of declined livers before transplantation: Hyperoxia and vasoplegia-important lessons from the first 12 cases”. In: *Transplantation* 101.5 (2017), pp. 1084–1098.

- [70] Mihai Calin Pavel et al. “Evolution Under Normothermic Machine Perfusion of Type 2 DCD Livers Discarded as Nontransplantable”. In: *Journal of Surgical Research* 235 (2019), pp. 383–394.
- [71] Markus Selzner et al. “Normothermic ex vivo liver perfusion using steen solution as perfusate for human liver transplantation: First North American results”. In: *Liver Transplantation* 22.11 (2016), pp. 1501–1508.
- [72] Charles J. Imber et al. “Optimisation of Bile Production during Normothermic Preservation of Porcine Livers”. In: *American Journal of Transplantation* 2.7 (Aug. 2002), pp. 593–599.
- [73] Serge Erlinger. “A HCO 3-umbrella protects human cholangiocytes against bile salt-induced injury”. In: *Clinics and Research in Hepatology and Gastroenterology* 36.1 (2012), pp. 7–9.
- [74] James H. Tabibian et al. “Physiology of cholangiocytes”. In: *Comprehensive Physiology* 3.1 (2013), pp. 541–565.
- [75] Murli Krishna. “Role of special stains in diagnostic liver pathology”. In: *Clinical Liver Disease* 2.SUPPL. 1 (2013), pp. 8–10.
- [76] S. Op Den Dries et al. “Ex vivo normothermic machine perfusion and viability testing of discarded human donor livers”. In: *American Journal of Transplantation* 13.5 (2013), pp. 1327–1335.
- [77] Charles J. Imber et al. “Advantages of normothermic perfusion over cold storage in liver preservation”. In: *Transplantation* 73.5 (2002), pp. 701–709.
- [78] Srikanth Reddy et al. “Non-heart-beating donor porcine livers: The adverse effect of cooling”. In: *Liver Transplantation* 11.1 (2005), pp. 35–38.
- [79] Christian Grosse-Siestrup et al. “The isolated perfused liver”. In: *Journal of Pharmacological and (Grosse-Siestrup et al., 2001) Toxicological Methods* 46.3 (Nov. 2001), pp. 163–168.
- [80] Stefan Nagel et al. “An Improved Model of Isolated Hemoperfused Porcine Livers Using Pneumatically Driven Pulsating Blood Pumps”. In: *Toxicologic Pathology* 33.4 (June 2005), pp. 434–440.

- [81] Jin Gong et al. “Preservation of non-heart-beating donor livers in extracorporeal liver perfusion and histidine - tryptophan - ketoglutarate solution”. In: *World Journal of Gastroenterology* 14.15 (2008), pp. 2338–2342.
- [82] Babak Banan et al. “Normothermic extracorporeal liver perfusion for donation after cardiac death (DCD) livers”. In: *Surgery (United States)* 158.6 (2015), pp. 1642–1650.
- [83] Ahmed Nassar et al. “Ex Vivo Normothermic Machine Perfusion Is Safe, Simple, and Reliable”. In: *Surgical Innovation* 22.1 (2015), pp. 61–69.
- [84] Qiang Liu et al. “Sanguineous normothermic machine perfusion improves hemodynamics and biliary epithelial regeneration in donation after cardiac death porcine livers”. In: *Liver Transplantation* 20.8 (Aug. 2014), pp. 987–999. arXiv: NIHMS150003.
- [85] Gianpiero Gravante et al. “Effects of Hypoxia Due to Isovolemic Hemodilution on an Ex Vivo Normothermic Perfused Liver Model”. In: *Journal of Surgical Research* 160.1 (2010), pp. 73–80.
- [86] Juan Echeverri et al. “Comparison of BQ123, epoprostenol, and verapamil as vasodilators during normothermic ex vivo liver machine perfusion”. In: *Transplantation* 102.4 (Nov. 2018), pp. 601–608.
- [87] Vincent N. Spetzler et al. “Subnormothermic ex vivo liver perfusion is a safe alternative to cold static storage for preserving standard criteria grafts”. In: *Liver Transplantation* 22.1 (2016), pp. 111–119.
- [88] Jan M. Knaak et al. “Subnormothermic ex vivo liver perfusion reduces endothelial cell and bile duct injury after donation after cardiac death pig liver transplantation”. In: *Liver Transplantation* 20.11 (Nov. 2014), pp. 1296–1305. arXiv: NIHMS150003.
- [89] Constantino Fondevila et al. “Superior preservation of DCD livers with continuous normothermic perfusion”. In: *Annals of Surgery* 254.6 (2011), pp. 1000–1007.
- [90] Michael R. Schön et al. “Liver Transplantation After Organ Preservation With Normothermic Extracorporeal Perfusion”. In: *Annals of Surgery* 233.1 (2001), pp. 114–123.

- [91] Janske Reiling et al. “Urea production during normothermic machine perfusion: Price of success?” In: *Liver Transplantation* 21.5 (May 2015), pp. 700–703. arXiv: NIHMS150003.
- [92] Arielle Cimeno et al. “N-glycolylneuraminic acid knockout reduces erythrocyte sequestration and thromboxane elaboration in an ex vivo pig-to-human xenoperfusion model”. In: *Xenotransplantation* 24.6 (2017), pp. 1–14.
- [93] Zhi Bin Zhang et al. “Protective role of normothermic machine perfusion during reduced-size liver transplantation in pigs”. In: *Liver Transplantation* 22.7 (2016), pp. 968–978.
- [94] David Nasralla et al. “A randomized trial of normothermic preservation in liver transplantation”. In: *Nature* (2018).
- [95] Ahmed Nassar et al. “Role of vasodilation during normothermic machine perfusion of DCD porcine livers”. In: *International Journal of Artificial Organs* 37.2 (2014), pp. 165–172.
- [96] Wenzel N. Schoening et al. “Iloprost donor treatment reduces ischemia-reperfusion injury in an isolated extracorporeal pig liver perfusion model”. In: *Experimental and Clinical Transplantation* 13.1 (2015), pp. 51–61.
- [97] David Alonso and Marek W. Radomski. “The nitric oxide - endothelin - 1 connection”. In: *Heart Failure Reviews* 8.1 (2003), pp. 107–115.
- [98] Baimeng Zhang et al. “NO-mediated vasodilation in the rat liver”. In: *Journal of Hepatology* 26.6 (July 1997), pp. 1348–1355.
- [99] Benedikt H.J. Pannen and Michael Bauer. “Differential regulation of hepatic arterial and portal venous vascular resistance by nitric oxide and carbon monoxide in rats”. In: *Life Sciences* 62.22 (Apr. 1998), pp. 2025–2033.
- [100] Masashi Yanagisawa et al. “A novel potent vasoconstrictor peptide produced by vascular endothelial cells”. In: *Nature* 332.6163 (1988), pp. 411–415.



- [101] Qiang Liu et al. “Lipid metabolism and functional assessment of discarded human livers with steatosis undergoing 24 hours of normothermic machine perfusion”. In: *Liver Transplantation* 24.2 (Nov. 2018), pp. 233–245.
- [102] Qiang Liu et al. “Ex situ 86-hour liver perfusion: Pushing the boundary of organ preservation”. In: *Liver Transplantation* 24.4 (Apr. 2018), pp. 557–561.
- [103] M. Bral et al. “Preliminary Single-Center Canadian Experience of Human Normothermic Ex Vivo Liver Perfusion: Results of a Clinical Trial”. In: *American Journal of Transplantation* 17.4 (2017), pp. 1071–1080.
- [104] R. Ravikumar et al. “Liver Transplantation After Ex Vivo Normothermic Machine Preservation: A Phase 1 (First-in-Man) Clinical Trial”. In: *American Journal of Transplantation* 16.6 (2016), pp. 1779–1787.
- [105] G. R. Kelman. “Digital computer subroutine for the conversion of oxygen tension into saturation.” In: *Journal of Applied Physiology* 21.4 (1966), pp. 1375–1376.
- [106] Juerg Peter Mueller et al. “The CentriMag: A new optimized centrifugal blood pump with levitating impeller”. In: *Heart Surgery Forum* 7.5 (2004), pp. 427–430.
- [107] M. Kocakulak et al. “Short term effects of pulsatile perfusion in high risk patients”. In: *2001 Conference Proceedings of the 23rd Annual International Conference of the IEEE Engineering in Medicine and Biology Society*. Vol. 1. IEEE, 2001, pp. 455–458.
- [108] Philip Hornick and Kenneth Taylor. “Pulsatile and nonpulsatile perfusion: The continuing controversy”. In: *Journal of Cardiothoracic and Vascular Anesthesia* 11.3 (1997), pp. 310–315.
- [109] Charlotte von Horn and Thomas Minor. “Isolated kidney perfusion: the influence of pulsatile flow”. In: *Scandinavian Journal of Clinical and Laboratory Investigation* 78.1-2 (2018), pp. 131–135.

- [110] Isabel M.A. Brüggewirth et al. “A Comparative Study of Single and Dual Perfusion During End-ischemic Subnormothermic Liver Machine Preservation”. In: *Transplantation Direct* (Oct. 2018), p. 1.
- [111] Marjolein P. Hoefijzers et al. “The pulsatile perfusion debate in cardiac surgery: Answers from the microcirculation?” In: *Journal of Cardiothoracic and Vascular Anesthesia* 29.3 (2015), pp. 761–767.
- [112] Charalambos Vlachopoulos, Michael O’Rourke, and Wilmer W. Nichols. *McDonald’s Blood Flow in Arteries 6th Edition: Theoretical, Experimental and Clinical Principles*. Ed. by Robert Reneman. CRC Press, July 2011.
- [113] Glenn S. Murphy, Eugene A. Hessel, and Robert C. Groom. “Optimal perfusion during cardiopulmonary bypass: An evidence-based approach”. In: *Anesthesia and Analgesia* 108.5 (2009), pp. 1394–1417.
- [114] Ahmed M. El-Sabbagh et al. “Effect of Air Exposure and Suction on Blood Cell Activation and Hemolysis in an In Vitro Cardiomy Suction Model”. In: *ASAIO Journal* 59.5 (2013), pp. 474–479.
- [115] Dustin Becker et al. “Model assisted analysis of the hepatic arterial buffer response during ex vivo porcine liver perfusion”. In: *IEEE Transactions on Biomedical Engineering* PP.c (2019), pp. 1–1.
- [116] Jaime Bosch and Juan Carlos García-Pagán. “Complications of cirrhosis. I. Portal hypertension”. In: *Journal of Hepatology* 32.SUPPL.1 (2000), pp. 141–156.
- [117] Philipp Kron et al. “Hypoxia-driven Hif2a coordinates mouse liver regeneration by coupling parenchymal growth to vascular expansion”. In: *Hepatology* 64.6 (2016), pp. 2198–2209.
- [118] Erik Schadde et al. “Hypoxia of the growing liver accelerates regeneration”. In: *Surgery (United States)* 161.3 (2017), pp. 666–679.
- [119] Martin von Siebenthal. “Analysis and modelling of respiratory liver motion using 4DMRI”. PhD thesis. 2008.

- [120] Ian E. Sambrook. “Studies on the flow and composition of bile in growing pigs”. In: *Journal of the Science of Food and Agriculture* 32.8 (1981), pp. 781–791.
- [121] Majid Esmaeilzadeh et al. “Technical guidelines for porcine liver allo-transplantation: A review of literature”. In: *Annals of Transplantation* 17.2 (2012), pp. 101–110.
- [122] Jay H. Lefkowitz. “Special stains in diagnostic liver pathology”. In: *Seminars in Diagnostic Pathology* 23.3-4 (Aug. 2006), pp. 190–198.
- [123] Richard Van Wijk and Wouter W Van Solinge. “Review article The energy-less red blood cell is lost : erythrocyte enzyme abnormalities of glycolysis”. In: *Blood* 106.13 (2015), pp. 4034–4043.
- [124] Liangyou Rui. “Energy Metabolism in the Liver”. In: *Comprehensive Physiology*. Vol. 4. 1. Hoboken, NJ, USA: John Wiley & Sons, Inc., Jan. 2014, pp. 177–197. arXiv: 15334406.
- [125] T Oku et al. “Hemolysis. A comparative study of four nonpulsatile pumps.” In: *ASAIO transactions* 34.3 (1988), pp. 500–4.
- [126] Constantine Mavroudis. “To Pulse or Not to Pulse”. In: *Annals of Thoracic Surgery* 25.3 (1978), pp. 259–271.
- [127] Ruofan Wang et al. “Modeling of pulsatile flow-dependent nitric oxide regulation in a realistic microvascular network”. In: *Microvascular Research* 113 (2017), pp. 40–49.
- [128] Neema Kaseje et al. “Donor hypernatremia before procurement and early outcomes following pediatric liver transplantation”. In: *Liver Transplantation* 21.8 (Aug. 2015), pp. 1076–1081. arXiv: NIHMS150003.
- [129] A.L. Ladron de Guevara Cetina et al. “Association between donor hypernatremia and liver transplant graft function”. In: *Hpb* 20 (2018), S78.
- [130] Patrizia Burra et al. “EASL Clinical Practice Guidelines: Liver transplantation”. In: *Journal of Hepatology* 64.2 (Feb. 2016), pp. 433–485.

- [131] Maria D’Apolito et al. “Urea-induced ROS cause endothelial dysfunction in chronic renal failure”. In: *Atherosclerosis* 239.2 (Apr. 2015), pp. 393–400.
- [132] Ilias Attaye et al. “The effects of hyperoxia on microvascular endothelial cell proliferation and production of vaso-active substances”. In: *Intensive Care Medicine Experimental* 5.1 (Dec. 2017), p. 22.
- [133] S Dallinger et al. “Endothelin-1 contributes to hyperoxia-induced vasoconstriction in the human retina.” In: *Investigative ophthalmology & visual science* 41.3 (Mar. 2000), pp. 864–9.
- [134] Jason R. Hickok et al. “Oxygen dependence of nitric oxide mediated signaling”. In: *Redox Biology* 1.1 (2013), pp. 203–209.
- [135] M. Bessems et al. “Machine Perfusion Preservation of the Pig Liver Using a New Preservation Solution, Polysol”. In: *Transplantation Proceedings* 38.5 (2006), pp. 1238–1242.
- [136] Zaher A. Radi et al. “Increased Serum Enzyme Levels Associated with Kupffer Cell Reduction with No Signs of Hepatic or Skeletal Muscle Injury”. In: *The American Journal of Pathology* 179.1 (July 2011), pp. 240–247.
- [137] Andrew Fedoravicius and Michael Charlton. “Abnormal liver tests after liver transplantation”. In: *Clinical Liver Disease* 7.4 (Apr. 2016), pp. 73–79.
- [138] L. Boone et al. “Selection and interpretation of clinical pathology indicators of hepatic injury in preclinical studies”. In: *Veterinary Clinical Pathology* 34.3 (Sept. 2005), pp. 182–188.
- [139] Robert H. Bartlett. “Vitalin: The rationale for a hypothetical hormone”. In: *Journal of the American College of Surgeons* 199.2 (2004), pp. 286–292.
- [140] Jennifer S. McLeod et al. “Ex Vivo Heart Perfusion for 72 Hours Using Plasma Cross Circulation”. In: *ASAIO Journal* (Aug. 2019), p. 1.
- [141] C-CIT Sensors AG. *CITSens Bio Technical Data Sheet*. 2019.

- [142] S Spichiger and U E Spichiger-Keller. “Process monitoring with disposable chemical sensors fit in the framework of process analysis technology (PAT) for innovative pharmaceutical development and quality assurance”. In: *Chimia (Aarau)* 64.11 (2010), pp. 803–807.
- [143] Stefan Spichiger and Ursula E. Spichiger-Keller. “New Single-Use Sensors for Online Measurement of Glucose and Lactate: The Answer to the PAT Initiative”. In: *Single-Use Biopharmaceutical Technology in Manufacture*. Ed. by Regine Eibl and Dieter Eibl. Hoboken, NJ, USA: John Wiley & Sons, Inc., Dec. 2010. Chap. 24, pp. 295–299.
- [144] Richard Johnstone et al. “Exponential convergence of recursive least squares with exponential forgetting factor”. In: *1982 21st IEEE Conference on Decision and Control*. IEEE, Dec. 1982, pp. 994–997.
- [145] J T Sorensen. “A physiologic model of glucose metabolism in man and its use to design and assess improved insulin therapies for diabetes”. PhD thesis. 1985, p. 557.
- [146] P. Guzelian and J. L. Boyer. “Glucose reabsorption from bile. Evidence for a biliohepatic circulation.” In: *Journal of Clinical Investigation* 53.2 (Feb. 1974), pp. 526–535.
- [147] C. Lopez-Quijada and P.M. Goñi. “Liver and insulin: Presence of insulin in bile”. In: *Metabolism* 16.6 (June 1967), pp. 514–521.
- [148] Claudio Cobelli et al. “An integrated mathematical model of the dynamics of blood glucose and its hormonal control”. In: *Mathematical Biosciences* 58.1 (Feb. 1982), pp. 27–60.
- [149] K. Mythreyi, Shankar C. Subramanian, and R. Krishna Kumar. “Nonlinear glucose-insulin control considering delays-Part II: Control algorithm”. In: *Control Engineering Practice* 28.1 (2014), pp. 26–33.
- [150] David C. Polidori et al. “Hepatic and extrahepatic insulin clearance are differentially regulated: Results from a novel model-based”. In: *Diabetes* 65.6 (2016), pp. 1556–1564.

- [151] C. J. E. Watson et al. “Preimplant Normothermic Liver Perfusion of a Suboptimal Liver Donated After Circulatory Death”. In: *American Journal of Transplantation* 16.1 (Jan. 2016), pp. 353–357.
- [152] S. A. Weinzimer et al. “Fully Automated Closed-Loop Insulin Delivery Versus Semiautomated Hybrid Control in Pediatric Patients With Type 1 Diabetes Using an Artificial Pancreas”. In: *Diabetes Care* 31.5 (May 2008), pp. 934–939.
- [153] David A Gough et al. “Function of an Implanted Tissue Glucose Sensor for More than 1 Year in Animals”. In: *Science Translational Medicine* 2.42 (July 2010), 42ra53–42ra53.
- [154] Lia Bally et al. “Closed-Loop Insulin Delivery for Glycemic Control in Noncritical Care”. In: *New England Journal of Medicine* (2018), NEJMoa1805233.
- [155] Federico Ribet, Göran Stemme, and Niclas Roxhed. “Real-time intradermal continuous glucose monitoring using a minimally invasive microneedle-based system”. In: *Biomedical Microdevices* 20.4 (Dec. 2018), p. 101.
- [156] Jeffrey I Joseph, Marc C. Torjman, and Paul J. Strasma. “Vascular Glucose Sensor Symposium: Continuous Glucose Monitoring Systems (CGMS) for Hospitalized and Ambulatory Patients at Risk for Hyperglycemia, Hypoglycemia, and Glycemic Variability”. In: *Journal of Diabetes Science and Technology* 9.4 (July 2015), pp. 725–738.
- [157] B Wayne Bequette. “A Critical Assessment of Algorithms and Challenges in the Development of a Closed-Loop Artificial Pancreas”. In: *Diabetes Technology & Therapeutics* 7.1 (Feb. 2005), pp. 28–47.
- [158] Yvonne Ho. *Patient-Specific Controller for an Implantable Artificial Pancreas*. Springer Theses. Singapore: Springer Singapore, 2019.
- [159] Patrick Gilon et al. “Control mechanisms of the oscillations of insulin secretion in vitro and in vivo”. In: *Diabetes* 51.SUPPL. (2002).

- [160] Rinaldo Bellomo et al. “Normothermic extracorporeal perfusion of isolated porcine liver after warm ischaemia: a preliminary report.” In: *Critical care and resuscitation : journal of the Australasian Academy of Critical Care Medicine* 14.3 (Sept. 2012), pp. 173–6.
- [161] Russell Burton-Opitz. “The vascularity of the liver. II. The influence of the portal blood-flow upon the flow in the hepatic artery”. In: *Quarterly Journal of Experimental Physiology* 4.1 (Jan. 1911), pp. 93–102.
- [162] W. Wayne Lautt. “Role and control of the hepatic artery”. In: *Hepatic Circulation in Health and Disease*. 1981, pp. 203–226.
- [163] Wayne Wayne Lautt. “Regulatory processes interacting to maintain hepatic blood flow constancy: Vascular compliance, hepatic arterial buffer response, hepatorenal reflex, liver regeneration, escape from vasoconstriction”. In: *Hepatology Research* 37.11 (Nov. 2007), pp. 891–903.
- [164] T Ayuse et al. “Pressure-flow analysis of portal vein and hepatic artery interactions in porcine liver.” In: *American journal of physiology. Heart and circulatory physiology* 267.4 Pt 2 (1994), H1233–42.
- [165] Diethard R. Monbaliu et al. “Flow competition between hepatic arterial and portal venous flow during hypothermic machine perfusion preservation of porcine livers”. In: *International Journal of Artificial Organs* 35.2 (2012), pp. 119–131.
- [166] John J. Reho, Xiaoxu Zheng, and Steven A. Fisher. “Smooth muscle contractile diversity in the control of regional circulations”. In: *American Journal of Physiology-Heart and Circulatory Physiology* 306.2 (Jan. 2014), H163–H172.
- [167] R. T. Mathie and B. Alexander. “The role of adenosine in the hyperaemic response of the hepatic artery to portal vein occlusion (the ‘buffer response’).” In: *British journal of pharmacology* 100.3 (July 1990), pp. 626–30.

- [168] Nikolai Siebert et al. "H<sub>2</sub>S contributes to the hepatic arterial buffer response and mediates vasorelaxation of the hepatic artery via activation of K<sup>+</sup> ATP channels". In: *American Journal of Physiology-Gastrointestinal and Liver Physiology* 295.6 (Dec. 2008), G1266–G1273.
- [169] Jarosław Biernat et al. "Role of afferent nerves and sensory peptides in the mediation of hepatic artery buffer response". In: *Journal of Physiology and Pharmacology* 56.1 (2005), pp. 133–145.
- [170] Masashi Ishikawa et al. "Hemodynamic changes in blood flow through the denervated liver in pigs". In: *Journal of Investigative Surgery* 8.1 (1995), pp. 95–100.
- [171] S. M. Sancetta. "Dynamic and Neurogenic Factors Determining the Hepatic Arterial Flow after Portal Occlusion". In: *Circulation Research* 1.5 (Sept. 1953), pp. 414–418.
- [172] R T Mathie et al. "The hepatic arterial blood flow response to portal vein occlusion in the dog: the effect of hepatic denervation." In: *Pflugers Archiv : European journal of physiology* 386.1 (July 1980), pp. 77–83.
- [173] J. Michael Henderson et al. "Hemodynamics during liver transplantation: The interactions between cardiac output and portal venous and hepatic arterial flows". In: *Hepatology* 16.3 (Sept. 1992), pp. 715–718.
- [174] D M Payen et al. "Portal and hepatic arterial blood flow measurements of human transplanted liver by implanted Doppler probes: interest for early complications and nutrition." In: *Surgery* 107.4 (Apr. 1990), pp. 417–27.
- [175] W. R. Ezzat and W. Wayne Lauth. "Hepatic arterial pressure-flow autoregulation is adenosine mediated". In: *American Journal of Physiology-Heart and Circulatory Physiology* 252.4 (Apr. 1987), H836–H845.
- [176] A M Rappaport. "Hepatic blood flow: morphologic aspects and physiologic regulation." In: *International review of physiology* 21 (1980), pp. 1–63.



- [177] J. Lutz, U. Peiper, and E. Bauereisen. “Auftreten und Verhalten veno-vasomotorischer Reaktionen in der Leberstrombahn”. In: *Pfluegers Archiv fuer die Gesamte Physiologie des Menschen und der Tiere* 299.4 (1968), pp. 311–325.
- [178] D. Harper and B. Chandler. “Splanchnic circulation”. In: *BJA Education* 16.2 (2016), pp. 66–71.
- [179] L. B. Hinshaw, D. A. Reins, and L. Wittmers. “Venous-Arteriolar Response in the Canine Liver”. In: *Experimental Biology and Medicine* 118.4 (Apr. 1965), pp. 979–982.
- [180] Nicola Brienza et al. “Effects of PEEP on Liver Arterial and Venous Blood Flows”. In: *American Journal of Respiratory and Critical Care Medicine* 152.2 (1995), pp. 511–518.
- [181] KM Hanson and PC Johnson. “Local control of hepatic arterial and portal venous flow in the dog”. In: *American Journal of Physiology-Legacy Content* 211.3 (Sept. 1966), pp. 712–720.
- [182] Charlotte Debbaut et al. “From vascular corrosion cast to electrical analog model for the study of human liver hemodynamics and perfusion”. In: *IEEE Transactions on Biomedical Engineering* 58.1 (2011), pp. 25–35.
- [183] Chloe Audebert et al. “Closed-loop lumped parameter modelling of hemodynamics during cirrhogenesis in rats”. In: *IEEE Transactions on Biomedical Engineering* (2018).
- [184] Harvey Ho et al. “Modeling the hepatic arterial buffer response in the liver”. In: *Medical Engineering and Physics* 35.8 (2013), pp. 1053–1058.
- [185] T D Bennett and C F Rothe. “Hepatic capacitance responses to changes in flow and hepatic venous pressure in dogs.” In: *The American journal of physiology* 240 (1981), H18–H28.
- [186] C. V. Greenway, K. L. Seaman, and I. R. Innes. “Norepinephrine on venous compliance and unstressed volume in cat liver”. In: *American Journal of Physiology-Heart and Circulatory Physiology* 248.4 (Apr. 1985), H468–H476.
- [187] Simon Gelman. “Venous Function and Central Venous Pressure”. In: *Anesthesiology* 108.4 (Apr. 2008), pp. 735–748.

- [188] Brian E. Carlson, Julia C. Arciero, and Timothy W. Secomb. "Theoretical model of blood flow autoregulation: roles of myogenic, shear-dependent, and metabolic responses". In: *American Journal of Physiology-Heart and Circulatory Physiology* 295.4 (2008), H1572–H1579.
- [189] W. Wayne Lautt, Dallas J Legare, and Waleed R Ezzat. "Quantitation of the hepatic arterial buffer response to graded changes in portal blood flow". In: *Gastroenterology* 98.4 (Apr. 1990), pp. 1024–1028.
- [190] Roberto Troisi et al. "Modulation of Portal Graft Inflow: A Necessity in Adult Living-Donor Liver Transplantation?" In: *Annals of Surgery* 237.3 (2003), pp. 429–436.
- [191] W G SCHENK et al. "Direct measurement of hepatic blood flow in surgical patients: with related observations on hepatic flow dynamics in experimental animals." In: *Annals of surgery* 156 (Sept. 1962), pp. 463–71.
- [192] Taku Aoki et al. "Intraoperative direct measurement of hepatic arterial buffer response in patients with or without cirrhosis." In: *Liver transplantation : official publication of the American Association for the Study of Liver Diseases and the International Liver Transplantation Society* 11.6 (June 2005), pp. 684–91.
- [193] Stephan M Jakob et al. "Splanchnic vasoregulation during mesenteric ischemia and reperfusion in pigs." In: *Shock (Augusta, Ga.)* 18.2 (Aug. 2002), pp. 142–7.
- [194] S Richter et al. "Impact of intrinsic blood flow regulation in cirrhosis: maintenance of hepatic arterial buffer response." In: *American journal of physiology. Gastrointestinal and liver physiology* 279.2 (Aug. 2000), G454–62.
- [195] J Lutz et al. "Das Druck-Volumendiagramm und Elastizitaetswerte des gesamten Lebergefassaesssystems der Katze in situ". In: *Pfluegers Archiv fuer die Gesamte Physiologie des Menschen und der Tierer die Gesamte Physiologie des Menschen und der Tiere* 295.4 (1967), pp. 315–327.
- [196] Harald Kjekshus et al. "Regulation of Hepatic Vascular Volume". In: *Circulation* 96.12 (Dec. 1997), pp. 4415–4423.

- [197] T. D. Bennett, C. L. MacAnespie, and C. F. Rothe. “Active hepatic capacitance responses to neural and humoral stimuli in dogs”. In: *American Journal of Physiology-Heart and Circulatory Physiology* 242.6 (June 1982), H1000–H1009.
- [198] W. Wayne Lutt. “Mechanism and role of intrinsic regulation of hepatic arterial blood flow: hepatic arterial buffer response”. In: *American Journal of Physiology-Gastrointestinal and Liver Physiology* 249.5 (Nov. 1985), G549–G556.
- [199] Lei Liu et al. “Effects of H<sub>2</sub>S on Myogenic Responses in Rat Cerebral Arterioles”. In: *Circulation Journal* 76.4 (2012), pp. 1012–1019.
- [200] Olan Jackson-Weaver et al. “Intermittent Hypoxia in Rats Increases Myogenic Tone Through Loss of Hydrogen Sulfide Activation of Large-Conductance Ca<sup>2+</sup>-Activated Potassium Channels”. In: *Circulation Research* 108.12 (June 2011), pp. 1439–1447.
- [201] K.M. Hanson. “Dilator Responses of the Canine Hepatic Vasculature”. In: *Journal of Vascular Research* 10.1 (1973), pp. 15–23.
- [202] Fuat H. Saner et al. “Positive end-expiratory pressure induces liver congestion in living donor liver transplant patients: Myth or fact”. In: *Transplantation* 85.12 (2008), pp. 1863–1866.
- [203] W. Wayne Lutt and Dallas J Legare. “The use of 8-phenyltheophylline as a competitive antagonist of adenosine and an inhibitor of the intrinsic regulatory mechanism of the hepatic artery”. In: *Canadian Journal of Physiology and Pharmacology* 63.6 (June 1985), pp. 717–722.
- [204] Melanie Senior. “Beating the organ clock transforming transplantation and offering new therapeutic”. In: *Nature Publishing Group* 36.6 (2018), pp. 488–492.
- [205] Dilmurodjon Eshmuminov et al. “Reply to “Ex situ normothermic machine perfusion of donor livers using a haemoglobin-based oxygen carrier: a viable alternative to red blood cells””. In: *Transplant International* 31.11 (Nov. 2018), pp. 1283–1284.

- [206] Rosanna Asselta and Flora Peyvandi. “Factor V Deficiency”. In: *Seminars in Thrombosis and Hemostasis* 35.04 (June 2009), pp. 382–389.
- [207] Bruno Levy et al. “Vasoplegia treatments: The past, the present, and the future”. In: *Critical Care* 22.1 (2018), pp. 1–11.
- [208] C. Eisenbach et al. “An Early Increase in Gamma Glutamyl-transpeptidase And Low Aspartate Aminotransferase Peak Values Are Associated With Superior Outcomes After Orthotopic Liver Transplantation”. In: *Transplantation Proceedings* 41.5 (2009), pp. 1727–1730.
- [209] Kim M. Olthoff et al. “Validation of a current definition of early allograft dysfunction in liver transplant recipients and analysis of risk factors”. In: *Liver Transplantation* 16.8 (Apr. 2010), pp. 943–949.
- [210] “Buying time for transplants”. In: *Nature Biotechnology* 35.9 (Sept. 2017), pp. 801–801.
- [211] Andrew Rhodes et al. “Surviving Sepsis Campaign: International Guidelines for Management of Sepsis and Septic Shock: 2016”. In: *Intensive Care Medicine* 43.3 (Mar. 2017), pp. 304–377.
- [212] Pierre Asfar, Peter Radermacher, and Marlies Ostermann. “MAP of 65: target of the past?” In: *Intensive Care Medicine* 44.9 (2018), pp. 1551–1552.
- [213] Eduardo De Santibañes and Pierre Alain Clavien. “Playing play-doh to prevent postoperative liver failure: The ”aLPPS” approach”. In: *Annals of Surgery* 255.3 (2012), pp. 415–417.

# List of publications

## Relevant journal publications

*First authors underlined.*

1. Becker, D., Eshmuminov, D., Hefti, M., Keller, R., Schuler, M. J., Bautista Borrego, L., Hagedorn, C., Muller, X., Mueller, M., Graf, P., Dutkowski, P., Tibbitt, M.W., Onder, C., Clavien, P., Rudolf von Rohr, P., (2020): Continuous blood glucose control during *ex vivo* liver perfusion, **submitted**
2. Eshmuminov, D., Becker, D., Bautista Borrego, L., Hefti, M., Schuler, M. J., Hagedorn, C., Muller, X., Mueller, M., Onder, C., Graf, P., Weber, A., Dutkowski, P., Rudolf von Rohr, P., Clavien, P., (2020): An integrated perfusion machine preserves injured human livers for 1 week. *Nature Biotechnology*, <https://doi.org/10.1038/s41587-019-0374-x>
3. Becker, D., Hefti, M., Schuler, M. J., Bautista Borrego, L., Hagedorn, C., Muller, X., Graf, P., Dutkowski, P., Tibbitt, M.W., Onder, C., Clavien, P., Eshmuminov, D., Rudolf von Rohr, P., (2019): Model assisted analysis of the hepatic arterial buffer response during *ex vivo* porcine liver perfusion. *IEEE Transactions on Biomedical Engineering*, <https://doi.org/10.1109/TBME.2019.2919413>
4. Eshmuminov, D., Leoni, F., Schneider, M. A., Becker, D., Muller, X., Onder, C., Hefti, M., Schuler, M. J., Dutkowski, P., Graf, R., Rudolf von Rohr, P., Clavien, P., Bautista Borrego, L., (2018): Perfusion settings and additives in liver normothermic machine perfusion with red blood cells as oxygen carrier. A systematic review of human and porcine perfusion protocols. *Transplant International*, 31:956—969, <https://doi.org/10.1111/tri.13306>

## Patents

1. **Becker, D.**, Eshmuminov, D., Hefti, M., Schuler, M. J., Rudolf von Rohr, P., Clavien, P., Graf, R., Bautista Borrego, L., Muller, X., Dutkowski, P.: (WO2019141809) Perfusion loop assembly for an ex-vivo liver perfusion and a method for ex-vivo liver perfusion, PCT/EP2019/051252, online version, *patent pending*.

## Conference contributions

1. **Becker, D.**, Eshmuminov, D., Hefti, M., Schuler, M. J., Bautista Borrego, L., Hagedorn, C., Muller, X., Onder, C., Graf, R., Dutkowski, P., Rudolf von Rohr, P., Clavien, P., (2019).: A Perfusion Device to Preserve Liver Function in an Ex Vivo Environment for Multiple Days. *ASAIO 65th Annual Conference 2019*, San Francisco, 2019.
2. **Becker, D.**, Eshmuminov, D., Hefti, M., Schuler, M. J., Bautista Borrego, L., Hagedorn, C., Muller, X., Müller, M., Onder, C., Graf, R., Dutkowski, P., Rudolf von Rohr, P., Clavien, P., (2019).: Keeping a liver fully functional outside of the body for multiple days. *Swiss Medtech Day 2019*, Bern, 2019.
3. **Becker, D.**, Eshmuminov, D., Hefti, M., Schuler, M. J., Bautista Borrego, L., Hagedorn, C., Muller, X., Onder, C., Graf, R., Dutkowski, P., Rudolf von Rohr, P., Clavien, P., (2018).: Technical aspects and challenges of a long-term ex vivo liver perfusion system. *Personalized Health Technologies and Translational Research Conference 2018*, Zurich, 2018.